Magneto-elastic interactions in the heavy rare-earth metals and the elastic properties of terbium

Jensen, J.

Publication date:
1971

Document Version
Publisher's PDF, also known as Version of record

Risö Report No. 252

Danish Atomic Energy Commission

Research Establishment Risö

Magneto - Elastic Interactions in the Heavy Rare-Earth Metals and the Elastic Properties of Terbium

by Jens Jensen

October 1971

Sales distributors: Jul. Gjellerup, 87, Sölvgade, DK-1307 Copenhagen K, Denmark

Available on exchange from: Library, Danish Atomic Energy Commission, Risö, DK-4000 Roskilde, Denmark

U. D. C.
546.66:539.17

October, 1971 Risö Report No. 252

MAGNETO - ELASTIC INTERACTIONS IN THE HEAVY RARE-EARTH METALS AND THE ELASTIC PROPERTIES OF TERBIUM

by

Jens Jensen

Danish Atomic Energy Commission
Research Establishment Risö
Physics Department

Abstract

With the Hamiltonian for linear magneto - elastic coupling proposed by Callen and Callen we deduced expressions for changes in the velocity of acoustic waves in terbium and dysprosium due to ferromagnetic ordering and the application of an external magnetic field. These calculations are in fair agreement with experimental results. We also examined the extent to which this simple picture may be used to explain the magnon - phonon interactions in terbium. The magneto - elastic contributions to the spin wave energies were considered in detail, and the "flexible lattice" calculations performed by Cooper were examined critically.

Experimental measurements of the elastic constants of terbium as functions of temperature are presented. Strong coupling between the lattice and the spin system is observed.

Recent experimental results for ferromagnetic terbium obtained by means of inelastic neutron scattering show that the two-ion exchange interaction in the c-direction is highly anisotropic.

This report is submitted to the Technical University, Lyngby, in partial fulfilment of the requirements for obtaining the Ph. D. (lic. techn.) degree.

Statens trykningskontor ISBN 87 550 0115 7

CONTENTS

INTRODUCTION

I. MAGNETO - ELASTIC INTERACTIONS IN TERBIUM AND DYSPROSIUM

We shall begin with a brief review of the knowledge available about the magnetic properties of the heavy rare-earth metals terbium and dysprosium. The magnetic excitations in these metals are described by the combination of indirect exchange interaction and crystal field effects, the exchange interaction giving rise to dispersion and the crystal field to magnetic anisotropy. Because of their large orbital moments, the heavy rare-earth metals display the largest known magnetostriction effects. This strong coupling between the magnetic moments and the lattice has the effect that the elastic constants and the sound wave velocities depend relatively strongly on the magnetization of the crystal. In chapter 5 we derive expressions for the change in sound velocities below the Curie temperature due to linear magneto - elastic interactions, in terms of the magnetostriction coefficients and the magnon energies. The extent to which these considerations apply to magnon - phonon interactions, which have been observed at finite wave vector in terbium by means of neutron scattering, is also discussed. In the light of the better understanding of the interaction between the spin wave system and the dynamic lattice, we examine critically the two models proposed for calculating the magneto - elastic contributions to the magnetic anisotropy, namely the "frozen lattice" approximation, where the lattice is assumed to be entirely rigid, and the opposite "flexible lattice" model.

II. EXPERIMENTAL MEASUREMENTS OF THE VELOCITY OF ACOUSTIC SOUND WAVES IN TERBIUM

The four elastic constants c_{11}, c_{33}, c_{44}, and c_{66} of terbium were determined from measurements of the velocity of sound waves propagating in symmetry directions. The sound velocities were measured by an ultrasonic pulse echo technique at a frequency of 20 MHz. By conventional cryogenic technique the temperature of the sample ranged from room temperature to liquid-helium temperature. However, difficulties were encountered in preserving the ultrasonic couplant between the quartz transducers and the terbium single crystal, when the samples were cooled down below the ferromagnetic transition temperature. The results show a very strong coupling between the lattice and the spin system in the neighbourhood of the transition temperatures, T_N and T_C, in the sense that the attenuation of the sound

waves increases drastically in this temperature region, and the velocities change rather abruptly.

III. RECENT EXPERIMENTAL RESULTS FOR TERBIUM

After the two first parts of this thesis were written, additional experiments have been performed on terbium (August-September 1971) with inelastic neutron scattering technique. The spin wave energy gap at zero wave vector has been studied and analysed. The magnon - phonon interaction in the c-direction has been examined in more detail at 4.2° K. Finally, by measurements of the spin wave energies in a high magnetic field, it has been observed that anisotropic exchange interaction is considerable in terbium.

I. MAGNETO - ELASTIC INTERACTIONS IN TERBIUM AND DYSPROSIUM

1. BASIC MODEL FOR MAGNETIC AND ELASTIC PROPERTIES

Tb and Dy (atomic numbers: 65 and 66) both belong to the group of rare earths (or the lanthanides). The electronic configurations of the rare-earth atoms are given by (pd core)$4f^n5s^25p^65d^m6s^2$. In their trivalent ionic state these elements present configurations of the type (Pd core)$4f^n5s^25p^6$, where n = 8 for Tb^{+3} and n = 9 for Dy^{+3}. The unfilled 4f-shell is an inner shell screened by the 5s and 5p shells. When these ions are in crystals, the electric field from the surrounding ions and electrons gives rise to crystal field splitting, but because of the screening electrons the crystal field potential is small in comparison with the spin - orbit interaction, so the crystal field splitting is small compared with the splitting between multiplets, and we can use a $LSJM_J$ representation to take matrix elements of the crystal field perturbations. The crystal field potential $V(x, y, z)$ that acts on the 4f-electrons can when we take matrix elements within the same J-multiplet be replaced by an equivalent operator expression, namely $a_J V(J_x, J_y, J_z)$, where a_J is a constant.

The effective magnetic moment found in the paramagnetic state[1, 2] is nearly identical to that of the corresponding free trivalent ions when they are in their ground state. The ground state of the ions can be obtained by means of Hund's rules. In the heavy rare earths, where the 4f-shell is more than half-filled, the multiplet with the largest J (J = L + S) has the smallest energy. The ground term for Tb^{+3} is then $^7F_6$ or S = 3, L = 3 and J = 6, and for Dy^{+3} it is $^6H_{15/2}$ or S = 5/2, L = 5 and J = 15/2. The

magnetic moments of the (free) ions are then given by

$$\mu = g\sqrt{[J(J+1)]}\,\mu_B \,, \tag{1.1}$$

where

$$g = 1 + \frac{J(J+1) + S(S+1) - L(L+1)}{2\,J(J+1)} \tag{1.2}$$

or $\mu = 9.72\,\mu_B$ for Tb^{+3} and $\mu = 10.65\,\mu_B$ for Dy^{+3}, where a Bohr magneton $\mu_B = 5.7884 \cdot 10^{-3}$ meV/kOe.

The direct overlap between the 4f-electrons in the crystal is negligible, but the ionic moments are coupled together strongly through the conduction electrons. This indirect exchange interaction is very well described[3] by an isotropic Heisenberg interaction

$$\tilde{H}_{Ex} = -\sum_{ij} \mathcal{J}(\bar{R}_i - \bar{R}_j)\,\bar{J}_i \cdot \bar{J}_j \,. \tag{1.3}$$

The crystal field potential $V(\xi,\eta,\zeta)$ can be expanded in spherical harmonics $Y_l^m(r)$ referring to the crystal ζ-axis (the constant, α_J, depends on l). This expansion can be greatly reduced by symmetry arguments. The Y_l^m has to fulfil the crystal symmetry, and furthermore when the spin operator equivalence is evaluated, only terms that have $l \leq 2J$ and l even (due to time reversal symmetry) are retained. The crystal field Hamiltonian for the hexagonal crystals of Tb and Dy is then

$$\tilde{H}_{C.F.} = \sum_j [V_2^0\ \tfrac{1}{3}(Q_2^0)_j + V_4^0(Q_4^0)_j + V_6^0(Q_6^0)_j + V_6^6(Q_6^6)_j \,]. \tag{1.4}$$

The definition[4,5] of the Q_l^m is given in Appendix A. Experimentally[6] it is found that the V_2^0-term is much bigger than the V_4^0- and V_6^0-terms, so we will henceforward neglect V_4^0 and V_6^0.

Besides from the magnetic energy we have contributions from the lattice binding energy to the total energy. In the harmonic approximation the lattice energy can be written

$$\tilde{H}_L = \tilde{H}_L^0 + E_{el} = E_L^0 + \sum_{k,s} \hbar\omega_{\bar{k},s}(\beta_{\bar{k},s}^{+}\beta_{\bar{k},s} + \tfrac{1}{2}) + E_{el} \,. \tag{1.5}$$

$\beta_{\bar{k},s}$ is the phonon annihilation operator, and E_{el} is the increase in elastic energy due to deformations of the lattice (see chapter 3).

The spin system and the lattice are not independent of each other. A deformation of the lattice will change the exchange energy and modify the crystal field so that magnetic ordering may be accompanied by deformations of the lattice which reduce the energy of the total system. Mason[7] has derived macroscopic expressions for the magnetostriction, while Callen and Callen[8] have developed a phenomenological theory of the magneto - elastic coupling. Using this theory, we write the interaction between the lattice and the spin system as

$$\begin{aligned}\tilde{H}_{S-L} = & -\sum_{ij\alpha}[(\partial\mathcal{J}_{ij}/\partial R_{i\alpha})\delta R_{i\alpha} + (\partial\mathcal{J}_{ij}/\partial R_{j\alpha})\delta R_{j\alpha}]\mathbf{J}_i\cdot\mathbf{J}_j \\ & + G_{01}\sum_j \tfrac{1}{3}(Q_2^0)_j(e_{11}+e_{22}) + G_{03}\sum_j \tfrac{1}{3}(Q_2^0)_j e_{33} \\ & - G_{22}\sum_j[(Q_2^2)_j(e_{11}-e_{22}) + (Q_2^{-2})_j e_{12}] \\ & - G_{12}\sum_j[\tfrac{1}{2}(Q_2^1)_j e_{23} + \tfrac{1}{2}(Q_2^{-1})_j e_{13}] \\ & + G_{44}\sum_j[(Q_4^4)_j(e_{11}-e_{22}) - (Q_4^{-4})_j e_{12}]\,.\end{aligned} \tag{1.6}$$

The strains $e_{\alpha\beta}$ are defined in terms of the elastic displacements $u_\alpha(\bar{r},t)$

$$e_{\alpha\beta} = (1 - \tfrac{1}{2}\delta_{\alpha\beta})(\partial u_\alpha/\partial x_\beta + \partial u_\beta/\partial x_\alpha)\,. \tag{1.7}$$

$\tilde{H}_{S-L}$ has the symmetry of the hexagonal lattice. The only two-ion term that is included is the one arising from the exchange energy. The G_{01}, G_{03}, G_{12}, and G_{22} terms comprise the total one-ion magneto - elastic Hamiltonian to the second power in the spin operators. Besides these we included one term of fourth power (G_{44}), which has about the same magnitude as G_{22} in Tb and Dy. The assumption that the terms have purely one-ion character is in accordance with experimental measurements[9,10,11,12], and it does not seem necessary to include terms of sixth power or the fourth power term

$$- G_{24} \sum_j [(Q_4^2)_j (e_{11} - e_{22}) + (Q_4^{-2})_j e_{12}]. \qquad (1.8)$$

The magnetic and elastic behaviour of Tb and Dy is then given by the total Hamiltonian

$$\tilde{H}_T = \tilde{H}_{Ex} + \tilde{H}_{C.F.} + \tilde{H}_L^0 + E_{el} + \tilde{H}_{S-L} + \tilde{H}_Z \ , \qquad (1.9)$$

where $\tilde{H}_Z$ is the Zeeman energy in the presence of a magnetic field

$$\tilde{H}_Z = - g\mu_B \sum_j \bar{J}_j \cdot \bar{H} . \qquad (1.10)$$

The equilibrium magnetic ordering arrangements for Tb and Dy are very similar. At T_N they go through a second-order transition from a paramagnetic phase to an antiferromagnetic state. This transition is mainly caused by $\tilde{H}_{Ex}$. In the temperature range between T_N and T_C the moments are arranged in a spiral with the moments lying in the basal plane (the moments of the ions lying in a given hexagonal layer are parallel). The magnetic moments then change their direction going down the c-axis, described either by a spiral turn angle between the moments of successive hexagonal layers, or by a wave vector $\bar{Q}$, parallel with the c-axis. The axial anisotropy[6] (the V_2^0-term in $\tilde{H}_{C.F.}$) is responsible for the basal plane alignment of the moments, that is V_2^0 is positive. The wave vector, $\bar{Q}$, has such a value that the Fourier-transformed exchange integral $\mathcal{J}(\bar{q})$ has its maximum at $\bar{q} = \bar{Q}$. In the molecular field approximation, the Neel temperature, T_N, is

$$T_N = \mathcal{J}(\bar{Q}) J(J+1)/3k_B \ ; \qquad (1.11)$$

k_B is the Boltzmann factor.

In Tb and Dy there is a spontaneous transformation (first-order transition) at the Curie temperature, T_C, to a ferromagnetic configuration. For Tb the ferromagnetic alignment below T_C is along a b-axis in the hexagonal plane, whereas for Dy it is along an a-axis in the hexagonal plane. This transition is almost entirely due to contributions to planar anisotropy from the magneto - elastic interaction term, $\tilde{H}_{S-L}$ [12,13,14,15,16]

The transition temperatures are rather sensitive to the quality of the crystals, however for Tb we have $T_N = 225^\circ$ K and $T_C = 216^\circ$ K, and for

Dy $T_N = 179^\circ$ K and $T_C = 85^\circ$ K.

2. SPIN WAVE THEORY

In this section we discuss the spin wave excitations for the ferromagnetic system (below T_C) characterized by the following Hamiltonian. (The magneto - elastic effects will be treated in chapter 6):

$$\tilde{H} = \tilde{H}_{Ex} + \tilde{H}_{C.F.} + \tilde{H}_z = - \sum_{ij} \mathcal{J}_{ij} \mathbf{J}_i \cdot \mathbf{J}_j + \sum_i [V_2^0 \tfrac{1}{3}(Q_2^0)_j + V_6^6 (Q_6^6)_j] - g\mu_B \sum_j \mathbf{J}_j \cdot \mathbf{H}. \qquad (2.1)$$

This is the Hamiltonian of the spin system in the (ξ, η, ζ) co-ordinate system. The co-ordinate system used for the hexagonal close-packed lattice of Tb and Dy is othogonal with the ξ-axis along the a $(11\bar{2}0)$ crystal axis, the η-axis along the b $(10\bar{1}0)$ direction, and the ζ-axis along the c (0001) crystal axis (see fig. 1).

The spin wave behaviour expected for such a system has been discussed by a number of authors[3, 5, 13, 18, 19]. Following Brooks et al.[5] we first transform the spin operators to the (x, y, z)-system. $\hat{z}$ is the direction of the net magnetization, assumed to lie in the basal plane. From Appendix A we have:

$$\tilde{H} = - \sum_{ij} \mathcal{J}_{ij} [J_{iz} J_{jz} + \tfrac{1}{2}(J_{i+} J_{j-} + J_{i-} J_{j+})] + V_2^0 \sum_j (\tfrac{1}{2} 0_2^2 - \tfrac{1}{6} 0_2^0)_j + V_6^6 \sum_j \tfrac{1}{16} (0_6^0 + \tfrac{15}{2} 0_6^2 + 3\, 0_6^4)_j \cos 6\varphi - g\mu_B H \sum_j (J_z \cos\delta + J_y \sin\delta)_j . \qquad (2.2)$$

The angle φ is defined as the angle between the ξ-axis and the z-axis, and δ is the angle between the z-axis and the direction of the magnetic field, also assumed to lie in the basal plane.

The hcp lattice is not a Bravais lattice, but has two atoms per unit cell, so that the spin wave spectrum has two branches, an acoustic and an optical branch. The hcp structure is considered as made of two identical interpenetrating hexagonal sublattices. Two kinds of spin deviation operators a_j and b_j (see eq. (A.4)) satisfying Bose commutation relations are introduced corresponding to each of the two sublattices:

$$a_j^{\pm} = \sqrt{(2/N)} \sum_{\vec{q}} a_q^{\pm} \exp(\mp i\, \vec{q} \cdot \vec{R}_j) \qquad b_j^{\pm} = \sqrt{(2/N)} \sum_{\vec{q}} b^{\pm} \exp(\mp i\, \vec{q} \cdot \vec{R}_j). \qquad (2.3)$$

N is the number of atoms in the crystal (or twice the number of primitive cells). The Fourier transform of the exchange integral is defined as

$$\gamma_q = \sum_{j \text{ same sublattice as } i} \gamma_{ij} \exp[i\, \vec{q} \cdot (\vec{R}_i - \vec{R}_j)]$$

$$\gamma'_q = \sum_{j \text{ other sublattice from } i} \gamma_{ij} \exp[i\, \vec{q} \cdot (\vec{R}_i - \vec{R}_j)] = |\gamma'_q| \exp(i\theta_q) \qquad (2.4)$$

γ_q is real, whereas γ'_q is generally complex. However, it is easy to see that

$$(\gamma'_q)^* = \gamma'_{-q}, \quad \text{or} \quad \theta_q = -\theta_{-q}. \qquad (2.5)$$

The Hamiltonian is now diagonalized by two successive transformations[3,5,19]

$$a_q = 1/\sqrt{2}\,(c_q + d_q)$$

$$b_q = 1/\sqrt{2}\,(c_q - d_q) \exp(i\theta_q), \qquad (2.6)$$

and the second canonical transformation

$$c_q = u_{1,q} a_{1,q} - v_{1,q} a^+_{1,-q}$$

$$d_q = u_{2,q} a_{2,q} - v_{2,q} a^+_{2,-q} \qquad (2.7)$$

where $a_i = a_1$ or a_2 are boson annihilation operators, annihilating acoustic and optical magnons respectively.

$$\tilde{H} = E_o + \sum_{i,q} \varepsilon_i(q)\, a^+_{i,q} a_{i,q}. \qquad (2.8)$$

Before the second transformation the Hamiltonian is

$$\tilde{H} = E_o + \sum_q A_1(q)\, c^+_q c_q + B_1(q)\, \tfrac{1}{2}(c_q c_{-q} + c^+_q c^+_{-q}) + \text{similar terms for the second mode,} \qquad (2.9)$$

where

$$A_i(q) = 2J(\gamma_o + \gamma'_o - \gamma_q + (-1)^i|\gamma'_q|) + J_1 V_2^o - 21\, J_5 V_6^6 \cos 6\varphi + g\mu_B H\cos\delta$$
$$B_i(q) = B = J_1 V_2^o + 15\, J_5 V_6^6 \cos 6\varphi . \tag{2.10}$$

J_n is defined in Appendix A (A. 7). The second transformation then is

$$u_{i,q}^2 - v_{i,q}^2 = 1$$
$$u_{i,q}^2 + v_{i,q}^2 = A_i(q)/\epsilon_i(q) \tag{2.11}$$
$$2\, u_{i,q} v_{i,q} = B/\epsilon_i(q) .$$

The spin wave excitation energy is

$$\epsilon_i(q) = [(A_i(q) + B)(A_i(q) - B)]^{1/2}. \tag{2.12}$$

The total magnetic energy at $T = 0^o$ K is

$$E_o = -NJ^2(\gamma_o + \gamma'_o) - \tfrac{1}{3}NJJ_1V_2^o + NJJ_5V_6^6\cos 6\varphi - g\mu_B NJH\cos\delta. \tag{2.13}$$

In Tb and Dy, V_2^o is positive so the moments are forced to lie in the basal plane. The sign of V_6^6 then determines the easy planar axis. V_6^6 greater than zero corresponds to an alignment of the moments parallel with a b-axis ($\varphi = \pi/6 + p \cdot \pi/3$).

If we apply a field along an easy planar axis, the acoustic magnons display an energy gap at $q = 0$ which is ($V_6^6 \rangle 0$)

$$\epsilon_1(0) = [(2\, J_1 V_2^o + 6\, J_5 V_6^6 + g\mu_B H)(36\, J_5 V_6^6 + g\mu_B H)]^{1/2} . \tag{2.14}$$

The effect of an applied field along a hard planar axis as treated by Cooper et al.[13, 20] is much more interesting. Such an applied field pulls the magnetization towards the hard direction. δ is here determined with the condition that the equilibrium magnetic energy, E_o, is minimized:

$$\partial E_o/\partial\delta = 0 \tag{2.15}$$

where $\varphi = \delta$.

δ is then given by the equation

$$g\mu_B H = 12\, J_5 V_6^6 (3 + 16\sin^4\delta - 16\sin^2\delta)\cos\delta, \tag{2.16}$$

or $\delta = 0$, when H is larger than the critical field, H_c

$$H_c = 36\, J_5 V_6^6 / g\mu_B , \tag{2.17}$$

and the spin wave energy gap then is

$$\epsilon(0)_{hard} = [(2\, J_1 V_2^o + 30\, J_5 V_6^6 + g\mu_B(H - H_c)) \cdot g\mu_B(H - H_c)]^{1/2}. \tag{2.18}$$

We see that $\epsilon(0)_{hard} = 0$ for $H = H_c$. That is $\epsilon(0)_{hard}$ goes to zero just when the moment is pulled fully around to the hard axis. One should include the appropriate demagnetizing fields in (2.14) and (2.18), which result from dipole - dipole interaction[5,13].

The spin wave dispersion law given by (2.10) and (2.12) holds at $T = 0^o K$. The renormalization of the anisotropy terms (at $q = 0$) has been evaluated by Cooper[13] by applying the phenomenological macroscopic resonance theory developed by Smit and Belgers[21]. The anisotropy terms in (2.1) (for zero applied field) correspond to a free energy of the form

$$F_M = F_{Ex} + K_2(T)(\cos^2\theta - \tfrac{1}{3}) + K_6^6(T)\sin^6\theta\cos 6\varphi, \tag{2.19}$$

where at $T = 0^o K$ (see Appendix A (A.12))

$$K_2(0) = NJJ_1 V_2^o \qquad \text{and} \qquad K_6^6(0) = NJJ_5 V_6^6 . \tag{2.20}$$

Then the uniform mode frequency is

$$\epsilon_T(0) = [g\mu_B / M(T)](F_{\theta\theta} F_{\varphi\varphi} - F_{\theta\varphi}^2)^{1/2}. \tag{2.21}$$

$F_{\theta\theta}$, etc. denote second derivatives of the free energy with respect to angle evaluated at the equilibrium position ($\theta = \pi/2$). M(T) is the magnetization at temperature T, and defining the reduced magnetization

$$\sigma = M(T)/M(0), \tag{2.22}$$

we have

$$M(T) = M(0)\sigma = Ng\mu_B[J(J+1)]^{1/2}\,\sigma \cong g\mu_B NJ\sigma . \tag{2.23}$$

Then the ferromagnetic resonance mode frequency is

$$\epsilon_T(0) = [\gamma/NJ\sigma]\,[(-36\,K_6^6(T)\cos 6\varphi)(2\,K_2(T) - 6\,K_6^6(T)\cos 6\varphi)]^{1/2} . \tag{2.24}$$

This expression corresponds to the spin wave energy gap at q = 0, (2.14) and $\epsilon_T(0) \to \epsilon_1(0)$ when $T \to 0^\circ K$. Then the temperature dependence of $\epsilon_1(0)$ can be introduced explicitly into (2.24) in terms of the reduced magnetization, using the theory of Callen and Callen[8]. They have calculated the temperature and field dependence of spin correlation functions arising from single-ion crystal field effects. For infinite spin they have

$$\langle\langle O_l^m \rangle\rangle = \langle O_l^m \rangle_{T=0} \cdot \hat{I}_{l+1/2}\,[\mathcal{L}^{-1}(\sigma)] , \tag{2.25}$$

where

$$\hat{I}_{l+1/2}(x) = I_{l+1/2}(x)/I_{1/2}(x) \tag{2.26}$$

is the ratio of hyperbolic Bessel functions, and $\mathcal{L}^{-1}(\sigma)$ is the inverse Langevin function of the reduced magnetization. For low temperature

$$\hat{I}_{l+1/2}\,[\mathcal{L}^{-1}(\sigma)] \sim \sigma^{l(l+1)/2} . \tag{2.27}$$

This proportionality is reasonably good throughout the ferromagnetically ordered region. Comparison between (2.24) and (2.14) shows that the temperature renormalization of $\epsilon_1(q)$ in the limit $q \to 0$ is

$$\epsilon_1(0) = [(2\,J_1V_2^0 \cdot \sigma^2 - 6\,J_5V_6^6 \cdot \sigma^{20}\cos 6\varphi)(-36\,J_5V_6^6 \cdot \sigma^{20}\cos 6\varphi)]^{1/2} \tag{2.28}$$

because

$$\frac{1}{\sigma}K_2(T) \sim \frac{1}{\sigma}\hat{I}_{5/2} \sim \sigma^2 \qquad \text{and} \qquad \frac{1}{\sigma}K_6^6(T) \sim \frac{1}{\sigma}\hat{I}_{13/2} \sim \sigma^{20} . \tag{2.29}$$

Brooks et al.[5] have obtained almost the same temperature dependence for $\epsilon_1(0)$ by applying a variational principle for the free energy

$$J_1V_2^0 \to J_1V_2^0 \cdot \sigma^{3/2} \qquad \text{and} \qquad J_5V_6^6 \to J_5V_6^6 \cdot \sigma^{24} . \tag{2.30}$$

Brooks[18] has later modified this result by using the ratio of axial anisotropy to exchange, rather than the angular deviation from the easy direction, as expansion parameter in a perturbation theory. At low temperature only acoustic magnons with small q-vectors are excited, and the main contribution to σ comes from the axial anisotropy rather than from the exchange interaction. At these temperatures the result is

$$J_1 V_2^0 \to J_1 V_2^0 \cdot \sigma^1 \qquad \text{and} \qquad J_5 V_6^6 \to J_5 V_6^6 \cdot \sigma^{35} . \tag{2.31}$$

At higher temperatures or for small anisotropy the result is identical with (2.28).

The simplest, reasonably accurate way to renormalize the exchange contribution in (2.12) is to use the random phase approximation and multiply the exchange energy terms in (2.13) by σ^2, which means that the exchange contribution to $A_i(q)$ in (2.10) is renormalized proportionally to σ. The effect of a non-zero field on $A_i(q)$ is independent of σ, corresponding to a renormalization of the Zeeman term in the free energy proportionally to σ.

3. MAGNETOSTRICTION

For elastic waves with wave lengths of more than 10^{-6} cm, which means for frequencies below 10^{11} or 10^{12} cps, a crystal can be considered as a homogeneous, continuous medium rather than as a periodic array of atoms. For sufficiently small deformations of the crystal we can make use of Hooke's law, which states that in an elastic solid the strain is directly proportional to the stress. Defining the stress and strain tensors in the usual way[22, 23], we have

$$T_{ij} = c_{ijkl} \epsilon_{kl} . \tag{3.1}$$

The co-ordinate system used for the hcp lattice of Tb and Dy is the othogonal system (ξ, η, ζ) defined in fig. 1, that is ξ is the 1-axis, etc. The strains $e_{\alpha\beta}$ defined in (1.7) are related to the strain tensor

$$e_{\alpha\beta} = (2 - \delta_{\alpha\beta}) \epsilon_{\alpha\beta} . \tag{3.2}$$

The indices are simplified as follows

$$11 \to 1, \quad 22 \to 2, \quad 33 \to 3, \quad 23 \to 4, \quad 13 \to 5, \quad 12 \to 6, \tag{3.3}$$

and Hooke's law is then

$$T_i = \sum_{j=1}^{6} c_{ij} e_j , \tag{3.4}$$

where c_{ij} for a hexagonal system defined as above is

$$c_{ij} = \begin{Bmatrix} c_{11} & c_{12} & c_{13} & 0 & 0 & 0 \\ c_{12} & c_{11} & c_{13} & 0 & 0 & 0 \\ c_{13} & c_{13} & c_{33} & 0 & 0 & 0 \\ 0 & 0 & 0 & c_{44} & 0 & 0 \\ 0 & 0 & 0 & 0 & c_{44} & 0 \\ 0 & 0 & 0 & 0 & 0 & c_{66} \end{Bmatrix} \tag{3.5}$$

where

$$c_{66} = \frac{1}{2}(c_{11} - c_{12}) . \tag{3.6}$$

The elastic properties of a hexagonal solid are determined by five independent elastic constants. These constants can be evaluated by measuring the velocities of sound waves propagating in different directions. In high symmetry directions the polarization of the sound waves is either longitudinal or transverse. If the density of the solid is ρ, we have

Sound waves in the c-direction:

$$c_{33} = \rho v_{long.}^2 , \quad c_{44} = \rho v_{tran.}^2 \tag{3.7}$$

Sound waves in the basal plane:

$$c_{11} = \rho v_{long.}^2 , \quad c_{44} = \rho v_{1, tran.}^2 , \quad c_{66} = \rho v_{2, tran.}^2 , \tag{3.8}$$

where $v_{1, tran.}$ is the velocity of transverse sound waves polarized in the c-direction, and the polarization of $v_{2, tran.}$ is parallel with the basal plane. c_{13} can be found by measuring the velocity of sound waves propagating in a direction at an angle of 45° with the c-axis.

The relation (3.4) can be conversed so that the strain components are linear functions of the stress components

$$\begin{Bmatrix} e_1 - e_2 \\ e_1 + e_2 \\ e_3 \end{Bmatrix} = \begin{bmatrix} \frac{1}{c_{66}} & 0 & 0 \\ 0 & \frac{2c_{33}}{\Delta} & -\frac{2c_{13}}{\Delta} \\ 0 & -\frac{2c_{13}}{\Delta} & \frac{c_{11}+c_{12}}{\Delta} \end{bmatrix} \cdot \begin{Bmatrix} \frac{1}{2}(T_1 - T_2) \\ \frac{1}{2}(T_1 + T_2) \\ T_3 \end{Bmatrix} \tag{3.9}$$

$e_i = T_i/c_{ii}$ when $i \geq 4$

where

$$\Delta = c_{33}(c_{11} + c_{12}) - 2c_{13}^2 . \tag{3.10}$$

The bulk modulus, B, or the inverse compressibility is

$$B = \Delta/(c_{11} + c_{12} + 2c_{33} - 4c_{13}) . \tag{3.11}$$

The elastic energy density, E_{el}, is a quadratic function of the strains in the approximation of Hooke's law. Thus we have

$$E_{el} = \frac{1}{2} \sum_{i,j} c_{ij} e_i e_j , \tag{3.12}$$

and the elastic energy density of a hexagonal crystal can be written

$$E_{el} = \frac{1}{2}(c_{11} - c_{66})(e_1 + e_2)^2 + \frac{1}{2}c_{33}e_3^2 + c_{13}(e_1 + e_2)e_3 +$$

$$+ \frac{1}{2}c_{44}(e_4^2 + e_5^2) + \frac{1}{2}c_{66}[(e_1 - e_2)^2 + e_6^2] . \tag{3.13}$$

The magnetostriction of a material is a result of the interaction between the magnetic anisotropy and exchange energies and the elastic energy. If, in the process of magnetization, it becomes energetically favourable, the crystal lattice will distort and produce a magnetostrictive strain. The total strain-dependent energy density, E_{MS}, leading to the magnetostriction is

$$E_{MS} = E_{el} + E_{me} , \tag{3.14}$$

where E_{me} is the magneto - elastic contribution. Mason[7] has derived an expression for the thermodynamic enthalpy for crystals characterized by hexagonal symmetry. The magnetostriction in a direction characterized by

direction cosines $\beta_1\beta_2\beta_3$ may then be written

$$\delta l/l = \sum_{ij} \hat{\epsilon}_{ij}\beta_i\beta_j , \tag{3.15}$$

and Mason obtains the following expressions for the magnetostrictive strains in a hexagonal material:

$$\begin{aligned}
\hat{e}_1 + \hat{e}_2 &= 2D'\sin^2\theta + 2J\cos^2\theta + 2F'\cos^2\theta\sin^2\theta \\
\hat{e}_3 &= G\sin^2\theta + K\cos^2\theta + (E' + F')\cos^2\theta\sin^2\theta \\
\hat{e}_4 &= \tfrac{1}{2}(H_o + I\cos^2\theta)\sin 2\theta\sin\varphi \\
\hat{e}_5 &= \tfrac{1}{2}(H_o + I\cos^2\theta)\sin 2\theta\cos\varphi \\
\hat{e}_1 - \hat{e}_2 &= 2C\sin^2\theta\cos 2\varphi - A\sin^4\theta\cos 4\varphi + \tfrac{1}{2}B\sin^2 2\theta\cos 2\varphi \\
\hat{e}_6 &= 2C\sin^2\theta\sin 2\varphi + A\sin^4\theta\sin 4\varphi + \tfrac{1}{2}B\sin^2 2\theta\sin 2\varphi
\end{aligned} \tag{3.16}$$

We made the following substitutions

$$D' = D + A/2 \qquad E' = E + A/2 \qquad F' = F - A/2 . \tag{3.17}$$

These expressions can be deduced from E_{MS} because it has to fulfil the equilibrium condition

$$(\partial E_{MS}/\partial e_j)_{\theta,\varphi} = 0 \qquad \text{when } e_i = \hat{e}_i . \tag{3.18}$$

Thus if we write E_{me} as

$$E_{me} = \sum_i B_i(\theta, \varphi; \sigma)e_i \tag{3.19}$$

where B_i is a function of θ and φ, we find

$$
\begin{aligned}
\tfrac{1}{2}(B_1 + B_2) &= -(c_{11} - c_{66})(\hat{e}_1 + \hat{e}_2) - c_{13}\hat{e}_3 \\
B_3 &= -c_{33}\hat{e}_3 - c_{13}(\hat{e}_1 + \hat{e}_2) \\
B_4 &= -c_{44}\hat{e}_4 \\
B_5 &= -c_{44}\hat{e}_5 \\
\tfrac{1}{2}(B_1 - B_2) &= -c_{66}(\hat{e}_1 - \hat{e}_2) \\
B_6 &= -c_{66}\hat{e}_6 \,.
\end{aligned}
\tag{3.20}
$$

This expression for the strain-dependent energy density can be compared with the average value of the spin lattice Hamiltonian, $\bar{H}_{S-L}$, (1.6) and (1.8) at $T = 0^{\circ}K$, by using the result from Appendix A (A.12), and we obtain[24] the following relations between the magnetostriction coefficients

$$
\begin{aligned}
D_{22} &= G_{22}J_1 - G_{24}J_3 = 2Cc_{66}/NJ \\
D_{24} &= G_{24}J_3 = 2Bc_{66}/7NJ \\
D_{44} &= G_{44}J_3 = Ac_{66}/NJ \\
G_{12} &= H_o c_{44}/NJJ_1 \\
\partial E_{ex}/\partial e_1 - \tfrac{1}{3}NJD_{01} &= -[2D'(c_{11} - c_{66}) + Gc_{13}] \\
\partial E_{ex}/\partial e_3 - \tfrac{1}{3}NJD_{03} &= -[2D'c_{13} + Gc_{33}]
\end{aligned}
\tag{3.21}
$$

where

$$
D_{01} = J_1 G_{01} \qquad \text{and} \qquad D_{03} = J_1 G_{03} \,. \tag{3.22}
$$

The derivatives of E_{Ex} with respect to e_1, e_2, and e_3 can be evaluated from the macroscopic equation

$$
\tfrac{1}{3}[2\partial E_{Ex}/\partial e_1 + \partial E_{Ex}/\partial e_3] = V\partial E_{Ex}/\partial V = -(E_{Ex}B/T_N)\partial T_N/\partial p \tag{3.23}
$$

(B is the bulk modulus (3.11) and p is the pressure) by assuming

$$
\partial E_{Ex}/\partial e_1 = \partial E_{Ex}/\partial e_2 \cong \partial E_{Ex}/\partial e_3 \,. \tag{3.24}
$$

(3.23) and (3.24) are consistent with the following considerations: The contribution from the first term in (1.6) arising from the exchange interaction can be calculated in the limit of homogeneous strain ($\delta R_{i\alpha} = e_{\alpha\alpha} R_{i\alpha}$) when we assume that $\langle \vec{J}_i \cdot \vec{J}_j \rangle \cong \langle \vec{J}_i \rangle \cdot \langle \vec{J}_j \rangle = J^2$, and we find

$$\partial E_{Ex}/\partial e_1 \cong \partial E_{Ex}/\partial e_3 \cong -2NJ^2(\mathcal{J}_o + \mathcal{J}'_o) = 2E_{Ex} . \tag{3.25}$$

Using $\mathcal{J}(\vec{Q}) \cong \mathcal{J}_o + \mathcal{J}'_o$ in the expression for T_N (1.11) and the experimental value[25] for $\partial T_N/\partial p = -1.1\,^oK/kbar$ in Tb, we have

$$E_{Ex} = -3k_B T_N NJ/(J+1) \tag{3.26}$$

and $V\partial E_{Ex}/\partial V = 2.1\, E_{Ex}$, which is in accordance with (3.25).

With the correspondance between E_{me} and $\tilde{H}_{S-L}$ (3.21) and the Callen and Callen theory for the temperature dependence of the spin correlation function (2.25), the terms in (3.16) renormalize in the following manner:

$$\begin{aligned} &H_o \sim \hat{I}_{5/2} \sim \sigma^3 \\ &A \text{ and } B \sim \hat{I}_{9/2} \sim \sigma^{10} \\ &C = \frac{NJ}{c_{66}} (J_1 G_{22} \hat{I}_{5/2} - J_3 G_{24} \hat{I}_{9/2}) \sim \sigma^3 \quad \text{when} \quad C \rangle\rangle \tfrac{1}{7} B . \end{aligned} \tag{3.27}$$

D' and G will be proportional to something between σ^2 and σ^3, corresponding to a σ^2-dependent contribution from the exchange term and a σ^3-dependence of NJD_{01} and NJD_{03} respectively.

This renormalization of the magnetostriction predicted by Callen and Callen[8], (3.16) and (3.27), has been verified experimentally[9,10,11] for Tb and Dy. The observed σ^3-dependence of C seems to indicate that B is much smaller than C (B has not been determined explicitly so far).

Finally we will write down the total strain-dependent energy density, E_{MS} (3.14), in the case where $\theta = \pi/2$, using (3.13), (3.16), (3.19), and (3.20)

$$\begin{aligned} E_{MS} = &-2D'^2(c_{11}-c_{66}) - \tfrac{1}{2}G^2 c_{33} - 2D'Gc_{13} - 2C^2 c_{66} - \tfrac{1}{2}A^2 c_{66} + \\ &+ 2ACc_{66}\cos 6\varphi \end{aligned} \tag{3.28}$$

so that E_{MS} added to the total magnetic energy, E_o (2.13), gives the total magneto - elastic energy density.

4. THE FREE ENERGY

Before we continue examining (in chapters 5 and 6) the behaviour of a system characterized by the Hamiltonian (1.9) in a more accurate and straightforward manner by using a model of elementary excitations, we shall in this chapter examine more closely the behaviour of the free energy of an equivalent system.

We do this to show an alternative way of deriving some of the results obtained in chapters 5 and 6. However, the real purpose is to obtain a basis for analysing the two models proposed for Tb and Dy, namely the "frozen lattice" model (introduced by Turov and Shavrov[26]) and the "flexible lattice" model. We shall show later (chapter 6) that the "flexible lattice" model proposed by Cooper[13] is not a well-defined model.

When the Hamiltonian is known, the free energy is expressed as

$$F = -\frac{1}{\beta} \ln Z = \langle \tilde{H} \rangle , \qquad \beta = 1/k_B T \tag{4.1}$$

where

$$Z = \mathrm{Tr}\, e^{-\beta \tilde{H}} . \tag{4.2}$$

Below we use the first and second derivatives of F with respect to different kinds of variables, and we have

$$\partial F/\partial x = \frac{1}{Z} \mathrm{Tr}\, [(\partial \tilde{H}/\partial x)\, e^{-\beta \tilde{H}}] = \langle \partial \tilde{H}/\partial x \rangle \tag{4.3}$$

and the second derivative

$$\partial^2 F/\partial x \partial y = \langle \partial^2 \tilde{H}/\partial x \partial y \rangle + \beta [\langle \partial \tilde{H}/\partial x \rangle \langle \partial \tilde{H}/\partial y \rangle - \langle (\partial \tilde{H}/\partial x)(\partial \tilde{H}/\partial y) \rangle] . \tag{4.4}$$

To avoid too many indices we simplify the Hamiltonian (1.9) so that only one strain variable is present. However, we generalize the interaction term $\tilde{H}_{S-L}$ (1.6) to take into account dynamic interactions between spin waves and elastic waves. The simplest way to make this generalization is to realize that the short-range character of the interaction between the spin system and the lattice for the crystal field terms (we shall not consider the exchange interaction term here) will imply that the interaction energy is proportional mainly to the local deformation of the lattice, i.e. proportional to the relative displacements of neighbouring ions. In the limit of small

wave vectors the relative displacements of neighbouring ions are identical with the local strains. The Hamiltonian to be considered is then

$$\tilde{H} = \frac{1}{2} \sum_j \frac{c}{N} (\hat{e} + e_j)^2 + \sum_j \tilde{B}_j(\theta, \varphi)(\hat{e} + e_j) + \tilde{H}_S(\theta, \varphi) . \qquad (4.5)$$

The first term corresponds to $\tilde{H}_L$ (1.5) when only acoustic phonons with small wave vectors are excited (which is the case when the temperature is much lower than the Debye temperature θ_D). $\tilde{H}_S(\theta, \varphi)$ is the Hamiltonian for the spin system and is a function of the direction of the net magnetization (θ, φ) and implicit of the reduced magnetization σ. The second term symbolizes the interaction, $\tilde{H}_{S-L}$ (1.6), between the lattice and the spin system. $\hat{e}$ is the homogeneous strain, and e_j is the deviation of the local strain from the homogeneous strain. The homogeneous strain, $\hat{e}$, is an essentially classical quantity, which results from the vanishing of the natural vibrational frequency (corresponding to $\omega_q \to 0$ when $q \to 0$ in (1.5)), and the term involving the momentum $p_{\hat{e}}$, conjugate to the strain $\hat{e}$, does not appear in the Hamiltonian. e_j can be expanded in normal phonon co-ordinates (which we shall do in the next chapter), however, e_j is off-diagonal in phonon operators so that

$$\langle e_j \rangle_o = 0 \quad \text{and} \quad \langle \sum_j e_j \rangle = 0. \qquad (4.6)$$

The second term in (4.5) is treated as a perturbation of the Hamiltonian $\tilde{H}_o$, defined as (4.5), setting $\tilde{B}_j = 0$. The use of $\tilde{H}_o$ instead of $\tilde{H}$ in the expression for Z (4.2) is indicated by the index o.

The parameters θ, φ, and $\hat{e}$ are evaluated by minimizing the free energy:

$$(\partial F/\partial \hat{e})_{\theta,\varphi} = \sum_j (\partial F/\partial e_j)_{\theta,\varphi} = \langle \sum_j [\frac{c}{N}(\hat{e} + e_j) + \tilde{B}_j(\theta, \varphi)] \rangle = 0, \qquad (4.7)$$

and defining γ to be equal to either θ or φ

$$(\partial F/\partial \gamma)_{\hat{e}} = \langle \partial \tilde{H}_S/\partial \gamma \rangle + \langle \sum_j (\partial \tilde{B}_j/\partial \gamma)(\hat{e} + e_j) \rangle = 0. \qquad (4.8)$$

with (4.6) equation (4.7) is immediately reduced to

$$c\hat{e} + \langle \sum_j \tilde{B}_j(\theta, \varphi) \rangle = 0. \qquad (4.9)$$

This equilibrium condition is identical with (3.18) and causes magnetostriction.

In the next chapter we shall investigate more carefully the influence of the interaction term, $\sum_j \tilde{B}_j(\theta,\varphi)e_j$; however, here we need the result that the spin system and the lattice are so weakly dynamically coupled that the magnon and the phonon excitations are still eigen-excitations of the Hamiltonian to the first order in $\tilde{B}_j$, (in the neighbourhood of points (in the q-space), where the corresponding dispersion curves cross each other this is not the case), furthermore the amplitude of the interaction is going to zero when q is going to zero. To a very good approximation we can replace $\tilde{H}$ by $\tilde{H}_o$ in (4.2), (especially at low temperatures).

Using this approximation, we have instead of (4.8)

$$\langle \partial \tilde{H}_S/\partial\gamma \rangle + \hat{e}\ \langle \sum_j \partial \tilde{B}_j/\partial\gamma \rangle = 0, \tag{4.10}$$

and the relation

$$(\partial F/\partial e_j)_{\theta,\varphi} = \langle \frac{c}{N} e_j + \tilde{B}_j \rangle - \frac{1}{N} \langle \sum_i \tilde{B}_i \rangle = 0 \tag{4.11}$$

is an identity.

On account of the weak dynamical coupling the new elastic constant is calculated as

$$c' = (\partial^2 F/\partial e^2)_{\theta,\varphi}\ , \tag{4.12}$$

and the derivatives to be used in the macroscopic formula (2.21) for the uniform spin excitation mode are

$$F_{\gamma\gamma} = (\partial^2 F/\partial\gamma^2)_{\hat{e}} = \tag{4.13}$$
$$\langle \partial^2 \tilde{H}_S/\partial\gamma^2 \rangle + \hat{e} \langle \sum_j \partial^2 \tilde{B}_j/\partial\gamma^2 \rangle - \beta [\langle (\partial \tilde{H}_S/\partial\gamma + \hat{e} \sum_j \partial \tilde{B}_j/\partial\gamma)^2 \rangle]\ ,$$

and for c' we find

$$c' = \langle \partial^2 \tilde{H}/\partial e^2 \rangle + \beta [\langle \partial \tilde{H}/\partial e \rangle^2 - \langle (\partial \tilde{H}/\partial e)^2 \rangle] = c - \beta \langle (\partial \tilde{H}/\partial e)^2 \rangle \tag{4.14}$$

or

$$c' - c = -\beta [\langle \sum_{ij} \tilde{B}_i \tilde{B}_j \rangle - \langle \sum_j \tilde{B}_j \rangle^2 + (c^2/N^2) \langle \sum_{ij} e_i e_j \rangle + (2c/N) \langle \sum_{ij} \tilde{B}_i e_j \rangle]. \tag{4.15}$$

This is in itself a second-order effect so we cannot use the above approximation.

Finally we shall write down the Hamiltonian after introducing explicitly the equilibrium condition (4. 9) into the Hamiltonian (4. 5)

$$\tilde{H} = \tilde{H}_o + \tilde{H}_m + \tilde{H}_{mp} + \tilde{H}_p \tag{4.16}$$

$\tilde{H}_o$ is the equilibrium magneto - elastic energy

$$\tilde{H}_o = -\frac{1}{2c}\langle\sum_j \tilde{B}_j\rangle^2 + \langle\tilde{H}_S\rangle \tag{4.17}$$

$\tilde{H}_m$ is the part determining the magnon excitation spectrum

$$\tilde{H}_m = \tilde{H}_S - \langle\tilde{H}_S\rangle - \frac{1}{c}\sum_j\langle\sum_i \tilde{B}_i\rangle\tilde{B}_j + \frac{1}{c}\langle\sum_j \tilde{B}_j\rangle^2 \tag{4.18}$$

and $\tilde{H}_p$ is the corresponding phonon part

$$\tilde{H}_p = \frac{1}{2}\sum_j \frac{c}{N} e_j^2 \tag{4.19}$$

$\tilde{H}_{mp}$ is the magnon - phonon interaction term

$$\tilde{H}_{mp} = \sum_j \tilde{B}_j e_j - \frac{1}{N}\sum_j\langle\sum_i \tilde{B}_i\rangle e_j \tag{4.20}$$

which causes a renormalization of the magnon and the phonon energies and contributes to the lifetime of the excitations. Furthermore the magnon - phonon interaction causes a mixing of the modes and energy gaps at some crossing points of the unperturbed dispersion curves. This is the subject of the next chapter.

5. DYNAMIC MAGNETO - ELASTIC INTERACTIONS

5.1. The Hamiltonian for Magnon - Phonon Interactions

As described in chapter 4 the Hamiltonian, $\tilde{H}_{S-L}$ (1. 6), is generalized to take into account dynamic interactions between spin waves and elastic waves, by replacing the strain $e_{\alpha\beta}$ by a sum of the homogeneous strain, $\hat{e}_{\alpha\beta}$, and the deviation of the local lattice deformation, $\tilde{e}_{\alpha\beta}(R_j)$, from the homogeneous strain. The effective dynamical interaction term then takes the form of (4. 20) (the last term in (4. 20) just ensures that we are left with the pure magnon - phonon terms).

The spin operator expressions, $\tilde{B}_j$, are evaluated in magnon operators by means of the procedure showed in chapter 3 and Appendix A. The first step is to make the co-ordinate system transformation, (A. 3), and the Hamiltonian is divided into three parts

$$\tilde{H}_{S-L} = \tilde{H}^{(o)}_{S-L} + \tilde{H}^{(1)}_{S-L} + \tilde{H}^{(2)}_{S-L} , \tag{5.1}$$

where $\tilde{H}^{(o)}_{S-L}$ is the magnetostriction part treated in chapter 3, and

$$\begin{aligned}\tilde{H}^{(1)}_{S-L} = &- G_{22} \sum_j (0^1_2)_j [(\tilde{e}_1 - \tilde{e}_2)\sin 2\varphi - \tilde{e}_6 \cos 2\varphi]_j + \\ &+ G_{44} \sum_j (0^3_4)_j [(\tilde{e}_1 - \tilde{e}_2)\sin 4\varphi + \tilde{e}_6 \cos 4\varphi]_j - \\ &- G_{12} \sum_j \tfrac{1}{2}(0^{-1}_2)_j [\tilde{e}_5 \cos\varphi + \tilde{e}_4 \sin\varphi]_j ,\end{aligned} \tag{5.2}$$

and further

$$\begin{aligned}\tilde{H}^{(2)}_{S-L} = &- \sum_{ij\alpha} [(\partial \mathcal{J}_{ij}/\partial R_{i\alpha})\delta R_{i\alpha} + (\partial \mathcal{J}_{ij}/\partial R_{j\alpha})\delta R_{j\alpha}] J_i \cdot J_j \\ &+ \sum_j (\tfrac{1}{2} 0^2_2 - \tfrac{1}{6} 0^0_2)_j [G_{01}(\tilde{e}_1 + \tilde{e}_2) + G_{03}\tilde{e}_3]_j \\ &- G_{22} \sum_j \tfrac{1}{2}(0^0_2 + 0^2_2)_j [(\tilde{e}_1 - \tilde{e}_2)\cos 2\varphi + \tilde{e}_6 \sin 2\varphi]_j \\ &+ G_{44} \sum_j \tfrac{1}{8}(0^0_4 + 40^2_4 + 0^4_4)_j [(\tilde{e}_1 - \tilde{e}_2)\cos 4\varphi - \tilde{e}_6 \sin 4\varphi]_j \\ &- G_{12} \sum_j \tfrac{1}{2}(0^{-2}_2)_j [\tilde{e}_5 \sin\varphi - \tilde{e}_4 \cos\varphi]_j - \text{the average value of the} \\ &\text{same expression}\end{aligned} \tag{5.3}$$

The displacement of the ion i from its equilibrium position, δR_i, is expanded in normal phonon co-ordinates

$$\delta R^{\gamma}_{i\alpha} = \sum_{s,k} F^{\gamma,s}_{k,\alpha} \exp(i\, k \cdot R^{\gamma}_i) (\beta_{s,k} + \beta^{+}_{s,-k}) , \tag{5.4}$$

where

$$F^{\gamma,s}_{k,\alpha} = [\hbar/(2NM\omega_s(k))]^{1/2} f^{\gamma,s}_{k,\alpha} . \tag{5.5}$$

M is the mass of the ions, and $f^{\gamma,s}_{k,\alpha}$ is the α component of the phonon polarization vector. $\beta_{s,k}$ is the phonon annihilation operator, where s denotes one of the three acoustic or three optical branches. The index γ refers to the existence of the two (identical) sublattices that correspond to the two kinds of spin deviation operators, a_j and b_j (2.3). The expressions are written in such a way that the polarization vector is a unit vector, and the polarization vectors for different branches have to be orthogonal to each other.

$$\sum_{\alpha} (f^{1,s}_{k,\alpha})^* f^{1,s'}_{k,\alpha} + (f^{2,s}_{k,\alpha})^* f^{2,s'}_{k,\alpha} = 2\,\delta_{ss'} . \tag{5.6}$$

Owing to the identity of the two sublattices we have

$$|f^{1,s}_{k,\alpha}|^2 = |f^{2,s}_{k,\alpha}|^2 \tag{5.7}$$

or

$$f^{2,s}_{k,\alpha} = f^{1,s}_{k,\alpha} \cdot \exp(i\varphi^{\alpha}_{s,k}) , \quad \text{where} \quad \varphi^{\alpha}_{s,-k} = -\varphi^{\alpha}_{s,k} + 2p\pi. \tag{5.8}$$

The relative displacements of neighbouring ions from their equilibrium positions, $\tilde{e}_{\alpha\beta}(R_i)$, are quite well described by the local strains, $e_{\alpha\beta}(R_i)$

$$\tilde{e}_{\alpha\beta}(R_i) \cong e_{\alpha\beta}(R_i) = (1 - \tfrac{1}{2}\delta_{\alpha\beta}) \sum_{s,k} i(k_\alpha F^{\gamma,s}_{k,\beta} + k_\beta F^{\gamma,s}_{k,\alpha}) \exp(i\,k\cdot R^{\gamma}_i) \cdot \cdot (\beta_{s,k} + \beta^{+}_{s,-k}) . \tag{5.9}$$

This approximation is satisfactory except in the neighbourhood of the zone boundaries if the k-vector (in front of the expression) is interpreted as the one lying in the first Brillouin zone.

The magnon and phonon operators are now introduced into (5.2) and (5.3) and the lattice sums are evaluated by using

$$\sum_{i_\gamma}^{N/2} \exp[i(q - q') \cdot R_i^\gamma] = \frac{1}{2} N \delta_{qq'} . \tag{5.10}$$

One example will show how this works

$$G = [2JJ_1^2]^{-1/2} \sum_j \frac{1}{2}(0_2^{-1})_j(\tilde{e}_5)_j = \sum_i (a_i^+ + a_i)(\tilde{e}_5)_i + \sum_j (b_j^+ + b_j)(\tilde{e}_5)_j \tag{5.11}$$

according to (A. 6). Using (2. 3) and (5. 9), we have

$$G = i\sqrt{(2/N)} \quad \{ \sum_{iqks} [a_q^+ e^{-iqR_i} + a_q e^{iqR_i}][k_1 F_{k,3}^{1,s} + k_3 F_{k,1}^{1,s}](\beta_{s,k}^+ + \beta_{s,-k}^+) e^{ik} \tag{5.12}$$

$$+ \sum_{jqks} [b_q^+ e^{-iqR_j} + b_q e^{iqR_j}][k_1 F_{k,3}^{2,s} + k_3 F_{k,1}^{2,s}](\beta_{s,k}^+ + \beta_{s,-k}^+) e^{ikR_j} \} .$$

Defining

$$F_{k,\alpha}^s = \delta_{\alpha\gamma} F_{k,\gamma}^{1,s} \tag{5.13}$$

and using (5. 8) and (5. 10), we find

$$G = i\sqrt{(N/2)} \sum_{k,s,\gamma} (k_1 F_{k,3}^s + k_3 F_{k,1}^s)[a_k^+ + a_{-k} + (b_k^+ + b_{-k}) \exp(i\varphi_{s,k}^\gamma)] \cdot \tag{5.14}$$

$$\cdot (\beta_{s,k} + \beta_{s,-k}^+) .$$

Finally we have to introduce the magnon operators, and we use (2. 6), (2. 7), and (2. 11). This operation introduces, as does (5. 13), an uncertainty to the phase factor of the final expression, however, it is easily seen that this uncertainty has no physical effect.

To write down the final expression for the Hamiltonian, $\tilde{H}_{S-L}^{(1)}$, which gives rise to one-magnon one-phonon scattering processes, we have to define the following quantities:

$$K_{i,q} = [(A_i(q)+B)/(A_i(q)-B)]^{1/4} = [(A_i(q)+B)/\varepsilon_i(q)]^{1/2} \tag{5.15}$$

and

$$p^{j,\gamma}_{s,k} = \frac{1}{2}\left[1 - (-1)^j \exp(i\varphi^{\gamma}_{s,k} - i\theta_k)\right]. \tag{5.16}$$

Then, following the procedure shown above, we obtain

$$\tilde{H}^{(1)}_{S\text{-}L} = \sum_{k,sj}\left[W'_{s,j}(k)(a^{+}_{j,k} - a_{j,-k}) - iW''_{s,j}(k)(a^{+}_{j,k} + a_{j,-k})\right]\cdot(\beta_{s,k} + \beta^{+}_{s,-k}), \tag{5.17}$$

where in terms of the magnetostriction coefficients defined by (3.21) we have

$$W'_{s,j}(k) = \sum_{\gamma}(2NJ)^{1/2} K_{j,k}\, p^{j,\gamma}_{s,k}\left[(k_1 F^{s}_{k,1} - k_2 F^{s}_{k,2})(D_{22}\sin 2\varphi - 2D_{44}\sin 4\varphi)\right. \tag{5.18}$$

$$\left. - (k_1 F^{s}_{k,2} + k_2 F^{s}_{k,1})(D_{22}\cos 2\varphi + 2D_{44}\cos 4\varphi)\right]$$

and

$$W''_{s,j}(k) = \sum_{\gamma}(2NJ)^{-1/2} H_o c_{44} K^{-1}_{j,k}\, p^{j,\gamma}_{s,k}\left[(k_1 F^{s}_{k,3} + k_3 F^{s}_{k,1})\cos\varphi\right. + \tag{5.19}$$

$$\left. + (k_2 F^{s}_{k,3} + k_3 F^{s}_{k,2})\sin\varphi\right].$$

$\tilde{H}^{(1)}_{S\text{-}L}$ is a hermitean operator owing to the relation

$$W^{*}_{s,j}(k) = - W_{s,j}(-k). \tag{5.20}$$

Within a phase factor, $\tilde{H}^{(1)}_{S\text{-}L}$ is the one-magnon one-phonon interaction treated in Appendix B, and the results can be obtained from that Appendix by replacing $|V_q|$ in expressions (B.17) and (B.20) by the effective interaction amplitude

$$W_{s,j}(k) = \left[|W'_{s,j}(k)|^2 + |W''_{s,j}(k)|^2\right]^{1/2}, \tag{5.21}$$

which can be seen by making a suitable phase transformation of the magnon operators. Furthermore the assumption made in (B.19) is fulfilled in the limit of small wave vectors because

$$W_{s,j}(k) \sim k\,[\omega_s(k)]^{-1/2} \to 0 \qquad \text{when} \qquad k \to 0 \tag{5.22}$$

which is valid both for acoustic and optical phonons.

Using relations (2.5) and (5.8) we see that in the limit of small wave vectors

$$\theta_{k=0} = 0 \qquad \text{and} \qquad \varphi^{\gamma}_{a,\,k=0} = 0\,, \quad \varphi^{\gamma}_{o,\,k=0} = \pi, \tag{5.23}$$

where the subindices a and o denote acoustic and optical phonon modes respectively. There is nothing to prevent θ_o from being equal to π instead of zero, however, choosing $\theta_o = 0$ implies that the branch which has the lowest energy of the two magnon branches is labelled as the acoustic branch (corresponding to i = 1 in equation (2.10)). (5.23) together with (5.16) lead to the result that acoustic phonons with small wave vectors interact with acoustic magnons, and similarly optical phonons interact only with optical magnons in this limit.

The other part of the Hamiltonian, $\tilde{H}^{(2)}_{S-L}$ (5.3), which gives rise to two-magnon one-phonon scattering processes, can be written in terms of magnon and phonon operators following the scheme sketched above

$$\tilde{H}^{(2)}_{S-L} = \sum_{ij,\,s}\sum_{q,\,k} [(U^{s}_{ij}(k,q)\alpha^{+}_{i,\,q+k}\alpha_{j,\,q} + V^{s}_{ij}(k,q)\tfrac{1}{2}(\alpha^{+}_{i,\,q+k}\alpha^{+}_{j,\,-q} + \alpha_{i,\,-q-k}\alpha_{j,\,q})]\cdot [\beta_{s,\,k} + \beta^{+}_{s,\,-k}]\,. \tag{5.24}$$

The interaction amplitudes, U and V, are functions of great complexity, and to write these functions properly requires definition of several other functions.

$$g^{\gamma,\,s}_{ij}(k,q) = \tfrac{1}{2}\,\delta_{ij}\,[1 + \exp i(\varphi^{\gamma}_{s,\,k} + \theta_q - \theta_{q+k})\,] + \tfrac{1}{2}(1 - \delta_{ij})\,[1 - \exp i(\varphi^{\gamma}_{s,\,k} + \theta_q - \theta_{q+k})\,] \tag{5.25}$$

and

$$d^{\gamma,\,s}_{ij}(k,q) = \delta_{ij}\cos\tfrac{1}{2}(\varphi^{\gamma}_{s,\,k} + \theta_{q+k} - \theta_q - 2\theta_k)/\cos\tfrac{1}{2}(\theta_{q+k} - \theta_q - \varphi^{\gamma}_{s,\,k}) + (1 - \delta_{ij})\sin\tfrac{1}{2}(\varphi^{\gamma}_{s,\,k} + \theta_{q+k} - \theta_q - 2\theta_k)/\sin\tfrac{1}{2}(\theta_{q+k} - \theta_q - \varphi^{\gamma}_{s,\,k}) \tag{5.26}$$

and the exchange part

$$Q_{ij}^{\gamma,s}(k,q) = -2J\,\bar{F}_k^s \cdot [\,\bar{k}(\gamma_k + d_{ij}^{\gamma,s}(k,q)\,|\gamma_k'|) + \bar{q}(\gamma_q - (-1)^j|\gamma_q'|) - \\ - (\bar{q}+\bar{k})\,(\gamma_{q+k} - (-1)^i|\gamma_{q+k}'|)\,] \tag{5.27}$$

and the crystal field part

$$\mathcal{A}_{s,k} = k_3F_{k,3}^s\,D_{03} + (k_1F_{k,1}^s + k_2F_{k,2}^s)\,D_{01} \\ + (k_1F_{k,1}^s - k_2F_{k,2}^s)\,(3D_{22}\cos 2\varphi - 10D_{44}\cos 4\varphi) \\ + (k_1F_{k,2}^s + k_2F_{k,1}^s)\,(3D_{22}\sin 2\varphi + 10D_{44}\sin 4\varphi) \tag{5.28}$$

$$\mathcal{B}_{s,k} = k_3F_{k,3}^s\,D_{03} + (k_1F_{k,1}^s + k_2F_{k,2}^s)\,D_{01} \\ + (k_1F_{k,1}^s - k_2F_{k,2}^s)\,(-D_{22}\cos 2\varphi + 6D_{44}\cos 4\varphi) \\ + (k_1F_{k,2}^s + k_2F_{k,1}^s)\,(-D_{22}\sin 2\varphi - 6D_{44}\sin 4\varphi) \tag{5.29}$$

$$\mathcal{C}_{s,k} = [\,(k_3F_{k,1}^s + k_1F_{k,3}^s)\sin\varphi - (k_2F_{k,3}^s + k_3F_{k,2}^s)\cos\varphi\,]H_0c_{44}/NJ. \tag{5.30}$$

Using (5.13) and (5.15) and defining

$$\mathcal{A}_{ij}^{\gamma,s}(k,q) = Q_{ij}^{\gamma,s}(k,q) + \mathcal{A}_{s,k}, \tag{5.31}$$

we have

$$U_{ij}^s(k,q) = \frac{i'}{2}\sum_{\gamma} g_{ij}^{\gamma,s}(k,q)\,[(K_{i,\,q+k}K_{j,\,q} + 1/K_{i,\,q+k}K_{j,\,q})\mathcal{A}_{ij}^{\gamma,s}(k,q) \\ - (K_{i,\,q+k}K_{j,\,q} - 1/K_{i,\,q+k}K_{j,\,q})\mathcal{B}_{s,k} \\ + i'(K_{i,\,q+k}/K_{j,\,q} - K_{j,\,q}/K_{i,\,q+k})\mathcal{C}_{s,k}\,] \tag{5.32}$$

where $i' = \sqrt{(-1)}$,

$$v_{ij}^{s}(k,q) = \frac{i'}{2}\sum_{\gamma} g_{ij}^{\gamma,s}(k,q)\,[(K_{i,q+k}K_{j,q} + 1/K_{i,q+k}K_{j,q})\mathcal{B}_{s,k}$$

$$- (K_{i,q+k}K_{j,q} - 1/K_{i,q+k}K_{j,q})\mathcal{A}_{ij}^{\gamma,s}(k,q) \qquad (5.33)$$

$$+ i'(K_{i,q+k}/K_{j,q} + K_{j,q}/K_{i,q+k})\mathcal{C}_{s,k}\,].$$

Strictly speaking the Hamiltonian (5.24) is not a hermitean operator when $\mathcal{C}_{s,k}$ is different from zero ((C.25) is only valid when $\mathcal{C}_{s,k} = 0$). However, if we write down the correct expression for the Hamiltonian (which is hermitean), we obtain results which are identical with the results obtained in Appendix C, (C.27) and (C.28), using (5.32) and (5.33) as the effective interaction amplitudes. The phase factor, i, in front of the $\mathcal{C}_{s,k}$-term indicates that this interaction term is othogonal to the other terms (just as in the case of $\tilde{H}_{S-L}^{(1)}$, see equation (5.21)).

5.2. Acoustic Velocities

The Hamiltonian, $\tilde{H}_{S-L}$ (5.17) and (5.24), will not change the acoustic phonon energy at zero wave vector (the energy remains zero), but the phase velocities, $\omega_s(k)/k$, which are equal to the slope of the corresponding energy dispersion curves (the group velocities), will change according to the results obtained in the preceding section and Appendices B and C. Using (B.20) and (C.35) in addition to the interaction amplitudes deduced in section 5.1, we can write the resulting changes in velocities due to the linear magneto - elastic coupling, $\tilde{H}_{S-L}$, as[24]

$$\Delta v_a/v_a = (\Delta v_a/v_a)_1 + (\Delta v_a/v_a)_2\,, \qquad (5.34)$$

where the first term arises from the one-magnon one-phonon interaction, $\tilde{H}_{S-L}^{(1)}$,

$$(\Delta v_a/v_a)_1 = -2\Gamma_a^2\, NJ/[c_{aa}(A_1(0) - B)], \qquad (5.35)$$

and the term arising from the two-magnon one-phonon interaction, $\tilde{H}_{S-L}^{(2)}$, is

$$(\Delta v_a/v_a)_2 = 1/2c_{aa}\sum_{q,i}[\varepsilon_i(q)]^{-2}[[\mathcal{A}_{i,a}(q)A_i(q) - \mathcal{B}_a B]^2\,\partial n_i(q)/\partial\varepsilon_i(q) -$$

$$- [\mathcal{A}_{i,a}(q)B - \mathcal{B}_a A_i(q)]^2 n_i(q)/\varepsilon_i(q)\,]. \qquad (5.36)$$

For proporgation in high symmetry directions, the parameters of equations (5.35) and (5.36) have the following values:

(I) Longitudinal sound waves in symmetry directions (a = 1, 2, and 3 here represents the direction of the k-vector):

$$\mathcal{A}_{i,a}(q) = -2J(\gamma_0 + \gamma'_0 - \gamma_q + (-1)^i|\gamma'_q|) + \mathcal{A}_a \tag{5.37}$$

where

$$\mathcal{A}_1 = D_{01} + 3D_{22}\cos 2\varphi - 10D_{44}\cos 4\varphi$$
$$\mathcal{B}_1 = D_{01} - D_{22}\cos 2\varphi + 6D_{44}\cos 4\varphi \tag{5.38}$$

$$\mathcal{A}_2 = D_{01} - 3D_{22}\cos 2\varphi + 10D_{44}\cos 4\varphi$$
$$\mathcal{B}_2 = D_{01} + D_{22}\cos 2\varphi - 6D_{44}\cos 4\varphi \tag{5.39}$$

$$\mathcal{A}_3 = D_{03} \quad \text{and} \quad \mathcal{B}_3 = D_{03} \tag{5.40}$$

$$\Gamma_1 = \Gamma_2 = D_{22}\sin 2\varphi - 2D_{44}\sin 4\varphi, \quad \text{and} \quad \Gamma_3 = 0. \tag{5.41}$$

(II) Transverse sound waves in the basal plane (either in a 1- or 2-direction) with the polarization vector in the basal plane (a = 6):

$$\mathcal{A}_{i,6}(q) = \mathcal{A}_6 = 3D_{22}\sin 2\varphi + 10D_{44}\sin 4\varphi$$
$$\mathcal{B}_6 = -D_{22}\sin 2\varphi - 6D_{44}\sin 4\varphi \tag{5.42}$$

and

$$\Gamma_6 = D_{22}\cos 2\varphi + 2D_{44}\cos 4\varphi. \tag{5.43}$$

(III) Transverse sound waves in the c-direction (φ can here be considered as the angle between the polarization vector and the z-axis). This velocity (and change in velocity) is equal to the velocity (change) of the transverse sound waves in the basal plane with the polarization vector parallel to the c-axis:

$$(\Delta v_5/v_5)_1 = -H_0^2 c_{44}\cos^2\varphi / [2NJ(A_1(0) + B)] \tag{5.44}$$

and

$$(\Delta v_5/v_5)_2 = - H_o^2 c_{44} \sin^2\varphi / [\, 2N^2 J^2 \,] \sum_{q,i} n_i(q)/\varepsilon_i(q) \,. \qquad (5.45)$$

An external magnetic field will, besides a possible change of the angle φ, (2.16), modify the strength of the magneto - elastic interaction. This is mainly due to the H-dependence of $\varepsilon_i(q)$ (see equation (2.10)) which implies

$$\partial(\Delta v/v)/\partial H = g\mu_B \sum_{q,i} d(\Delta v/v)/dA_i(q) \qquad (5.46)$$

so that

$$\alpha_\parallel = [\partial(\Delta v_5/v_5)/\partial H]_{\varphi=0} = H_o^2 c_{44} g\mu_B / [\, 2NJ(A_1(0) + B)^2 \,] \qquad (5.47)$$

and

$$\alpha_\perp = [\partial(\Delta v_5/v_5)/\partial H]_{\varphi=\pi/2} = S \cdot H_o^2 c_{44} g\mu_B / [\, 2NJ^2 \,] = \qquad (5.48)$$

$$\frac{H_o^2 c_{44} g\mu_B}{2N^2 J^2} \sum_{q,i} \frac{A_i(q) n_i(q)}{\varepsilon_i(q)^2} \left[\frac{n_i(q)+1}{k_B T} + \frac{1}{\varepsilon_i(q)} \right].$$

The expression used by Moran and Lüthi[27] in the analysis of their experimental results for $\alpha_\parallel$ and $\alpha_\perp$ is almost identical with expression (5.47) for $\alpha_\parallel$, except that $A_1(0) + B$ has been replaced by $\varepsilon_1(0)$. This expression used by Moran and Lüthi originates from a calculation made by Schlömann[28] who used a more phenomenological Hamiltonian than the one we have considered.

These expressions for the relative change in the velocity of sound waves can be compared with expression (4.15) in chapter 4 for the change of the elastic constants derived from the free energy by means of

$$\Delta c/c = 2\,\Delta v/v. \qquad (5.49)$$

When considering the $\tilde{H}^{(1)}_{S-L}$ part of the Hamiltonian, we do not have contributions from the last two terms in (4.15), and it is easily seen that we obtain the same expressions for $(\Delta v/v)_1$ as above if we replace β in (4.15) by $1/\varepsilon_1(0) n_1(0)$, which is correct when $k_B T \rangle\rangle \varepsilon_1(0)$. The derivation of $(\Delta v/v)_2$ from (4.15) is more difficult because of contributions from the last two terms, however, the two terms in front of expression (4.15) do give

changes of the velocities, which is consistent with $(\Delta v/v)_2$ derived in this section.

The simplest way to obtain the temperature dependence of the velocity changes is to generalize the results obtained in the spin wave theory, i. e. J is everywhere replaced by σJ (see (2. 28) and chapter 6). The magnetostriction coefficients have a temperature dependence given by (3. 27), and the temperature dependence of $A_i(q)$ and B is taken from the spin wave theory. For instance we have

$$(\Delta v_5/v_5)_1 \sim (\sigma^3)^2/(\sigma.\sigma^2) = \sigma^3 \tag{5. 50}$$

if we approximate the temperature dependence of $A_1(0) + B$ to σ^2. At sufficiently high temperatures we can use the following approximation for the occupation number of the magnons

$$n_i(q) \approx k_B T/\varepsilon_i(q) . \tag{5. 51}$$

The behaviour of the elastic constants of the heavy rare earths has been investigated experimentally by a number of authors. The elastic properties of polycrystalline rare-earth metals have been measured by Rosen[29]. Furthermore the temperature dependence of the elastic constants of single crystals has been investigated rather carefully[16, 23, 27, 30-33]. However, it is difficult to isolate the magneto - elastic contributions to the temperature dependence without knowing the third-order elastic constants. The lattice distortions which occur owing to the magnetic ordering below T_N, give rise to changes in the elastic constants which are equal to the third-order elastic constants multiplied by the magnetostrictive strains. These anharmonic effects are of the same order of magnitude as the contributions from the magneto - elastic interactions[33]. However, by means of a magnetic field it is possible to distinguish between these two kinds of contributions, because the magnetostriction is almost independent of an applied field if we do not change the direction of the magnetization (the so-called forced magnetostriction is quite small[9]), so that the major contribution to $\partial v/\partial H$ arises from the magneto - elastic interaction corresponding to formulas (5. 47) and (5. 48).

Palmer and Lee[33] have measured the elastic constants of Dy and Ho as functions of temperature in a zero field and in a field of 25 kOe along the magnetically easy direction, in order to eliminate spurious contributions to the elastic constants from domain re-orientation effects (ΔE-effect). The

differences between the two cases should, however, probably be interpreted as being due to domain effects rather than to domain re-orientation effects. Below T_C we have a distribution of domains in the Dy-crystal which have different angles between the 1-direction and the direction of magnetization (corresponding to $\varphi = p\pi/3$) in a zero field, whereas when applying a saturating magnetic field along the easy direction, we are left with only one domain ($\varphi = 0$). The application of a field has no effect on c_{33} in Dy below T_C in agreement with the result that c_{33} is independent of φ, whereas c_{11} and c_{66} are modifield rather much. In the case of an applied field the change of c_{11} is given by $(\Delta v_1/v_1)_2$, (5.36). In a zero field $(\Delta v_1/v_1)_1$ will contribute considerably in domains where $\varphi = \pm \pi/3$ and $\pm 2\pi/3$ due to $A_1(0) - B$ in the denominator of equation (5.35), which is in accordance with the experimental result that $(\Delta c_{11})_{H=0}$ is much greater than $(\Delta c_{11})_{H=25\ kOe}$.

The only measurements of $\partial v/\partial H$ that exist have been performed by Moran and Lüthi[27] who have measured $a_{\parallel}$, $a_{\perp}$ and $\Delta = (\Delta v_5/v_5)_{\varphi=\pi/2} - (\Delta v_5/v_5)_{\varphi=0}$ in Tb at $T = 140^oK$ and in Dy at $T = 78^oK$. For Tb they obtained

$$\Delta = 3.0 \cdot 10^{-3}, \quad a_{\parallel} = 3.6 \cdot 10^{-5}\ 1/kOe, \quad \text{and} \quad a_{\perp} = 7.2 \cdot 10^{-5}\ 1/kOe,$$

and for Dy

$$\Delta = -2.9 \cdot 10^{-3}, \quad a_{\parallel} = 2.4 \cdot 10^{-5}\ 1/kOe, \quad \text{and} \quad a_{\perp} = 1.3 \cdot 10^{-5}\ 1/kOe.$$

From these experimental values we deduce:

For Tb, where we have used $A_1(0) + B = 4.9$ meV and $\sigma = 0.83$ at $T = 140^oK$

$$H_o = 1.5 \cdot 10^{-2}$$

in fair agreement with the value deduced from magnetostriction measurements[11] $H_o = 2.3 \cdot 10^{-2}$ at $T = 140^oK$. Further we obtain

$$\frac{1}{N}\sum_{q,i} n_i(q)/\varepsilon_i(q) = 0.86\ 1/meV \quad \text{and} \quad S = 0.41\ 1/meV^2.$$

Using the approximation (5.51) and $A_i(q) \approx \varepsilon_i(q)$, we find

$$\frac{1}{N}\sum_{q,i} 1/\varepsilon_i(q)^2 \approx 1/[3.7\ meV]^2 \quad \text{and} \quad \frac{1}{N}\sum_{q,i} 1/\varepsilon_i(q)^3 \approx 1\ [4.3\ meV]^3.$$

The spin wave parameters of Dy are not so well determined as in Tb, but using $A_1(0) + B = 3.6$ meV when $\sigma = 0.9$, we find

$$H_o = 1.0 \cdot 10^{-2}$$

and from the magnetostriction measurements[10]: $H_o = 0.83 \cdot 10^{-2}$ at $T = 78^oK$.

$$\frac{1}{N} \sum_{q,i} n_i(q)/\varepsilon_i(q) = 2.3\ 1/\text{meV} \qquad \text{and} \quad S = 0.28\ 1/\text{meV}^2$$

and as above

$$\frac{1}{N} \sum_{q,i} 1/\varepsilon_i(q)^2 \approx 1/[1.7\ \text{meV}]^2 \quad \text{and} \quad \frac{1}{N} \sum_{q,i} 1/\varepsilon_i(q)^3 \approx 1/[4.2\ \text{meV}]^3.$$

The values of the energy sums are reasonable when compared with the experimentally determined dispersion relations for the spin waves[34-36]. The sum of $1/\varepsilon_i(q)^2$ is the most uncertain, because the evaluation of this sum involves the value of Δ (which can be modified by anharmonic effects). However, the sums of $1/\varepsilon_i(q)^3$ display the great similarity between Tb and Dy.

5.3. Magnon - Phonon Interactions

The interaction amplitudes (5.18) and (5.19) derived in section 5.1 in the case of one-magnon one-phonon processes are completely correct only for small wave vectors. When considering $H^{(1)}_{S-L}$ at finite wave vectors, we shall use the relative displacements of neighbouring ions instead of the local strains (5.9). Following Evenson and Liu[15] we construct functions which are isomorphic to the strain tensors

$$\delta_{\alpha\beta}(i,j) = \frac{1}{2}[(R_{i\alpha} - R_{j\alpha})(\delta R_{i\beta} - \delta R_{j\beta}) + (R_{i\beta} - R_{j\beta})(\delta R_{i\alpha} - \delta R_{j\alpha})]. \qquad (5.52)$$

The relative displacements of neighbouring ions can then be constructed out of these functions as follows:

$$\tilde{e}_{\alpha\beta}(R_i) = \frac{1}{n} \sum_{\tau} \delta_{\alpha\beta}(i, i+\tau)\,, \qquad (5.53)$$

where τ denotes one of the twelve nearest neighbours of i, and n is a factor which provides that

$$\tilde{e}_{\alpha\beta}(R_i) = e_{\alpha\beta}(R_i) \tag{5.54}$$

in the limit of small wave vectors. Using this procedure and defining

$$q^{j,\gamma}_{s,k} = \frac{1}{2}\left[\exp(i\varphi^{\gamma}_{s,k}) - (-1)^j \exp(-i\theta_k)\right] \tag{5.55}$$

$$r^{j,\gamma}_{s,k} = \frac{1}{2}\left[\exp(i\varphi^{\gamma}_{s,k}) + (-1)^j \exp(-i\theta_k)\right] \tag{5.56}$$

we obtain in the case where the k-vector is parallel with an a-axis:

$$\begin{aligned}\tilde{W}'_{s,j}(k) = \sum_{\gamma} (2NJ)^{1/2} K_{j,k} \{ & \frac{1}{2a}\left[p^{j,\gamma}_{s,k}(\sin(ka)+\sin(ka/2)) + q^{j,\gamma}_{s,k}\sin(ka/2)\right] \cdot \\ & \cdot \left[F^{s}_{k,1}(D_{22}\sin 2\varphi - 2D_{44}\sin 4\varphi) - F^{s}_{k,2}(D_{22}\cos 2\varphi + 2D_{44}\cos 4\varphi)\right] \\ & + \frac{i}{2b} r^{j,\gamma}_{s,k}(1-\cos(ka/2))\left[F^{s}_{k,2}(D_{22}\sin 2\varphi - 2D_{44}\sin 4\varphi)\right. \\ & \left. + F^{s}_{k,1}(D_{22}\cos 2\varphi + 2D_{44}\cos 4\varphi)\right]\}\end{aligned} \tag{5.57}$$

and instead of (5.19)

$$\begin{aligned}\tilde{W}''_{s,j}(k) = (2NJ)^{-1/2} H_o c_{44} K^{-1}_{j,k} F^{s}_{k,3} \{ & \frac{1}{2a}\left[p^{j,3}_{s,k}(\sin(ka)+\sin(ka/2)) \right. \\ & \left. + q^{j,3}_{s,k}\sin(ka/2)\right]\cos\varphi - \frac{i}{2b} r^{j,3}_{s,k}(1-\cos(ka/2))\sin\varphi\}\end{aligned} \tag{5.58}$$

where a and b are the lattice parameters. These expressions are similar to (5.18) and (5.19) except for the terms proportional to (1 - cos(ka/2)) which disappear when k goes to zero. However, this term implies that the interaction amplitudes are different from zero at the point M on the Brillouin zone boundary ($k = 2\pi/a$).

As shown in Appendix B the one-magnon one-phonon interaction, $\tilde{H}^{(1)}_{S-L'}$ gives rise to energy gaps in the magnon and phonon energy spectrum at the nominal crossing points of the magnon and phonon dispersion relations which are

$$\Delta = 2\,|\tilde{W}(k)|\ , \tag{5.59}$$

and the excitations have neither pure phonon nor pure magnon character.

This mixing between the magnons and the phonons whenever $|\epsilon(k) - \hbar\omega_s(k)|$ is of the same order of magnitude as $|\tilde{W}(k)|$ implies that the neutron cross sections of the two kinds of modes are comparable.

In the hcp-lattice we have a mirror plane perpendicular to the a-axis which implies that in the a-direction

$$\theta_k = 0 \quad \text{and} \quad \varphi^{\gamma}_{s,k} = 0 \quad \text{or} \quad \pi \ , \quad \text{for all k-vectors.} \tag{5.60}$$

The eigenvectors of phonons in symmetry directions for Tb have been calculated by Gylden Houmann and Nicklow[37]. The different phonon modes are labelled in accordance with the character of the modes at small wave vectors, and when k is parallel with an a-axis, we have: The $TA_\perp$ and $TO_\perp$ modes are purely acoustic and optical transverse modes respectively with the polarization vector parallel with the c-axis. In the a-direction there is a strong mixing of the LA and $TO_\parallel$ modes around K ($k = 4\pi/3a$); this mixing goes to zero when k goes to either zero or $2\pi/a$. In the same way the LO and $TA_\parallel$ modes are mixed strongly around K, but at $k = 2\pi/a$ the LO mode attained a pure $TA_\parallel$-eigenvector and vice versa.

In fig. 2 we show the magnon dispersion curves for Tb[3, 35] at 4.2°K and in fig. 3 the phonon dispersion relations for Tb[37] at room temperature. In the a-direction we have a strong mixing of phonons and acoustic magnons around $k = 0.6\ \text{Å}^{-1}$ (fig. 2). Comparison with the phonon dispersion curves shows that the LA mode is quite close to the magnon dispersion curves and probably crosses it at $k = 0.5\ \text{Å}^{-1}$. With (5.57) and (5.59) the energy gap should be

$$\Delta_{LA,1} = 2\hbar\left[\frac{J}{M(A_1(k) - B)}\right]^{1/2} \left|\left[f_{k,1}\frac{1}{2a}\left[\sin(ka) + 2\sin(ka/2)\right]\right.\right. \\ \left.\left. + i\, f_{k,2}\,\frac{1}{2b}\,\left[1 - \cos(ka/2)\right]\right] \cdot \left[D_{22}\sin 2\varphi - 2D_{44}\sin 4\varphi\right]\right| \ , \tag{5.61}$$

and using $f_{k,1} \approx 1$, we obtain

$$\Delta_{LA,1} \cong 2\hbar\left[\frac{J}{M(A_1(k) - B)}\right]^{1/2} \frac{1}{2a}\left[\sin(ka) + 2\sin(ka/2)\right] \cdot \\ \left|D_{22}\sin 2\varphi - 2D_{44}\sin 4\varphi\right| \ . \tag{5.62}$$

Owing to the multi-domain character of a ferromagnetic crystal in the absence of a magnetic field, three neutron groups of equal magnitude should be observed at the crossing point in a constant $\vec{q}$-scan. One neutron group arises from domains in which $\varphi = \pm \pi/2$ (where the magnetization is perpendicular to the wave vector, the a-direction we are considering corresponds to $\varphi = 0$); and two groups show energy splitting in the domains where $\varphi = \pm \pi/6$ and $\pm 5\pi/6$. The neutron data may in fact be satisfactorily interpreted in this manner, and we obtain an energy gap equal to 0.7 meV, which agrees with the value of 0.57 meV obtained from (5.62) with the parameters determined by neutron diffraction[35]. This interaction should disappear when we apply a saturating magnetic field in the b-direction perpendicular to the a-direction we are considering, and so should the interaction between the neighbouring TO_g-phonons and the acoustic magnons, whereas a weak interaction between the magnons and the LO mode lying just above the magnon dispersion curve will remain.

In the case where the k-vector is parallel with a b-axis (2- axis), we find

$$\tilde{W}'_{s,j}(k) = \sum_{\gamma} (2NJ)^{1/2} K_{j,k} \frac{1}{b} \left[\frac{3}{2} p^{j,\gamma}_{s,k} \sin(kb/2) + s^{j,\gamma}_{s,k} \sin(kb/4) \right] \cdot \left[-F^{s}_{k,2}(D_{22}\sin 2\varphi - 2D_{44}\sin 4\varphi) - F^{s}_{k,1}(D_{22}\cos 2\varphi + 2D_{44}\cos 4\varphi) \right] \tag{5.63}$$

where

$$s^{j,\gamma}_{s,k} = \frac{1}{2} \left[\exp(ik\varphi^{\gamma}_{s,k} + ikb/12) - (-1)^{j} \exp(-i\theta_{k} - ikb/12) \right] \tag{5.64}$$

and further

$$\tilde{W}''_{s,j}(k) = \sum_{\gamma} (2NJ)^{-1/2} H_{o} c_{44} K^{-1}_{j,k} \frac{1}{b} \left[\frac{3}{2} F^{j,\gamma}_{s,k} \sin(kb/2) + s^{j,\gamma}_{s,k} \sin(kb/4) \right] F^{s}_{k,3} \sin\varphi . \tag{5.65}$$

We do not have a mirror plane perpendicular to the b-direction, so generally θ_k and $\varphi^{\gamma}_{s,k}$ are different from zero. However, the eigenvectors of the phonons[37] are either parallel or perpendicular to the wave vector, so that the modes are purely longitudinal or transverse modes, but neither purely acoustic nor optic. At $k = 2\pi/b$, that is at the point M in the reciprocal lattice,

$$\theta_k = \varphi^{\gamma}_{sa,k} = \varphi^{\gamma}_{so,k} - \pi = -\pi/3 , \tag{5.66}$$

where sa and so denote "acoustic" and "optical" modes respectively. The phase angles are quite close to being linear functions of k, that is

$$\theta_k \cong \varphi^{\gamma}_{sa,k} = \varphi^{\gamma}_{so,k} - \pi \cong -kb/12 . \tag{5.67}$$

With this approximation (5.63) and (5.65) are reduced owing to the following relations

$$p^{j,\gamma}_{sa,k} \cong s^{j,\gamma}_{sa,k} \cong \tfrac{1}{2}(1 - (-1)^j) = \delta_{1j} \tag{5.68}$$

and

$$p^{j,\gamma}_{so,k} \cong -s^{j,\gamma}_{so,k} \cong \tfrac{1}{2}(1 + (-1)^j) = \delta_{2j} . \tag{5.69}$$

As in the a-direction we have interaction between the LA phonon mode and the acoustic magnons with the crossing point lying at $k = 0.4\ \text{Å}^{-1}$ (fig. 2). Using the approximation above, we obtain an energy gap at the crossing point which is

$$\Delta_{LA,1} = 2h\,[\frac{J}{M(A_1(k) - B)}]^{1/2}\,\frac{1}{b}\,[\frac{3}{2}\sin(kb/2) + \sin(kb/4)] \cdot$$

$$\cdot\,|D_{22}\sin 2\varphi - 2D_{44}\sin 4\varphi| \tag{5.70}$$

or $\Delta_{LA,1} = 0.53$ meV in the domains where $\varphi = \pm\pi/6$ and $\pm 5\pi/6$, in agreement with the experimental result ($\Delta_{Exp} \cong 0.4$ meV).

The LA-mode seems to have a neutron cross section which is comparable with the cross section of the magnons all the way out to the Brillouin zone boundary (M). In the neighbourhood of M it is probably a mixing of the LA, $TO_{\parallel}$, and $TO_{\perp}$ modes which is seen. $TO_{\parallel}$ and $TO_{\perp}$ have a magnetic cross section, too, due to interactions with the optical magnons. That the interactions are finite at the zone boundary is in agreement with the expressions above. The point M in the reciprocal lattice is lying at $k = 2\pi/b$ in the b-direction or at $k = 2\pi/a$ in the a-direction. The one-magnon one-phonon interaction does not destroy the symmetry at this point, because the magnon - phonon interactions at $k = 2\pi/a$ and k parallel with an a-axis are identical with the interactions at $k = 2\pi/b$ and k perpendicular to the a-axis. We have for instance

$$|\tilde{W}'_{LA,j}(M)|_{k\parallel b} = |\tilde{W}'_{TO_{\parallel},j}(M)|_{k\parallel a} = \delta_{j1}\frac{\hbar}{b}\left[\frac{J\,\varepsilon_j(M)}{NM\hbar\omega_s(M)(A_j(M)-B)}\right]^{1/2}\cdot \tag{5.71}$$

$$\cdot\,|D_{22}\sin 2\varphi - 2D_{44}\sin 4\varphi|\,.$$

Finally we have the case where the k-vector is parallel with the c-axis, and using (5.53), we obtain for the interaction amplitudes

$$\tilde{W}'_{s,j}(k) = 0 \tag{5.72}$$

and

$$\tilde{W}''_{s,j}(k) = (2NJ)^{-1/2}H_o c_{44}K^{-1}_{j,k}\frac{2}{c}\sin(kc/2)(F^s_{k,1}\cos\varphi + F^s_{k,2}\sin\varphi)\,\delta_{j,s}\,, \tag{5.73}$$

where $\delta_{j,s}$ is equal to one if the modes are both acoustic or optical, otherwise $\delta_{j,s}$ is zero. In the c-direction the eigenvectors of the phonons are purely longitudinal or transverse eigenvectors, and both the magnons and the phonons are either purely acoustic or optical excitations (corresponding to the double zone scheme representation).

An examination of (5.73) shows that the acoustic (optical) magnons interact only with the transverse acoustic (optical) phonons polarized parallel with the magnetization. In fig. 4 is shown the neutron results[35] in the c-direction of Tb at 79°K, and this kind of interaction occurs at $k = 0.25\ \text{Å}^{-1}$ giving rise to an energy gap which is 0.6 meV in agreement with the expression above or

$$\Delta_{TA,1}(k) = 2\hbar\frac{1}{c}\left[\frac{J}{M(A_1(k)+B)}\right]^{1/2}H_o c_{44}/(NJ)\sin(kc/2)\,, \tag{5.74}$$

which is equal to 0.8 meV at $k = 0.25\ \text{Å}^{-1}$ with $H_o = \sigma^3\cdot 4.0\cdot 10^{-2}$. Besides this interaction (Δ_1) we also show in fig. 4 what seems to be an interaction between the transverse acoustic phonon mode and the optical magnon mode (Δ_2). Although the neutron experiment indicates strongly that this interaction takes place, one has to be cautious with the interpretation of the neutron data until this interaction has been investigated more carefully. However, this interaction between acoustic magnons and optical phonons in the c-direction, which probably exists, leads us to an inspection of the approximations and assumptions we have used.

If the assumption that the H_o-interaction is due to single ion crystal field effects is correct, then we should have calculated the interactions from first principle by evaluating the behaviour of the crystal field when the ions are displaced from their equilibrium positions. Lindgård[38] has calculated the magnetostriction coefficients C and A using a point charge model, and N. Tsuya et al.[39] conclude that C and H_o mainly originate from changes in the crystal field caused by deformations of the conduction electron distribution. A calculation from first principle will probably show that the magnetostriction coefficients will display a (slight) k-dependence due to contribution from the conduction electrons and the ions which are not nearest neighbours. The leading terms will, however, still be proportional to the relative displacements of neighbouring ions, which implies that the results obtained above should be correct at long wave lengths. A first-principle calculation will possibly show that the equivalence of the two sublattices is destroyed giving rise to the Δ_2-interaction between acoustic magnons and optical phonons in the c-direction; however, one would expect this interaction to be much smaller than the Δ_1-interaction calculated above, whereas experimentally $\Delta_2 \cong \Delta_1$. This discrepancy cannot be removed by assuming that the H_o-interaction is due to the exchange interaction rather than to changes in the crystal field, because this two-ion interaction will preserve the equivalence of the two sublattices. The temperature dependence of H_o is only known within a short temperature interval, because it takes a big magnetic field to pull the magnetization out of the basal plane at low temperature. The magnetostriction measurements[10,11], however, indicate that the origin of H_o is the crystal field and not the exchange interaction, corresponding to a σ^3- instead of a σ^2-dependence of H_o.

The two-magnon one-phonon interaction, $\tilde{H}^{(2)}_{S-L}$, does not give rise to energy gaps in the energy spectrums, however, it renormalizes the energies of the phonons and the magnons as shown in Appendix C (C. 27) and (C. 28). Besides this renormalization we obtain changes in the excitation energies owing to the zero point motion of the lattice, corresponding to the factor 1/2 in (C. 27) and (C. 28) which is still left at zero temperature.

Unlike the one-magnon one-phonon interaction $\tilde{H}^{(2)}_{S-L}$ influences the spin wave energy gap at zero wave vector. This contribution to the spin wave energy gap is, however, almost independent of φ, because the numerical values of D_{01} and D_{03} are 5-10 times larger than D_{22}. Using the interaction amplitudes derived in section 5.1, (5. 32) and (5. 33), without introducing the relative displacements *(5. 53)* instead of the strains *(5. 9)* (which implies an overestimation of the energy changes), we obtained a φ-independen

contribution from the zero point motion to the energy gap which is less than 5 per cent of the actual energy gap, and a φ-dependent part which is 5-10 times as small. At finite temperature the relative energy changes of the magnons and phonons are probably of the same order of magnitude as the relative velocity changes, that is maximum 5-10 per cent, whereas the magnon - magnon interaction implies a much greater renormalization of the magnon energies.

The effect of $\tilde{H}^{(2)}_{S-L}$ on the lifetime of the magnons has been considered by Abrahams and Kittel[40]. However, in accordance with the renormalization of the magnon energies one would expect the magnon - magnon interaction to be the most important mechanism in limiting the magnon lifetime.

6. MAGNETO - ELASTIC CONTRIBUTIONS TO THE SPIN WAVE ENERGIES

In chapter 2 we formulated the spin wave theory for the ferromagnetic hcp metals Tb and Dy without taking the magneto - elastic contributions arising from $\tilde{H}_{S-L}$, (1.6) into account. $\tilde{H}_{S-L}$ has been generalized to a Hamiltonian which describes the interaction of both the static and the dynamic lattice with the spin system. The dynamic interaction is given by $\tilde{H}^{(1)}_{S-L}$ and $\tilde{H}^{(2)}_{S-L}$ in chapter 5, (5.2) and (5.3), whereas the interaction between the homogeneous (time-dependent) strain and the spin system, $\tilde{H}^{(o)}_{S-L}$ equation (5.1), corresponds to the magneto - elastic terms in (4.17) and (4.18).

The Hamiltonian $\tilde{H}^{(o)}_{S-L}$ contributes to the equilibrium magneto - elastic energy, (4.17), and thereby gives rise to magnetostriction, (4.9), and it influences the direction of the magnetization, (4.10). With the actual Hamiltonian and magnetostriction coefficients (4.10) looks as follows:

$$(\partial F/\partial \varphi)_e = -6\,NJ(J_5 V_6^6 + \tfrac{1}{2} c_\gamma AC)\sin 6\varphi = 0 \qquad (6.1)$$

in a zero magnetic field and for $\theta = \pi/2$, where

$$c_\gamma = 4\,c_{66}/(NJ)\,. \qquad (6.2)$$

When we apply a magnetic field in a hard direction, we obtain an equation similar to (2.16), where the critical field is now given by

$$H_c = (36\,J_5 V_6^6 + 18\,c_\gamma AC)/g\mu_B. \qquad (6.3)$$

In the magnetically ordered phase the lattice is distorted from its equilibrium configuration. When there are no deformations of the lattice, the crystal field gives rise to the magnetic anisotropy terms, V_2^o and V_6^6. When the lattice is strained, the changes (of the symmetry) of the lattice will result in new magnetic anisotropy terms besides the V_2^o- and V_6^6-terms. These new terms are described by the Hamiltonian $\tilde{H}_{S-L}^{(o)}$, and as V_2^o and V_6^6 influence the spin wave energies, $\tilde{H}_{S-L}^{(o)}$ will imply changes of the spin wave energy spectrum corresponding to equation (4.18). These magneto - elastic contributions to the spin wave energies have first been considered by Turov and Shavrov[26], and because the lattice is assumed to be static when the time dependence of the homogeneous strain, $\tilde{H}_{S-L}^{(1)}$ and $\tilde{H}_{S-L}^{(2)}$ is not taken into account, they called it "the frozen lattice" approximation. In this approximation the spin wave energy gap at zero wave vector can be deduced by a straightforward calculation. The equilibrium strains ((3.16) with $\theta = \pi/2$) are substituted into $\tilde{H}_{S-L}$, (1.6) and (1.8), and with the quantization scheme applied in chapter 2, we obtain

$$A_1(0) + B = 2J_1V_2^o - 6J_5V_6^6\cos 6\varphi + g\mu_B H\cos\delta + V_a + c_\gamma [2C^2 + A^2 - 3AC\cos 6\varphi - B(2C - A\cos 6\varphi)] \quad (6.4)$$

and

$$A_1(0) - B = -36J_5V_6^6\cos 6\varphi + g\mu_B H\cos\delta + c_\gamma [4C^2 + 4A^2 - 10AC\cos 6\varphi] \quad (6.5)$$

where the a-mode contribution is

$$V_a = \frac{12}{NJ} [2D'^2(c_{11} - c_{66}) + \frac{1}{2}G^2c_{33} + 2D'Gc_{13}] - 12(2D' + G)J(\gamma_o + \gamma'_o). \quad (6.6)$$

The q-dependence is then given by adding the exchange term in (2.10) to $A_1(0)$ (the exchange integrals are modified slightly owing to a-mode contributions). This is the result also obtained by Lindgård[38], and when the A and B terms are cancelled, these expressions are similar to those of Cooper[13]. However, it is necessary to include the A terms when interpretating the neutron experiment[12] with Tb + 10% Ho. The most important effect of the magnetic anisotropy arising from static magneto - elastic interaction is that $\varepsilon(0)_{hard}$ does not go to zero when a field is applied in a hard

direction as the energy gap given by equation (2.18). Instead we obtain a minimum value of the energy gap at H equal to the critical field, H_c, which is

$$\varepsilon(0)_{hard} = [[\, 2J_1 V_2^0 + 30 J_5 V_6^6 + V_a + c_\gamma (2C^2 + A^2 + 15AC - 2BC + AB)\,] \cdot$$

$$\cdot\, [\, 4\, c_\gamma (C + A)^2\,]]^{1/2} \qquad (6.7)$$

in Tb where the hard direction is an a-axis. In Dy, where V_6^6 is negative, the hard direction is a b-axis, and we obtain a similar expression, only the sign of V_6^6 and A is the opposite.

The energy gap, (6.4) - (6.6), can also be evaluated by means of the second derivatives of the free energy with respect to θ and φ, keeping the strains constant, (4.13), in the macroscopic formula for the uniform spin mode (2.21). The last term in equation (4.13) gives rise to correlation effects, which, however, is physically untenable (the value of the energy gap is, irrespective of its origin, scaled by a factor which goes to zero when the temperature goes to zero). Following Cooper[13] and chapter 2 this can be used for determining the temperature dependence of the magneto-elastic terms, and in accordance with the results in chapter 2 the temperature dependence is given by the temperature dependence of the macroscopic magnetostriction coefficients divided by the relative magnetization. For instance we have

$$c_\gamma A^2 \sim (\sigma^{10})^2/\sigma = \sigma^{19} \qquad (6.8)$$

where we have ignored the temperature dependence of the elastic constants.

Besides by application of an external magnetic field the energy gap can be modified by a uniaxial stress. To find the equilibrium configuration when the stress is kept constant, we have to minimize an enthalpy function defined as

$$h = F + [\, c_{ij}\,]^{-1} T_i B_j\,; \qquad (6.9)$$

F is defined in chapter 4, and the definitions of T_i and B_j are found in chapter 3, (3.4) and (3.20). The energy gap is greatly changed when a uniaxial pressure, p, is applied along a direction in the basal plane, and we define

$$T_1 - T_2 = -p\cos 2\alpha \qquad \text{and} \qquad T_6 = -\frac{1}{2}p\sin 2\alpha\,, \qquad p \geq 0. \tag{6.10}$$

With a pressure along an a-direction in Tb the most energetically favourable direction of the magnetization is along the b-axis perpendicular to the pressure. This pressure stabilizes the configuration, and the energy gap will increase.

$$[A_1(0) + B]_p = [A_1(0) + B]_{p=0} + 2(A + C)\cdot p/NJ \tag{6.11}$$

and

$$[A_1(0) - B]_p = [A_1(0) - B]_{p=0} + 4(2A + C)\cdot p/NJ. \tag{6.12}$$

With a pressure along a b-axis the domains which are magnetized along this b-axis will disappear, and the pressure will turn the direction of magnetization of the other domains so that when p is greater than a critical pressure, p_c, the magnetization will be along the a-axis perpendicular to the pressure (this is only true when C is greater than 2A).

$$p_c = 9\,NJ(J_5V_6^6 + \tfrac{1}{2}c_\gamma AC)/(C - 2A)\,. \tag{6.13}$$

At this critical pressure the energy gap attains to its minimum value which is just the energy gap $\epsilon(0)_{hard}$ given by equation (6.7). When the pressure is greater than p_c, the energy gap will increase

$$[A_1(0) + B]_p = [A_1(0) + B]_{p=p_c} + 2(C - A)\,(p - p_c)/NJ \tag{6.14}$$

and

$$[A_1(0) - B]_p = [A_1(0) - B]_{p=p_c} + 4(C - 2A)(p - p_c)/NJ\,. \tag{6.15}$$

In the "frozen lattice" approximation $\epsilon(0)_{hard}$ is an absolute minimum value of the energy gap in the sense that a combination of an external field and a uniaxial stress can never bring the energy gap below this value.

In chapter 5 we treated the interaction between the spin system and the dynamic lattice, $\tilde{H}^{(1)}_{S-L}$ and $\tilde{H}^{(2)}_{S-L}$, without setting any restrictions on the lattice. We assumed the phonon lifetime to be infinite, because the limiting of the lifetime due to phonon - phonon and magnon - phonon interactions is expected to be of smaller importance. However, this is "the flexible lattice model", where the lattice responds to any alterations instantaneously. In section 5.3 we considered the influence of $\tilde{H}^{(1)}_{S-L}$ and $\tilde{H}^{(2)}_{S-L}$ on the magnon

energy spectrum. $\tilde{H}^{(1)}_{S-L}$ does not change the energy gap at zero wave vector at all (the interaction goes to zero when the wave vector goes to zero), whereas $\tilde{H}^{(2)}_{S-L}$ has a slight effect on the energy gap which, however, is almost independent of φ and probably much smaller than the renormalization due to magnon - magnon interaction. This implies that the spin wave energy gap at zero wave vector is practically independent of magnon - phonon interaction.

In a model where the lifetime of the phonons is assumed to be infinite, the strains are constant in time ($\delta\hat{e} = 0$). For instance thermal expansion of a crystal is only possible if one takes anharmonic terms (or phonon - phonon interaction) into account. When a finite lifetime is introduced, the strains can be adjusted to minimize the free energy. The presence of the total impulse of the crystal in the Hamiltonian implies fluctuations of the strains which correspond to the uncertainty in determining the position of the total crystal; these fluctuations are independent of magnon - phonon and phonon - phonon interactions. So when the internal properties of a crystal are considered, its total impulse can be neglected, and the strains commute with the Hamiltonian. The derivative of a homogeneous strain with respect to time is then

$$\frac{d\hat{e}}{dt} = \frac{i}{\hbar}\,[\tilde{H},\ \hat{e}] + \frac{\partial\hat{e}}{\partial t} = \frac{\partial\hat{e}}{\partial t} \tag{6.16}$$

where the explicit time dependence of the strain is obtained by minimizing the free energy. When the total impulse of the crystal is neglected and the phonon lifetime is finite, the free energy can be minimized instantaneously, and in the case of magneto - elastic interactions we have (equation (4.9))

$$\frac{\partial F}{\partial e} = \hat{e}(t) + \Big\langle \sum_j \tilde{B}_j(\theta,\varphi) \Big\rangle_t = 0 \tag{6.17}$$

where the index t indicates that the wave functions are time-dependent. This equation implies that the homogeneous strain follows the motion of the total magnetization vector (specified by the time dependence of θ and φ). The only difference between the strain defined by equation (6.17) and the one used in the frozen lattice approximation is that the strain now follows the precession of the magnetization (which corresponds to excitations of spin waves with infinite wave length). However, this motion will only perturb the strain slightly and does not change the way in which the homogeneous strain con-

tributes to the spin wave energy gap (the strains can still be treated as classical quantities).

We can conclude that neither the time dependence of the homogeneous strain nor the magnon - phonon interaction modify the results obtained above with the "frozen lattice" approximation. Although the lattice is completely "flexible", the spins will perceive the lattice as being "frozen". This can be understood in the following way:

If we consider the motion of a spin in a magnetic field, we know that the frequency of the spin precession can be specified, but that the phase is arbitrary. This arbitrariness in the phase of the precession of a single spin in the crystal (also for collective spin wave excitations) implies that the ions cannot follow the motion of the spins, which means that the anisotropy crystal field produced by the relative displacement of neighbouring ions cannot be reduced by allowing the ions to move freely.

We can illustrate this by considering equation (6.17) which can never be exact. If we include the total impulse of the crystal in the Hamiltonian, this will give rise to a phase difference between the two terms in (6.17) (on account of the inertia of the crystal); furthermore this phase difference will have an arbitrary magnitude, because now the strain does not commute with the Hamiltonian. The strain can follow the precession of the magnetization within an arbitrary phase factor.

The only kinds of interaction between a "flexible" lattice and the spin system are the one due to changes in the z-component of the spins ($\tilde{H}^{(2)}_{S-L}$), and resonance phenomena occurring when the wave vector and the frequency of the collective motions are equal ($\tilde{H}^{(1)}_{S-L}$).

The expression (6.4) - (6.6) for $\varepsilon(0)_{easy}$ is in agreement with neutron experiments[12,35] and with the magnon energy gap determined from infrared resonance[41]. When a field is applied in a hard direction, the neutron experiments[12,35] are also consistent with the results above, (6.7), and this is also the case for the ferromagnetic resonance experiments at 100 GHz[42], whereas the ferromagnetic resonance experiments at frequencies lower than the frequency corresponding to equation (6.7) seem to contradict the conclusion above, namely the Dy-resonance at 37 GHz[43] and the two resonance experiments performed with Tb at 10 GHz[44,45] and at 24 GHz[46].

Cooper[13] has attempted to explain these resonance experiments by introducing a "flexible lattice" model which is defined in principle as above. Cooper does not analyse this model on a microscopic basis, but attacks it macroscopically by using the free energy equation for the spin wave mode (2.21), and instead of keeping the strains constant when evaluating the

derivatives of the free energy with respect to the angles, θ and φ, he introduces explicitly the θ- and φ-dependence of the strains given by equation (6.17) into the free energy before calculating the derivatives. In the result obtained by Cooper with this model, (6.5) is replaced by

$$[A_1(0) - B]_C = -(36\, J_5 V_6^6 + 18\, c_\gamma AC)\cos 6\varphi + g\mu_B H\cos\delta$$
$$= g\mu_B(H\cos\delta - H_c\cos 6\varphi), \tag{6.18}$$

and (6.4) by

$$[A_1(0) + B]_C = A_1(0) + B - H_o^2 c_{44}/NJ\,. \tag{6.19}$$

When a field is applied in a hard direction, the energy gap should be zero when H is equal to the critical field, H_c, and the low-frequency resonance experiments would then be explained as resonance occurring at the critical field.

Brooks[47] has later modified this model by pointing out that (6.17) can only be fulfilled for frequencies below the phonon - phonon scattering frequency.

However, this model presupposes a classical nature of the spin wave excitations without taking the arbitrariness of the spin precession into account (the lattice is allowed to follow the spin precession in phase).

Finally Vigren and Liu[46] have proposed the use of the equilibrium equation (6.17) as a dynamic "operator" expression

$$\hat{e} = -\frac{1}{c}\sum_j \tilde{B}_j(\theta,\varphi)\,. \tag{6.20}$$

Using this expression for the strains in the Hamiltonian, they obtained a result which fits the experiments very well. This interpretation of the magnetostriction equation does not change the "frozen lattice" spin wave energies for wave vectors different from zero, whereas, when the wave vector is exactly zero (corresponding to the low-frequency resonance experiments), they obtained the expressions (6.18) and (6.19) for the energy gap. However, as seen above, this equation is only valid within an arbitrary phase factor. This can also be said in the following way: The reason why this uniform "flexible lattice mode" does not exist, is simply that the eigenfrequency of the lattice at infinite wave length is zero.

The low-frequency resonance experiments cannot be explained as being due to a "flexible lattice mode". The ferromagnetic resonance in Dy at 37 GHz[43] is observed at a field which corresponds very well to the critical field deduced from the anisotropy measurements performed by Rhyne and Clark[6] (for a comparison, see fig. 5). The frequency used in this experiment corresponds to an energy equal to 0.15 meV. Although the energy gap parameters of Dy have not been determined completely so far, it is very likely that $\varepsilon(0)_{hard}$ in Dy is only about twice the value of the resonance energy in the temperature range considered. The ultrabroad resonance observed in Dy is probably the tail of the resonance curve of the uniform spin wave mode.

The resonance field obtained in Tb at 10 and 24 GHz agrees very well with the resonance field (equal to H_c below 140°K) calculated by Vigren and Liu[46] and shown in fig. 6. The line width of the 10 GHz resonance is rather broad and increases when the temperature decreases, which indicates that the resonance is either an off-resonance, or it is due to domain effects (a pure on-resonance would have displayed the opposite behaviour). In Tb $\varepsilon(0)_{hard}$ is about 1 meV and the energy at which the ferromagnetic resonance is observed is only .04 - .08 meV, so the off-resonance explanation is not satisfactory in this case. Instead we propose that the absorption peaks in Tb at 10 and 24 GHz are due to domain or/and domain wall effects occurring when the field is equal to the domain alignment field which is identical with the critical field, H_c.

The line width of the absorption peaks observed by Hart and Stanford[46] at 24 GHz is only 3-4 kOe; however, the theory proposed by Vigren and Liu offers no satisfactory explanation of the absorption peaks observed for H aligned from 3 to 10° from the a-axis in the basal plane of the sample when T is below 140°K. A second discrepancy between this theory and the experiment is that no absorption peak is observed when H is aligned exactly along the a-axis. The experimental results reveal that peaks occur for H equal to H_c when H is aligned from 1 to 2° off the a-axis.

When the external magnetic field makes an angle δ with the a-axis and is smaller than the sum of the critical field, H_c, and the demagnetization field, H_D, the crystal will consist of two kinds of domains making an angle $\pm\varphi$ with the a-axis, owing to the self-energy of the crystal arising from H_D. The relative difference between the volume of the two kinds of domains will be

$$n = H\sin\delta/H_D\sin\varphi. \qquad (6.21)$$

It is easily seen that the absorption, χ, due to domain wall motion when a radiofrequency field, H_{rf}, is applied, will be proportional to

$$\chi \sim H_{rf}\, \omega_{rf}\, f(\delta, \varphi)\, \frac{\partial n}{\partial \delta} \tag{6.22}$$

where $f(\delta, \varphi)$ is a function which depends on the energy bound in the domain walls. For $\delta = 0$ we have

$$f(0, \varphi) \to 0 \quad \text{for} \quad \varphi \to 0\,. \tag{6.23}$$

The behaviour of the absorption, χ, will be quite similar to a resonance absorption. At constant frequency the absorption will be proportional approximately to $\cot\varphi$ for $\delta \neq 0$, which means that the absorption peak will be proportional to $\cot\delta$; only for $\delta = 0$ will this absorption peak disappear due to the relation (6.23). Without taking $f(\delta, \varphi)$ into account the peak will be very narrow (~ 1 kOe); $f(\delta, \varphi)$ will give rise to a somewhat broader peak. At constant field the absorption will be proportional to the frequency until relaxation in the motion of the domain walls (at $H = H_c + H_D$) will diminish the absorption.

The great similarity between the behaviour of χ, (6.22), and the resonance observed by Hart and Stanford indicates that this resonance is due to domain wall motion.

II. EXPERIMENTAL MEASUREMENTS OF THE VELOCITY OF ACOUSTIC SOUND WAVES IN TERBIUM

7. EXPERIMENTAL METHODS

Several experimental methods exist for determination of the elastic properties of a material. Static measurements call for a rather big sample, and resonance measurements in the kHz region are difficult when the material is anisotropic. Thus when the material to be investigated is a small anisotropic single crystal, we have to use acoustic sound waves with a frequency above 1 MHz. In this ultrasonic frequency region the driffraction is reduced to such a degree that the sound wave can exist as a plane wave for a distance of approx. 1 cm.

A number of methods for determining the velocity of ultrasound waves are described in the litterature[22, 23, 27, 29, 48, 49]. The different methods

have many features in common. The sample is prepared with two parallel plane surfaces, and a sound wave excited by e. g. a piezoelectric quartz crystal is transmitted into the sample. A greater or smaller part of this wave is then reflected by the surfaces, and by measuring the time between successive reflections the velocity and thereby the elastic constant can be determined.

In this experiment three different Tb-crystals were used. Tb I (Metals Research Ltd.), which has been used to determine c_{33}, is an old crystal which is not entirely faultless. Tb II and Tb III are new crystals of much better quality grown by P. Touborg, The Technical University of Denmark. A Tb-disk with very large internal tensions was prepared (by shock cooling of melted Tb). When this disk is annealed at high temperatures (1200°C) for some hours, single crystals without internal tensions will appear. To avoid impurities in the crystals all steps have to be carried out in vacuum.

Tb I and T II had faces cut perpendicular to the c-axis, whereas Tb III had faces containing the c- and a-axes (perpendicular to the b-axis). The crystal orientations were found by the back-reflection Laue technique and were accurate to within $\pm \frac{1}{2}°$. All the preparations of the crystals were made without mechanical action on the specimens. The cutting-out of the samples and the preparation of the two parallel plane faces were made with a spark cutting apparatus (Metals Research Ltd.). The faces of the specimens were flat and parallel to within ± 3 microns. The length of the crystals was about 3 mm and the diameter about 6 mm.

The sound velocities were measured by an ultrasonic pulse echo technique. A simplified diagram of the experimental set-up is shown in fig. 7. With intervals of about 1 msec a pulse train with a frequency of 20 MHz and a length of about 1 μsec is transmitted through the total system of transducer - quartz buffer - sample - quartz buffer - transducer. The transmitted signal is then amplified and finally analysed with an oscilloscope. This signal consists of a direct transmitted pulse train followed by pulse trains which have been reflected at discontinuities in the system. The first pulse train following the direct transmitted pulse train is the one that has travelled once back and forth in the sample before being detected. By measuring of the time delay of this pulse train, the velocity can be determined, and by comparison of the amplitudes of the two pulse trains the attenuation of the sound wave in the sample can be found. The buffers were used because the capacitive transmitted signal is then greatly damped, and the acoustic-bonding buffer sample is defined better than the transducer sample[49]. A transducer frequency of 20 MHz was used, and longitudinal

waves were produced with X-cut quartz transducers and shear waves with Y-cut transducers (Valpey Corporation). More details about the experimental set-up can be found in[23].

The temperature range was covered by using a conventional cryogenic technique, and the temperature was measured with a calibrated copper - constantan thermocouple above 100°K and a germanium resistance below this temperature. All temperature measurements should be accurate to within $\pm$ 0.2°K.

It was extremely difficult to find suitable adhesives for bonding the quartz buffers to the crystal. Several kinds of silicone materials were used without success. The most suitable "demountable" material seems to be a low-temperature varnish from General Electric (number 7031). Palmer and Lee[33] report similar difficulties when measuring the sound velocities in dysprosium and holmium, and instead of using a visco-elastic material as bonding, they used an Araldite epoxy-resin, which necessitates relapping of the specimens after removal of the transducers.

The most important source of error in evaluations of the sound velocities is the phase shift at the bondings which contributes about 0.1% to the probable error of the velocities. Other sources of error (the length and orientation of the crystal, time measuring, diffraction) contribute about the same amount so that the total probable error of the velocities is 0.2%. A more careful analysis of the sources of error can be found in[23]. In addition to these sources of error we have the variation in the quality of the crystals. Internal tensions and a great concentration of dislocation can decrease the accuracy of the result by an order of magnitude. The probable error of the relative velocity changes is much smaller. The most important contribution in this case is the probable error of the time measurements, and in this experiment we have a probable error of the relative velocities of 0.02%.

8. EXPERIMENTAL RESULTS

The elastic properties of a hexagonal solid are determined by means of five independent elastic constants as described in chapter 3, (3.5) and (3.6). In this experiment we measured four of these constants as functions of temperature. The Tb I crystal was used for measuring the velocity of longitudinal sound waves propagating in the c-direction, and from this velocity c_{33} can be calculated (3.7). From the velocity of shear waves propagating in the c-direction c_{44} was determined with the Tb II crystal.

Finally the longitudinal and transverse (polarized perpendicular to the c-axis) sound velocities were measured in the Tb III crystal, determining c_{11} and c_{66} respectively, (3.8).

A density of 8.204 g/cm^3 at 300°K for terbium was used in calculating the elastic constants. This density was obtained from the lattice parameters measured by Darnell[50]. The variation of density with temperature and the corrections in path lengths as a result of thermal expansion and magnetostriction were evaluated from the data given by Rhyne and Legvold[9]. The density at zero temperature should then be 8.235 g/cm^3.

The results are shown in figs. 8 - 17. c_{44} and the attenuation of the corresponding sound wave, α_{44}, show almost no anomaly at the transition temperatures, as also observed by Lüthi et al.[27, 51]. The critical behaviour of the longitudinal sound wave propagating in the c-direction has been exhaustively examined by Lüthi et al. At a second-order transition from a paramagnetic state to an ordered spin structure the critical attenuation[52] and the critical velocity change[52, 53] have been calculated to be proportional to

$$\alpha \sim \omega^2 C \tau_c \sim \omega^2 \epsilon^{-\eta} \qquad (8.1)$$

$$\Delta v/v \sim - \omega_o C \qquad (8.2)$$

where ω is the cyclic sound wave frequency, C is the specific heat with a logarithmic singularity at T_N, τ_c is a characteristic decay time of the spin fluctuations, and ϵ is the reduced temperature difference. The expression for the critical attenuation was found to be valid in a temperature range of $7 \cdot 10^{-3} < \epsilon < 7 \cdot 10^{-2}$ with an exponent equal to $\eta = 1.24$ in agreement with the theoretical prediction[52] of 4/3 for a paramagnet to anisotropic antiferromagnet transition. In the same temperature range the relative velocity followed the logarithmic temperature dependence very well.

Our measurements of v_{33} and α_{33} are consistent with this picture. However, the poor quality of the Tb I crystal was reflected in the presence of two domains in the crystal, a main domain having $T_N = 119.7$°K and a somewhat smaller domain displaying a critical velocity change at $T_N' = 223.3$°K (fig. 9). Our attenuation measurements (fig. 10) are not sufficiently precise to allow determination of the critical exponent, but the qualitative behaviour is in accordance with the measurement performed by Lüthi et al.[51], showing a critical increase of the attenuation at T_N (119.7°K) and a strong damping of the sound waves at the Curie temperature, $T_C \approx 210$°K, $\alpha_{33}(T_C) \approx 30$

dB/msec. The velocity change was only slightly disturbed by the small domain transition at T_N', and showed logarithmic behaviour at T_N, as also observed by Lüthi et al. The longitudinal sound velocity, $v_{33} = 3.10 \cdot 10^3$ m/sec at room temperature measured by Lüthi et al., is more reliable than the value we obtained with the Tb I crystal. This sound velocity corresponds to an elastic constant $c_{33} = 7.88 \cdot 10^{11}$ ergs/cm^3, which is about 5% above the value we obtained.

A critical change at T_N of the velocities v_{22} and v_{66} was also observed (figs. 12 and 14), and the change of the shear wave velocity, v_{66}, was followed by an increase of the attenuation (fig. 15). However, these critical velocity changes, which amount to $\frac{1}{2}$% for v_{22} and 1% for v_{66}, are not so pronounced as the critical change of v_{33}, which is about 5%. We observed a marked increase of the attenuation of the longitudinal and the transverse sound waves in the basal plane at the Curie temperature (figs. 13 and 15), with a maximum value for both kinds of waves of about 100 dB/msec. Furthermore the transition at the Curie temperature is also accompanied by a rather abrupt change of the velocities. From these measurements the Neel and Curie temperatures for the Tb III crystal are established to be $T_N = 223.7^\circ$K and $T_C = 214.7^\circ$K.

It is not possible to analyse quantitatively these experimental results obtained in the ferromagnetic region. The behaviour of the elastic constants below T_C cannot be expected to be well defined as long as, in the absence of an external field, the crystal is divided into domains whose magnetic polarizations differ from each other. As observed by Palmer and Lee[33] in Dy and Ho, an external field greatly affects the behaviour of c_{11} and c_{66}.

The abrupt change of v_{22} and v_{66} near T_C is probably due to the one-magnon one-phonon interaction giving rise to the $(\Delta v/v)_1$-change of the velocities (see section 5.2 (5.35), note that $(\Delta v_{33}/v_{33})_1 = 0$), whereas the main contribution to the attenuation near T_C probably arises from the two-magnon one-phonon interaction (corresponding to the velocity change $(\Delta v/v)_2$, (5.36)). The one-magnon one-phonon interaction contributes only indirectly to the attenuation of the sound waves through magnon - magnon interaction. a_{11} is about three - four times larger than a_{33} at the Curie temperature; the reason for this is probably that D_{01} is about twice D_{03}, (5.39) and (5.40), which corresponds to $a_{11} \approx 4a_{33}$.

In table I we compare the elastic constants of Tb at room temperature with the corresponding constants of Dy[16,33] and Ho[33]. C_{33} for Tb is the value obtained by Lüthi et al.[27,51], and c_{13}, which has not been measured so far, is indicated to be approximately the mean value of the c_{13} of Dy

and Ho. Furthermore the experimentally determined elastic constants for Tb are compared with those calculated by Gylden Houmann and Nicklow[37], who have fitted the phonon dispersion relations at room temperature of Tb with a Born - von Karman force model which includes interactions out to the eight-nearest neighbour.

Finally we calculated the bulk modulus, B (3.11), and the Debye temperature, θ_D, using the elastic constants at room temperature given in table I. This calculated bulk modulus, $B_{cal.} = 3.95 \cdot 10^{11}$ erg/cm^3, agrees very well with the value of $B = 4.05 \cdot 10^{11}$ erg/cm^3 obtained by Rosen[29] who measured the velocity of sound waves in polycrystalline Tb. From these measurements Rosen has obtained a Debye temperature of $\theta_D = 174^oK$, which is identical with the value we have deduced using $v_t = \frac{2}{3}v_{66} + \frac{1}{3}v_{44}$ and $v_l = \frac{2}{3}v_{22} + \frac{1}{3}v_{33}$ in the formula

$$\theta_D = \frac{h}{k_B}\left(\frac{9N}{4\pi V}\right)^{1/3}\left[\int\left(\frac{1}{v_1^3} + \frac{1}{v_2^3} + \frac{1}{v_3^3}\right)\frac{dV}{4\pi}\right]^{-1/3} \qquad (8.3)$$

where to a good approximation $v_1 = v_l$ and $v_2 = v_3 = v_t$, owing to the almost isotropic character of Tb.

The elastic properties of paramagnetic Tb, Dy, and Ho have by now been determined satisfactorily, and the critical behaviour at T_N is well understood. However, the behaviour of the velocity of sound waves in the ferromagnetic phase of Tb and Dy should be examined in much more detail now. The most interesting kinds of experiments are the ones commenced by Lüthi et al.[27], who isolated the magneto - elastic contributions to the velocity of the transverse sound waves propagating in the c-direction. By measuring the velocity changes due to the application of an external field it should be possible to determine the magnetostriction coefficients (section 5.2), and thereby impart a better understanding of the magneto - elastic properties of the heavy rare-earth metals, which still present many unanswered questions.

III. RECENT EXPERIMENTAL RESULTS FOR TERBIUM

9. INELASTIC NEUTRON SCATTERING STUDIES OF FERROMAGNETIC TERBIUM

The interaction between the acoustic magnons and the optical phonons in the c-direction was examined in more detail at 4.2°K. By application of a field in the easy and in the hard directions the magneto - elastic contributions to the spin wave energy gap at zero wave vector were deduced. The spin wave dispersion relation in the c-direction of Tb at 4.2°K was studied more closely by applying an external field along a b-direction, disclosing a rather anisotropic behaviour of the exchange interaction.

9.1. Magnon-Phonon Interaction

The further investigation of the acoustic magnon - optical phonon interaction in the c-direction of Tb at 4.2°K removed any doubt about the existence of this interaction. The position of the crossing point of the unperturbed dispersion relations is determined to be

$$q = 0.45\ \text{Å}^{-1}, \quad \varepsilon(q) = 6.25\ \text{meV},$$

and the energy gap at this position is determined to be $\Delta_2 = 1.35$ meV. At this wave vector the neutron groups on each side of the energy gap in a constant q-scan are of equal intensity and linewidth. The linewidths are reasonable when compared with the linewidth of neutron groups at different q-values. The variation of the two branches in the neighbourhood of the nominal crossing point is as one would expect for such an interaction (figs. 2 and 4). Finally, as should be the case, the sum of the squared intensities is almost constant over the range where the interaction takes place.

9.2. Spin Wave Energy Gap

The behaviour of the spin wave energy gap at zero wave vector when an external field was applied was analysed using the following expressions:

$$\varepsilon(0)^2_{easy} = \left[2P_2J + c_\gamma(2C^2 + A^2) + \Delta M + g\mu_B\left(\tfrac{1}{6}H_c + H\right)\right] \cdot \left[4c_\gamma(C - A)^2 + g\mu_B(H_c + H)\right] \qquad (9.1)$$

when applying a field in the easy direction (b-direction), and when the field is along a hard direction

$$\varepsilon(0)^2_{hard} = [\, 2P_2J + c_\gamma(2C^2 + A^2) - \Delta M + g\mu_B(-\tfrac{1}{6}H_c + H)\,] \cdot$$

$$\cdot\,[\,4c_\gamma(C + A)^2 + g\mu_B(-H_c + H)] \qquad (9.2)$$

in the case where the field is greater than the critical field, H_c,

$$g\mu_B H_c = 36\, J_5 V_6^6 + 18\, c_\gamma AC\,. \qquad (9.3)$$

These are the expressions deduced in chapter 6, (6.3) - (6.7), with the exception that the new results for Tb indicate that it is necessary to include also the sixth power magneto - elastic terms[38] (G_{26} and G_{46}, notice that G_{m1} is minus one half of the coefficients, B_1^m, defined by Lindgård[38]).

$$2P_2J = 2J_1V_2^o + V_a - 28CJ_3G_{24} + 72CJ_5G_{26} - 22AJ_5G_{46} \qquad (9.4)$$

and

$$\Delta M = -44CJ_5G_{46} - 14AJ_3G_{24} + 36AJ_5G_{26} \qquad (9.5)$$

and further

$$\tfrac{1}{2}c_\gamma C = J_1G_{22} - J_3G_{24} + J_5G_{26} \qquad (9.26)$$

$$\tfrac{1}{4}c_\gamma A = J_3G_{44} - J_5G_{46}\,. \qquad (9.7)$$

In table II we have written down the experimental results for Tb+10%Ho[12] and pure Tb in connection with the macroscopically determined magnetic anisotropy[6] and magnetostriction terms[9,10] for Tb and Dy. The theoretical temperature dependences also shown in the table are those predicted by the theory of Callen and Callen[8] taking into account only the most important term involved in the different expressions.

The results for pure Tb shown in table II constitute the best fit to the observed behaviour of the energy gap as a function of temperature and magnetic field. However, these results still have a temporary character, e. g. the temperature dependence of ΔM is smaller than expected. The later ob-

servation of a strongly anisotropic exchange interaction may cause some modifications of the interpretation of the energy gap behaviour.

9.3. Anisotropic Exchange Interaction

When a field is applied along the easy direction in the basal plane, the energy of the spin waves will increase according to the following expression:

$$\varepsilon_i(q, H) = [\,(A_i(q) + B_i(q) + g\mu_B H)(A_i(q) - B_i(q) + g\mu_B H)\,]^{1/2}, \qquad (9.8)$$

see chapter 2, (2.10) and (2.12). By measuring the variation of the spin wave energies with a magnetic field it is possible to determine $A_i(q)$ and $B_i(q)$ explicitly. This has recently been done for spin waves propagating in the c-direction at 4.2°K[54]. If the indirect exchange interaction in Tb is satisfactorily described by an isotropic Heisenberg exchange interaction, (1.3), then $B_i(q)$ should be q-independent, and the following relation should be fulfilled

$$2\,A_i(q) = 2[\varepsilon_i^2(q) + B_i^2(0)]^{1/2}\,. \qquad (9.9)$$

The experimental results shown in fig. 18 disclose that this relation does not hold true. The interpretation of these results demands the introducing of a more complex two-ion spin interaction. Following Lindgård et al.[19] a general Hamiltonian for two-ion spin interaction can be written

$$\tilde{H}_{Ex} = -\sum_{\alpha\beta}\sum_{ij} K^{\alpha\beta}(\bar{R}_i - \bar{R}_j)\, J_{i,\alpha} J_{j,\beta}\,. \qquad (9.10)$$

With this expression instead of (1.3) in the spin wave formalism introduced in chapter 2 the energy of magnons with the wave vector parallel with the c-axis is found to be

$$\varepsilon(q) = [[\,2J(K^{\zeta\zeta}(0) - K^{\zeta\zeta}(q)) + A_o + B_o\,]\,[\,2J(K^{\xi\xi}(0) - K^{\xi\xi}(q)) + A_o - B_o\,]]^{1/2}. \qquad (9.11)$$

The high symmetry in the c-direction implies that only terms which have $\alpha = \beta$ will occur in the spin wave energies, and because of the identity symmetry of the two sublattices we can use a double scheme representation.

The q-dependence of $K^{\zeta\zeta}$ and $K^{\xi\xi}$ is shown in figs. 19 and 20. The two-ion spin interaction is strongly anisotropic in the c-direction with $2J[K^{\zeta\zeta}(0) - K^{\zeta\zeta}(q)]$ lying between plus and minus 2 meV, whereas $2J[K^{\xi\xi}(0) - K^{\xi\xi}(q)]$ changes by an amount of 16 meV. This anisotropic behaviour implies that a division of the two-ion spin interaction into an isotropic and an anisotropic part can only be arbitrarily defined.

A complete description of the two-ion spin interaction in the c-direction involves the q-dependence of $K^{\eta\eta}$, which can be determined by applying a field in a hard direction. In the case where the net magnetization is along a hard direction $K^{\xi\xi}$ is replaced by $K^{\eta\eta}$ in the expression for the spin wave energies, (9.11).

The occurrence of anisotropic exchange interaction modifies the expressions for the spin wave energy gap at zero wave vector. Contrary to an isotropic interaction an anisotropic interaction can contribute to the energy gap at zero wave vector. This modification can be taken into account by introducing some effective parameters instead of the corresponding parameters in equations (9.1) and (9.2)

$$[2J_1V_2^0]_{eff.} = 2J_1V_2^0 + J[K^{\eta\eta}(0) + K^{\xi\xi}(0) - 2K^{\zeta\zeta}(0)] \qquad (9.12)$$

$$[36J_5V_6^6]_{eff.} = 36J_5V_6^6 + 2J[K^{\eta\eta}(0) - K^{\xi\xi}(0)] \qquad (9.13)$$

$$[\Delta M]_{eff.} = \Delta M + \frac{2}{3}J[K^{\eta\eta}(0) - K^{\xi\xi}(0)]. \qquad (9.14)$$

The way the anisotropic exchange parameters enter into (9.12) makes it difficult to distinguish between the crystal field part and the exchange interaction part of the axial anisotropy. The two-ion spin Hamiltonian defined by (9.10) is an effective Hamiltonian quadratic in the spin operator, which, however, also describes the effect of terms that involve more than bilinear spin operators[19]. If the two-ion spin Hamiltonian contains terms which are a product of six or more spin operators (corresponding to O_6^6), then $K^{\eta\eta}(0)$ can differ from $K^{\xi\xi}(0)$, and this difference will then modify the spin wave energy gap.

The anisotropic behaviour of the exchange interaction implies some changes of the amplitudes of the two-magnon one-phonon interaction, (5.32) and (5.33); the amplitudes of the one-magnon one-phonon interaction, (5.18) and (5.19), are implicitly altered because of the q-dependence of B(q). The anisotropic exchange interaction does not explicitly destroy the identity

symmetry in the c-direction of the two sublattices, however, a connection between the anisotropic exchange interaction and the occurrence of the acoustic magnon - optical phonon interaction in the c-direction can be possible.

CONCLUSION

Beginning with the magneto - elastic Hamiltonian, we deduced general expressions for the modification of the velocity of acoustic waves in a ferromagnetic metal due to magnetic ordering and the application of a magnetic field. It was shown that these expressions agree with the experimental results for Tb and Dy. The same Hamiltonian, with macroscopic magneto - elastic parameters and expanded to include explicitly the relative displacements of neighbouring ions, also gives an adequate account of the magnon - phonon interactions at short wave lengths which have been observed in Tb by means of inelastic neutron scattering, with the exception of the interaction between the acoustic magnons and optical transverse phonons in the c-direction. Finally the magneto - elastic contributions to the magnon energy gap at zero wave vector are found to be practically independent of the relaxation of the lattice, contrary to the "flexible lattice" calculations performed by Cooper.

The four elastic constants c_{11}, c_{33}, c_{44}, and c_{66} of Tb were measured by an ultrasonic pulse echo technique as functions of temperature. Strong coupling between the lattice and the spin system near the transition temperatures was observed.

Recent studies of ferromagnetic Tb by means of inelastic neutron scattering have been presented. The observation of a strongly anisotropic exchange interaction in the c-direction implies some modifications of the theory for the two-magnon one-phonon interaction and can possibly alter the interpretation of the behaviour of the spin wave energy gap at zero wave vector slightly. New investigations of the magnon - phonon interaction in the c-direction of Tb have confirmed the previous supposition about the occurrence of the acoustic magnon - optical phonon interaction.

ACKNOWLEDGEMENTS

The author is very grateful to Professor A. R. Mackintosh for valuable discussions and critism of the theoretical and experimental part of this work. The experiments described in part III were carried out in collaboration with

H. Bjerrum Møller and J. C. Gylden Houmann, and the author is indebted to them for allowing the presentation of these results for the first time. Helpful discussions with M. Nielsen and P. A. Lindgård are gratefully acknowledged.

APPENDIX A

Spin Operators

The definition of the shorthand notation of the spin operator expressions:

$$
\begin{aligned}
0_2^2 &= \tfrac{1}{2}(J_+^2 + J_-^2) \\
0_2^0 &= 3J_z^2 - J(J+1) \\
0_2^{-2} &= \tfrac{1}{2i}(J_+^2 - J_-^2) \\
0_4^4 &= \tfrac{1}{2}(J_+^4 + J_-^4) \\
0_4^2 &= \tfrac{1}{4}[(7J_z^2 - J(J+1) - 5)(J_+^2 + J_-^2) + (J_+^2 + J_-^2)(7J_z^2 - J(J+1) - 5)] \\
0_4^0 &= 35J_z^4 - 30J(J+1)J_z^2 + 25J_z^2 - 6J(J+1) + 3J^2(J+1)^2 \\
0_4^{-2} &= \tfrac{1}{4i}[(7J_z^2 - J(J+1) - 5)(J_+^2 - J_-^2) + (J_+^2 - J_-^2)(7J_z^2 - J(J+1) - 5)] \\
0_4^{-4} &= \tfrac{1}{2i}(J_+^4 - J_-^4) \\
0_6^6 &= \tfrac{1}{2}(J_+^6 + J_-^6)
\end{aligned}
\qquad \text{(A.1)}
$$

and further

$$
\begin{aligned}
0_2^{-1} &= J_zJ_x + J_xJ_z \\
0_2^1 &= J_zJ_y + J_yJ_z \\
0_4^1 &= \tfrac{1}{2}[(J_zJ_y + J_yJ_z)(7J_x^2 - J(J+1) - 5) + (7J_x^2 - J(J+1) - 5)(J_zJ_y + J_yJ_z)] \\
0_4^3 &= (J_zJ_y + J_yJ_z)(J_z^2 - J_y^2) + (J_z^2 - J_y^2)(J_zJ_y + J_yJ_z)
\end{aligned}
$$

where

$$J_+ = J_x + iJ_y \quad \text{and} \quad J_- = J_x - iJ_y .$$

The Q_1^m are defined as the 0_1^m, only (x, y, z) are replaced by (ξ, η, ζ).

In the case where $\hat{x}$ is parallel with $\hat{\zeta}$, and $\hat{z}$ (lying in the plane perpendicular to the ζ-axis) makes an angle, φ, with the ξ-axis (the definition of the co-ordinate systems is shown in fig. 1), we have

$$J_\xi = J_z \cos\varphi + J_y \sin\varphi$$

$$J_\eta = J_z \sin\varphi - J_y \cos\varphi \qquad \text{(A. 2)}$$

$$J_\zeta = J_x .$$

After some manipulations the spin operators become

$$Q_2^2 = \frac{1}{2}(0_2^0 + 0_2^2)\cos 2\varphi + 0_2^1 \sin 2\varphi$$

$$Q_2^0 = \frac{3}{2} 0_2^2 - \frac{1}{2} 0_2^0$$

$$Q_2^{-2} = \frac{1}{2}(0_2^0 + 0_2^2)\sin 2\varphi - 0_2^1 \cos 2\varphi$$

$$Q_4^4 = \frac{1}{8}(0_4^0 + 4\ 0_4^2 + 0_4^4)\cos 4\varphi + 0_4^3 \sin 4\varphi$$

$$Q_4^2 = \frac{1}{8}(-\ 0_4^0 + 4\ 0_4^2 + 7\ 0_4^4)\cos 2\varphi + 0_4^1 \sin 2\varphi$$

$$Q_4^0 = \frac{3}{8}\ 0_4^0 - \frac{5}{2}\ 0_4^2$$

$$Q_4^{-2} = \frac{1}{8}(-\ 0_4^0 + 4\ 0_4^2 + 7\ 0_4^4)\sin 2\varphi - 0_4^1 \cos 2\varphi$$

$$Q_4^{-4} = \frac{1}{8}(0_4^0 + 4\ 0_4^2 + 0_4^4)\sin 4\varphi - 0_4^3 \cos 4\varphi$$

$$Q_6^6 = \frac{1}{16}(0_6^0 + \frac{15}{2}\ 0_6^2 + 3\ 0_6^4)\cos 6\varphi \qquad \text{(A. 3)}$$

and further

$$Q_2^{-1} = 0_2^{-1}\cos\varphi + 0_2^{-2}\sin\varphi$$

$$Q_2^1 = 0_2^{-1}\sin\varphi - 0_2^{-2}\cos\varphi .$$

For construction of a spin wave theory the spin operators are expressed in terms of spin deviation operators satisfying the Bose commutation rules. The Holstein-Primakoff[17] transformation is

$$J_+ = (2J - a^+ a^-)^{1/2}\ a^-$$

$$J_- = a^+ (2J - a^+ a^-)^{1/2} \qquad \text{(A. 4)}$$

$$J_z = J - a^+ a^- .$$

In the final expressions all terms which involve more than two operators are neglected, and furthermore it is reasonable to make the approximation[5)]

$$J_+J_+ = 2\,[J(J-\tfrac{1}{2})]^{1/2}\,(1-\frac{a^+a^-}{2J})a^-a^-$$
$$J_-J_- = 2\,[J(J-\tfrac{1}{2})]^{1/2}\,a^+a^+(1-\frac{a^+a^-}{2J})\,. \qquad \text{(A. 5)}$$

These approximations introduce errors which are small at low temperature and for large angular momenta. To minimize the influence of these errors we place all a^+ operators to the left of all a^- operators before we start cancelling terms. The factor $[J(J-\frac{1}{2})]^{1/2}$ gives in some cases physically unreasonable results, and Brooks[18)] has shown that this factor is replaced by $(J-\frac{1}{2})$ in a spin wave theory based on the Oguchi expansion technique.

Replacing $[J(J-\frac{1}{2})]^{1/2}$ in (A. 5) by $(J-\frac{1}{2})$ the result is

$$O_2^0 = 2\,JJ_1 - 6\,J_1\,a^+a^-$$
$$O_2^2 = 2\,J_1\,\tfrac{1}{2}(a^+a^+ + a^-a^-)$$
$$O_4^0 = 8\,JJ_3 - 80\,J_3\,a^+a^-$$
$$O_4^2 = 12\,J_3\,\tfrac{1}{2}(a^+a^+ + a^-a^-)$$
$$O_6^0 = 16\,JJ_5 - 336\,J_5\,a^+a^-$$
$$O_6^2 = 32\,J_5\,\tfrac{1}{2}(a^+a^+ + a^-a^-)$$
$$O_4^4 = O_6^4 = O_6^6 = 0 \qquad \text{(A. 6)}$$

and further

$$O_2^{-1} = \sqrt{(2J)}\,J_1(a^+ + a^-)$$
$$O_2^1 = i\sqrt{(2J)}\,J_1(a^+ - a^-)$$
$$O_2^{-2} = i\,J_1(a^+a^+ - a^-a^-)$$
$$O_4^1 = -i\sqrt{(2J)}\,J_3(a^+ - a^-)$$
$$O_4^3 = 21\sqrt{(2J)}\,J_3(a^+ - a^-)$$

where we have used the abbreviation

$$J_n = (J - \tfrac{1}{2})(J - 1) \ldots . (J - \tfrac{n}{2}) . \qquad (A.7)$$

The matrix elements of the spin operator expressions can be calculated more directly at $T = 0^oK$. Instead of using the Holstein - Primakoff transformation we can use the relations

$$\begin{aligned} J_z|m\rangle &= J|m\rangle \\ J_+|m\rangle &= [J(J+1) - m(m+1)]^{1/2}|m+1\rangle \\ J_-|m\rangle &= [J(J+1) - m(m-1)]^{1/2}|m-1\rangle \end{aligned} \qquad (A.8)$$

and the commutation relations

$$[J_z, J_+] = J_+ , \qquad [J_z, J_-] = -J_- , \qquad [J_+, J_-] = 2 J_z . \qquad (A.9)$$

The matrix elements to be evaluated at $T = 0^oK$ are $\langle J|0_1^m|J\rangle = \langle 0_1^m\rangle$, and we have

$$\begin{aligned} &\langle J_z^n\rangle = J^n \\ &\langle J_x^2\rangle = \langle J_y^2\rangle = \tfrac{1}{2} J \\ &\langle J_x^4\rangle = \langle J_y^4\rangle = \tfrac{3}{4} J^2 - \tfrac{1}{4} J \\ &\langle J_x^6\rangle = \langle J_y^6\rangle = \tfrac{15}{8} J^2(J-1) + \tfrac{1}{2} J \\ &\langle \tfrac{1}{2}(J_x^2 J_y^2 + J_y^2 J_x^2)\rangle = -\tfrac{1}{4} J^2 + \tfrac{1}{4} J . \end{aligned} \qquad (A.10)$$

The matrix elements found in this way are in accordance with (A. 6).

In the case where $\hat{z}$ makes an angle, θ, with the ζ-axis, we make use of the following transformation:

$$\begin{aligned} J_\xi &= J_z \sin\theta\cos\varphi - J_x \cos\theta\cos\varphi + J_y \sin\varphi \\ J_\eta &= J_z \sin\theta\sin\varphi - J_x \cos\theta\sin\varphi - J_y \cos\varphi \\ J_\zeta &= J_z \cos\theta + J_x \sin\theta . \end{aligned} \qquad (A.11)$$

This corresponds to (A. 2) when $\theta = \pi/2$. Using (A. 8) and (A. 9), we find at $T = 0^{o}K$

$$\begin{aligned}
\langle Q_2^2 \rangle &= JJ_1 \sin^2\theta\cos 2\varphi \\
\langle Q_2^0 \rangle &= JJ_1(3\cos^2\theta - 1) \\
\langle Q_2^{-2} \rangle &= JJ_1 \sin^2\theta \sin 2\varphi \\
\langle Q_4^4 \rangle &= JJ_3 \sin^4\theta\cos 4\varphi \\
\langle Q_4^{-4} \rangle &= JJ_3 \sin^4\theta \sin 4\varphi \\
\langle Q_4^2 \rangle &= \tfrac{7}{4}\, JJ_3 \sin^2 2\theta\cos 2\varphi - JJ_3 \sin^2\theta\cos 2\varphi \\
\langle Q_4^{-2} \rangle &= \tfrac{7}{4}\, JJ_3 \sin^2 2\theta \sin 2\varphi - JJ_3 \sin^2\theta \sin 2\varphi \\
\langle Q_6^6 \rangle &= JJ_5 \sin^6\theta\cos 6\varphi
\end{aligned} \qquad (A.12)$$

and further

$$\begin{aligned}
\langle Q_2^{-1} \rangle &= JJ_1 \sin 2\theta\cos\varphi \\
\langle Q_2^1 \rangle &= JJ_1 \sin 2\theta \sin\varphi .
\end{aligned}$$

APPENDIX B

The One-Magnon One-Phonon Hamiltonian

The Hamiltonian

$$\tilde{H} = \sum_q \varepsilon_q a_q^+ a_q + iV_q[(a_q^+ + a_{-q})\beta_q - (a_q + a_{-q}^+)\beta_q^+] + \omega_q \beta_q^+ \beta_q \qquad (B.1)$$

where

$$V_q = V_q^* = -V_{-q} \qquad (B.2)$$

can be diagonalized exactly by means of three successive canonical transformations.

1 Transformation

$$a_q = a_q \cos\theta_q + ib_q \sin\theta_q \qquad (B.3)$$

$$\beta_q = b_q \cos\theta_q + ia_q \sin\theta_q \qquad (B.4)$$

where

$$\tan 2\theta_q = 2V_q/(\omega_q - \varepsilon_q), \qquad \theta_{-q} = -\theta_q \qquad (B.5)$$

which results in

$$\tilde{H} = \sum_q \varepsilon'_q a_q^+ a_q + \tilde{H}'_q + \omega'_q b_q^+ b_q \qquad (B.6)$$

where

$$\varepsilon'_q = \varepsilon_q \cos^2\theta_q + \omega_q \sin^2\theta_q - V_q \sin 2\theta_q \qquad (B.7)$$

$$\tilde{H}'_q = iV_q[(a_{-q}b_q - a_{-q}^+ b_q^+)\cos 2\theta_q + i\sin 2\theta_q \tfrac{1}{2}(a_{-q}a_q + a_{-q}^+ a_q^+ - b_{-q}b_q - b_{-q}^+ b_q^+)] \qquad (B.8)$$

$$\omega'_q = \omega_q \cos^2\theta_q + \varepsilon_q \sin^2\theta_q + V_q \sin 2\theta_q \,. \qquad (B.9)$$

2 Transformation

$$a_q = \gamma_q \cosh\varphi_q + i\tau^+_{-q} \sinh\varphi_q \tag{B.10}$$

$$b_q = \tau_q \cosh\varphi_q + i\gamma^+_{-q} \sinh\varphi_q \tag{B.11}$$

where

$$\sinh 2\varphi_q = 2V_q \cos 2\theta_q / (\omega'_q - \varepsilon'_q) \quad , \qquad \varphi_{-q} = -\varphi_q \, , \tag{B.12}$$

and we find

$$\tilde{H} = \sum_q \varepsilon''_q \gamma^+_q \gamma_q + \tilde{H}''_q + \omega''_q \tau^+_q \tau_q \tag{B.13}$$

where

$$\varepsilon''_q = \varepsilon'_q \cosh^2\varphi_q + \omega'_q \sinh^2\varphi_q - V_q \cos 2\theta_q \sinh 2\varphi_q \tag{B.14}$$

$$\tilde{H}''_q = \frac{1}{2} V_q \sin 2\theta_q \cosh 2\varphi_q \left[(\tau^+_q \tau^+_{-q} + \tau_q \tau_{-q}) - (\gamma^+_q \gamma^+_{-q} + \gamma_q \gamma_{-q}) \right] \tag{B.15}$$

$$\omega''_q = \omega'_q \cosh^2\varphi_q + \varepsilon'_q \sinh^2\varphi_q + V_q \cos 2\theta_q \sinh 2\varphi \, . \tag{B.16}$$

3 Transformation. This transformation is identical with the one used in the spin wave theory (2. 7) and (2.11) and will not be written down here.

The V_q-term in the Hamiltonian (B. 1) gives rise to energy gaps in the magnon and the phonon energy spectrum at the nominal crossing points of the magnon and phonon dispersion relations which are

$$\Delta = \left| \left[\varepsilon_q (\varepsilon_q + 2V_q) \right]^{1/2} - \left[\varepsilon_q (\varepsilon_q - 2V_q) \right]^{1/2} \right| \tag{B.17}$$

or

$$\Delta \tilde{=} 2 |V_q| \qquad \text{when} \quad |V_q| \ll \varepsilon_q \, . \tag{B.18}$$

In the limit of small wave vectors ($q \to 0$) both ω_q and V_q are going to zero, whereas ε_q remains finite so that

$$\omega_q \ll \varepsilon_q \qquad \text{and} \quad |V_q| \ll \varepsilon_q \qquad \text{when} \quad q \to 0 \, . \tag{B.19}$$

Thus we find

$$\Delta\omega_{q \to 0} = \omega''_q - \omega_q = - 2V_q^2/\varepsilon_q . \qquad \text{(B. 20)}$$

APPENDIX C

The Two-Magnon One-Phonon Hamiltonian

The Hamiltonian to be considered is

$$H = H_o + \lambda H_1 \tag{C.1}$$

where the nonperturbed Hamiltonian is

$$H_o = \sum_q \varepsilon_o(q) a_q^+ a_q + \sum_k \omega_o(k) \beta_k^+ \beta_k \,, \tag{C.2}$$

and the perturbation is

$$H_1 = \sum_{q,k} [\, U(k,q) a_{q+k}^+ a_q + V(k,q) \tfrac{1}{2} (a_{q+k}^+ a_{-q}^+ + a_q a_{-q-k})] \cdot (\beta_k + \beta_{-k}^+) \tag{C.3}$$

where

$$U(k,-q-k) = U(k,q) \,, \qquad U^*(k,q) = U(-k,-q) \tag{C.4}$$

and further

$$U(k,q) \to 0 \qquad \text{when} \quad k \to 0 \tag{C.5}$$

and the similar relations for $V(k,q)$. These relations ensure that H_1 is a hermitean operator.

The Hamiltonian (C.1) can be diagonalized approximately with the equation of motion method. This is essentially a second-order perturbation calculation, and the perturbation parameter, λ, is introduced to ensure a consistent solution of the Hamiltonian corresponding to λ equal to one.

$$[[\pi_q, H], \pi_q^+] = \varepsilon(q) \qquad \text{and} \qquad [[a_q, H_o], a_q^+] = \varepsilon_o(q) \tag{C.6}$$

where

$$\varepsilon(q) = \varepsilon_o(q) + \lambda \varepsilon_1(q) + \lambda^2 \varepsilon_2(q) + \ldots\ldots \tag{C.7}$$

$$\pi_q = a_q + \lambda a1_q + \lambda^2 a2_q + \ldots\ldots \,. \tag{C.8}$$

First the Hamiltonian is diagonalized to first power in λ, and we have

$$[\pi_q, H] = \varepsilon_0(q)a_q + \lambda([a1_q, H_0] + [a_q, H_1])$$
$$= \varepsilon_0(q)a_q + \lambda[\varepsilon_1(q)a_q + \varepsilon_0(q)a1_q] \quad . \tag{C.9}$$

The new operators have to fulfil the Bose commutation relations, that is

$$[\pi_q, \pi_q^+] = 1 + \lambda([a_q, a1_q^+] + [a1_q, a_q^+]) = 1 \quad . \tag{C.10}$$

Owing to the vanishing of the interaction amplitudes when k goes to zero (C. 5), we have

$$[[a_q, H_1], a_q^+] = 0 \quad \text{and} \quad [[[a1_q, a_q^+], H_0], H_0] = 0 \quad . \tag{C.11}$$

These three equations give as results

$$\varepsilon_1(q) = 0 \tag{C.12}$$

$$[a1_q, a_q^+] = 0 \tag{C.13}$$

$$\varepsilon_0(q)a1_q = [a1_q, H_0] + [a_q, H_1] \quad . \tag{C.14}$$

The first-order contribution to $\varepsilon(q)$ is zero, and $a1_q$ is given implicitly by equations (C. 13) and (C. 14).

To second power in λ we have

$$[\pi_q, \pi_q^+] = 1 + \lambda^2([a1_q, a1_q^+] + [a2_q, a_q^+] + [a_q, a2_q^+]) = 1 \quad , \tag{C.15}$$

and from

$$[[\pi_q, H], \pi_q^+] = \varepsilon_0(q) + \lambda^2\varepsilon_2(q) \tag{C.16}$$

we find

$$\varepsilon_2(q) = \varepsilon_0(q)[a1_q, a1_q^+] + \varepsilon_0(q)[a_q, a2_q^+] + [[a1_q, H_1], a_q^+] + [[a2_q, H_0], a_q^+] . \tag{C.17}$$

This expression can be reduced by using the relations above

$$\varepsilon_2(q) = [\alpha 1_q, [H_1, \alpha_q^+]] - \frac{1}{2}[[\alpha 1_q, \alpha 1_q^+], H_o] . \tag{C.18}$$

When calculating the energy change we neglect all terms which are not diagonal in magnon and phonon operators. In the actual case we find

$$\langle [[\alpha 1_q, \alpha 1_q^+], H_o] \rangle = 0 , \tag{C.19}$$

and we have finally

$$\Delta\varepsilon(q) = \varepsilon(q) - \varepsilon_o(q) = \langle [\alpha 1_q, [H_1, \alpha_q^+]] \rangle . \tag{C.20}$$

By means of completely identical calculations we obtain

$$\Delta\omega(k) = \langle [\beta 1_k, [H_1, \beta_k^+]] \rangle \tag{C.21}$$

where

$$\alpha 1_q = \sum_k \frac{U(k,-q)}{\varepsilon(q) - \varepsilon(q-k) - \omega(k)} \alpha_{q-k}\beta_k - \frac{U(k,q)}{\varepsilon(q) - \varepsilon(q+k) + \omega(k)} \alpha_{q+k}\beta_k^+$$

$$+ \frac{V(k,-q)}{\varepsilon(q) + \varepsilon(q-k) - \omega(k)} \alpha_{-q+k}^+\beta_k - \frac{V(k,q)}{\varepsilon(q) + \varepsilon(q+k) + \omega(k)} \alpha_{-q-k}^+\beta_k^+ \tag{C.22}$$

and

$$\beta 1_k = \sum_q - \frac{U(k,q)}{\varepsilon(q) - \varepsilon(q+k) + \omega(k)} \alpha_q^+\alpha_{q+k} + \frac{1}{2}\frac{V(k,q)}{\varepsilon(q) + \varepsilon(q+k) - \omega(k)} \alpha_{q+k}\alpha_{-q}$$

$$- \frac{1}{2}\frac{V(k,q)}{\varepsilon(q) + \varepsilon(q+k) + \omega(k)} \alpha_q^+\alpha_{-q-k}^+ \tag{C.23}$$

$\varepsilon(q)$ and $\omega(k)$ without indices refer now to the unperturbed values.

Until now we have only considered the case where we have one magnon mode and one single phonon mode. In the actual case we have an acoustic and an optical magnon mode and furthermore six phonon modes; instead of H_1 (C. 3) we have

$$\tilde{H}^{(2)}_{S-L} = \sum_{ij}^{2} \sum_{s}^{6} \sum_{q,k} [U^{s}_{ij}(k,q) a^{+}_{i,q+k} a_{j,q} + V^{s}_{ij}(k,q) \frac{1}{2} (a^{+}_{i,q+k} a^{+}_{j,-q} + a_{i,-q-k} a_{j,q})] \cdot [\beta_{s,k} + \beta^{+}_{s,-k}] \tag{C.24}$$

where

$$U^{s}_{ij}(k,-q-k) = U^{s}_{ji}(k,q), \quad U^{s*}_{ij}(k,q) = U^{s}_{ij}(-k,-q) \text{ and } U^{s}_{ij}(0,q) = 0. \tag{C.25}$$

Defining

$$G(\pm i, \pm j, \pm s) = \frac{1}{\pm \varepsilon_i(q) \pm \varepsilon_j(q+k) \pm \omega_s(k)} \tag{C.26}$$

where the upper or lower signs correspond to each other, we have the following second-order changes in energies

$$\Delta\omega_s(k) = -\sum_{ij} \sum_{q} \{|U^{s}_{ij}(k,q)|^2 [G(+j,-i,-s) + G(+j,-i,+s)] + |V^{s}_{ij}(k,q)|^2 [G(+j,+i,-s) + G(+j,+i,+s)]\} \cdot [\langle a^{+}_{i,q+k} a_{i,q+k} \rangle + \frac{1}{2}], \tag{C.27}$$

and for the magnon energies

$$\Delta\varepsilon_j(q) = \sum_{i,s} \sum_{k} \{|U^{s}_{ij}(k,q)|^2 [G(+j,-i,-s) + G(+j,-i,+s)] - |V^{s}_{ij}(k,q)|^2 [G(+j,+i,-s) + G(+j,+i,+s)]\} \cdot [\langle \beta_{s,k} \beta_{s,k} \rangle + \frac{1}{2}] + \{|U^{s}_{ij}(k,q)|^2 [G(+j,-i,-s) - G(+j,-i,+s)] + |V^{s}_{ij}(k,q)|^2 [G(+j,+i,-s) - G(+j,+i,+s)]\} \cdot [\langle a^{+}_{i,q+k} a_{i,q+k} \rangle + \frac{1}{2}]. \tag{C.28}$$

In the limit of small k it is possible to reduce expression (C. 27) for the change in energy of acoustic phonons. Using the relations

$$U^s_{ij}(k, -q-k) = U^s_{ij}(k, q) \rightarrow \delta_{ij} U^s_{ij}(k, q) \quad \text{when } k \rightarrow 0 \tag{C. 29}$$

(this holds only for acoustic phonons), and defining

$$\langle a^+_{i,q} a_{i,q} \rangle = n_i(q) = 1/[\exp\beta\epsilon_i(q) - 1], \quad \beta = 1/k_B T, \tag{C. 30}$$

we have

$$\Delta\omega_s(k)_{k\to 0} = -\sum_{q,i} \{ \tfrac{1}{2} |U^s_{ii}(k, q)|^2 [G(+i, -i, -s) + G(+i, -i, +s)] \cdot$$
$$\cdot [n_i(q+k) - n_i(q)] + |V^s_{ii}(k, q)|^2 n_i(q)/\epsilon_i(q) \}. \tag{C. 31}$$

In this limit of small k vectors we have

$$n(q+k) - n(q) \cong \vec{k} \cdot \nabla_q n(q) = -n(q)[n(q) + 1] \beta \vec{k} \cdot \nabla_q \epsilon(q) \tag{C. 32}$$

and further

$$G(+i, -i, -s) \cong 1/[-\vec{k} \cdot \nabla_q \epsilon(q) - \omega_s(k)]. \tag{C. 33}$$

For temperatures and frequencies where

$$\tfrac{1}{4} \beta^2 \omega_s^2(k) [n(q) + 1] [2n(q) + 1] \ll 1, \tag{C. 34}$$

we obtain the following expression for the change in energies of phonons with long wave lengths:

$$\Delta\omega_s(k) = \sum_{q,i} [|U^s_{ii}(k, q)|^2 \partial n_i(q)/\partial\epsilon_i(q) - |V^s_{ii}(k, q)|^2 n_i(q)/\epsilon_i(q)]. \tag{C. 35}$$

The derivation of this expression from (C. 27), which is valid in a frequency and temperature region where (C. 34) is fulfilled, is not immediately apparent. Because of that we shall go through the arguments that lead to these expressions. Neglecting the indices for the different modes we have (we shall only consider the first (U^s_{ij}-) part of (C. 27), the treatment of the other (V^s_{ij}-) part is obvious)

$$\Delta\omega(k) = -\sum_q U^2_{k,q}\left(\frac{1}{\varepsilon_1(k,q)}+\frac{1}{\varepsilon_2(k,q)}\right)\cdot n_{q+k} \qquad (C.36)$$

where

$$\varepsilon_1(k,q) = 1/G(+i,-i,-s) = \varepsilon(q) - \varepsilon(q+k) - \omega(k) = -\varepsilon_2(k,-q-k) \quad (C.37)$$

$$\varepsilon_2(k,q) = 1/G(+i,-i,+s) = \varepsilon(q) - \varepsilon(q+k) + \omega(k) = -\varepsilon_1(k,-q-k). \quad (C.38)$$

(C. 36) is just (the first part of) expression (C. 27) written in another way. Using condition (C. 4) or (C. 29) in addition to (C. 37-38), we have

$$\Delta\omega(k) = +\sum_q U^2_{k,q}\left(\frac{1}{\varepsilon_1(k,q)}+\frac{1}{\varepsilon_2(k,q)}\right)\cdot n_{-q}, \quad n_q = n_{-q} \qquad (C.39)$$

or

$$\Delta\omega(k) = -\frac{1}{2}\sum_q U^2_{k,q}\left(\frac{1}{\varepsilon_1(k,q)}+\frac{1}{\varepsilon_2(k,q)}\right)(n_{q+k}-n_q) \qquad (C.40)$$

corresponding to expression (C. 31). In the limit of small k vectors we can use the approximations (C. 32) and (C. 33)

$$\Delta\omega(k) = \frac{1}{2}\sum_q U^2_{k,q}\left(\frac{k\nabla\varepsilon(q)}{k\nabla\varepsilon(q)+\omega(k)}+\frac{k\nabla\varepsilon(q)}{k\nabla\varepsilon(q)-\omega(k)}\right)\beta n_q(n_q+1) \qquad (C.41)$$

so that

$$\Delta\omega(k) = -\sum_q U^2_{k,q}\beta n_q(n_q+1) + \Delta_1\omega(k) = \Delta_o\omega(k) + \Delta_1\omega(k) \qquad (C.42)$$

where

$$\Delta_1\omega(k) = -\frac{1}{2}\sum_q U^2_{k,q}\left(\frac{1}{\varepsilon_1(k,q)}-\frac{1}{\varepsilon_2(k,q)}\right)\omega(k)\beta n_q(n_q+1). \qquad (C.43)$$

Using the same procedure once more we obtain for $\Delta_1\omega(k)$

$$\Delta_1\omega(k) = \frac{1}{4}\beta\omega(k)\sum_q U^2_{k,q}\left(\frac{1}{\varepsilon_1(k,q)}-\frac{1}{\varepsilon_2(k,q)}\right)(n^2_{q+k}+n_{q+k}-n^2_q-n_q) \quad (C.44)$$

and

$$\Delta_1\omega(k) = \frac{1}{4}\beta^2\omega(k)\sum_q U^2_{k,q}\left(\frac{k\nabla\varepsilon(q)}{k\nabla\varepsilon(q)+\omega(k)}-\frac{k\nabla\varepsilon(q)}{k\nabla\varepsilon(q)-\omega(k)}\right)n_q(n_q+1)(2n_q+1) \qquad (C.45)$$

which finally leads to

$$\Delta_1 \omega(k) = \frac{1}{4} \beta^2 \omega^2(k) \sum_q U^2_{k,q} \left(\frac{1}{\varepsilon_1(k,q)} + \frac{1}{\varepsilon_2(k,q)} \right) n_q (n_q + 1)(2n_q + 1). \quad \text{(C. 46)}$$

This expression can be compared with expression (C. 39) for $\Delta\omega(k)$, and when the inequality (C. 34) is fulfilled, we have

$$\Delta\omega(k) \cong \Delta_0 \omega(k) \quad \text{(C. 47)}$$

corresponding to the result given above. For frequencies used in a ultrasonic experiment (C. 34) is fulfilled from $T = 0.1\,^{\circ}K$ up to $T = T_c$ (as long as $\varepsilon(0)$ is finite).

REFERENCES

1) D. E. Hegland, S. Legvold, and F. H. Spedding, Phys. Rev. 131, 158 (1963).

2) D. R. Behrendt, S. Legvold, and F. H. Spedding, Phys. Rev. 109, 1544 (1958).

3) A. R. Mackintosh and H. Bjerrum Møller, Magnetic Properties of Rare Earth Metals, edited by R. J. Elliott, chapter 5 (to be published).

4) R. J. Elliott and K. W. H. Stevens, Proc. R. Soc. A, 218, 553 (1953), ibid. 219, 387 (1953).

5) M. S. S. Brooks, D. A. Goodings, and H. I. Ralph, J. Phys. C 1, 132 (1968).

6) J. J. Rhyne and A. E. Clark, J. Appl. Phys. 38, 1379 (1967).

7) W. P. Mason, Phys. Rev. 96, 302 (1954).

8) E. Callen and H. B. Callen, Phys. Rev. 139, A 455 (1965).

9) J. J. Rhyne and S. Legvold, Phys. Rev. 138, A 507 (1965).

10) A. E. Clark, B. F. DeSavage, and R. Bozorth, Phys. Rev. 138, A 216 (1965).

11) P. De V. Du Plessis, Phys. Mag. 18, 145-169 (1968).

12) M. Nielsen, H. Bjerrum Møller, P. A. Lindgård, and A. R. Mackintosh, Phys. Rev. Letters 25, 1451 (1970).

13) B. R. Cooper, Solid State Physics, edited by F. Seitz and D. Turnbull (Academic Press, New York), vol. 21, 393-490 (1968).

14) B. R. Cooper, Phys. Rev. Letters 19, 900 (1967).

15) W. E. Evenson and S. H. Liu, Phys. Rev. 178, 783 (1969).

16) M. Rosen and H. Klimker, Phys. Rev. B1, 3748 (1970).

17) T. Holstein and H. Primakoff, Phys. Rev. 58, 1098 (1940).

18) M. S. S. Brooks, Phys. Rev. B1, 2257 (1970).

19) P. A. Lindgård, A. Kowalska, and P. Laut, J. Phys. Chem. Solids 28, 1357 (1967).

20) B. R. Cooper, R. J. Elliott, S. J. Nettel, and H. Suhl, Phys. Rev. 127, 57 (1962).

21) J. Smit and H.G. Belgers, Philips Research Repts. 10, 113 (1955).

22) H.B. Huntington, Solid State Physics, edited by F. Seitz and D. Turnbull (Academic Press, New York) vol. 7, 213 (1958).

23) J. Jensen, Thesis, Technical University of Denmark (1968).

24) J. Jensen, Intern. J. Magnetism 1, 271 (1971).

25) A.R. Wazzan, R.S. Vitt, and L.B. Robinson, Phys. Rev. 159, 400 (1967).

26) E.A. Turov and V.G. Shavrov, Fiz. Tverd. Tela 7, 217 (1965). English transl.: Soviet Phys. Solid State 7, 166 (1965).

27) T.J. Moran and B. Lüthi, J. Phys. Chem. Solids, 31, 1735 (1970), B. Lüthi, T.J. Moran and R.J. Pollina, ibid., 31, 1741 (1970).

28) E. Schlömann, J. Appl. Phys. 31, 1647 (1960).

29) M. Rosen, Phys. Rev. 174, 504 (1968).

30) E.S. Fisher and D. Dever, Trans. Met. Soc. AIME, 239, 48 (1967).

31) M. Long Jr., A.R. Wazzan, and R. Stern, Phys. Rev. 178, 775 (1969).

32) S.B. Palmer, J. Phys. Chem. Solids, 31, 143 (1970).

33) S.B. Palmer and E.W. Lee, Preprint.

34) H. Bjerrum Møller, J.C. Gylden Houmann, and A.R. Mackintosh, J. Appl. Phys. 39, 807 (1968).

35) H. Bjerrum Møller, J.C. Gylden Houmann, M. Nielsen, and A.R. Mackintosh, (to be published).

36) R.M. Nicklow, N. Wakabayashi, M.K. Wilkinson, and R.E. Reed, Phys. Rev. Letters 26, 140 (1971).

37) J.C. Gylden Houmann and R.M. Nicklow, Phys. Rev. B1, 3943 (1970), J.C. Gylden Houmann (private communication).

38) P.A. Lindgård, J. De Physique, 32, C1-238 (1971).

39) N. Tsuya, A.E. Clark, and R.M. Bozorth, Proceedings of the International Conference on Magnetisk, Nottingham, 250 (1964).

40) E. Abrahams and C. Kittel, Phys. Rev. 88, 1200 (1952) and Rev. Modern Phys. 25, 233 (1953).

41) H.S. Marsh and A.J. Sievers, J. Appl. Phys. 40, 1563 (1969), A.J. Sievers, J. Appl. Phys. 41, 980 (1970).

42) T. K. Wagner and J. L. Stanford, Phys. Rev. 184, 505 (1969).

43) F. C. Rossol and R. V. Jones, J. Appl. Phys. 37, 1227 (1966), F. C. Rossol, Ph. D. Thesis, Harvard University, Cambridge, Mass. (1966).

44) D. M. S. Bagguley and J. Liesegang, Proc. Roy. Soc. A 300, 497 (1967).

45) T. K. Wagner and J. L. Stanford, Phys. Rev. B1, 4488 (1970).

46) D. T. Vigren and S. H. Liu, Phys. Rev. Letters 27, 674 (1971) and L. W. Hart and J. L. Stanford, ibid., 27, 676 (1971).

47) M. S. S. Brooks, Preprint.

48) H. J. McSkimin, Physical Acoustics, edited by W. P. Mason (Academic Press, New York) vol. I, part A (1964).

49) H. J. McSkimin, J. Acoust. Soc. Am. 22, 413 (1950).

50) F. J. Darnell, Phys. Rev. 132, 1098 (1963).

51) R. J. Pollina and B. Lüthi, Phys. Rev. 177, 841 (1969).

52) G. E. Laramore and L. P. Kadanoff, Phys. Rev. 187, 619 (1969).

53) H. S. Bennett, Phys. Rev. 185, 801 (1969).

54) H. Bjerrum Møller, J. C. Gylden Houmann and J. Jensen, (to be published).

	Tb	Tb (cal.)	Dy I	Dy II	Ho
c_{11}	7.15	7.38	7.07	7.31	7.61
c_{33}	7.88	8.00	7.90	7.81	7.76
c_{44}	2.22	2.31	2.48	2.40	2.57
c_{66}	2.30	2.04	2.46	2.39	2.57
c_{13}	2.1		2.08	2.23	2.06
ρ	8.204		8.545	8.560	8.800

Table I

Comparison between the five independent elastic constants at room temperature of Tb, of the calculated constants for Tb from ref. 37, of Dy I from ref. 16, of Dy II, and of Ho both from ref. 33. All the elastic constants are in 10^{11} erg/cm^3. The density at room temperature used in evaluation of the elastic constants is also shown (g/cm^3).

	Dy	Tb	Tb+10%Ho	σ^1	Tb	σ^1	σ^1
	macrosc.	macrosc.	neutron	Tb+10%Ho	neutron	Tb	theor.
$2J_1V_2^0$	4.3	5.5					2
$2P_2J$			4.80	2	7.08	2.1	2
$4c_\gamma(c^2+A^2)$	0.28	0.30	0.28	8	0.36	5.3	5
$6\mu_B H_o$	0.90	0.29	0.44	20	0.29	15.2	12/20
$18c_\gamma AC$	0.31	0.53	0.44	20	0.29	15.2	12
$36J_5V_6^6$			~0		~0	-	20
ΔN			~0		- 1.40	14.6	19/23

Table II

Anisotropy parameters in Tb and Dy at 4.2°K and the power law obeyed by these parameters as functions of the relative magnetization, σ (after refs. 6, 9, 10, 12, and 35). All values are in meV/ion.

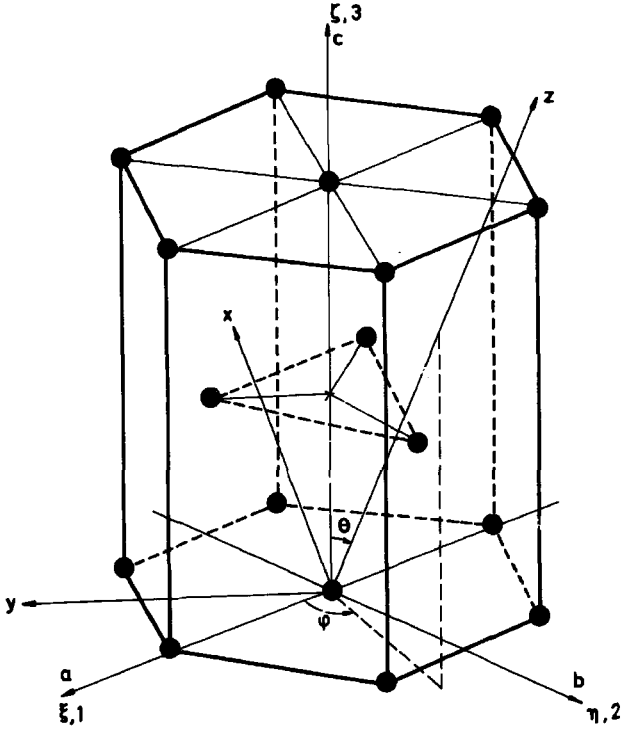

Fig. 1. The hexagonal close-packed structure and the definitions of the co-ordinate systems (ξ, η, ζ) identical with (1, 2, 3) and the (x, y, z) system defining the polar angles θ and φ.

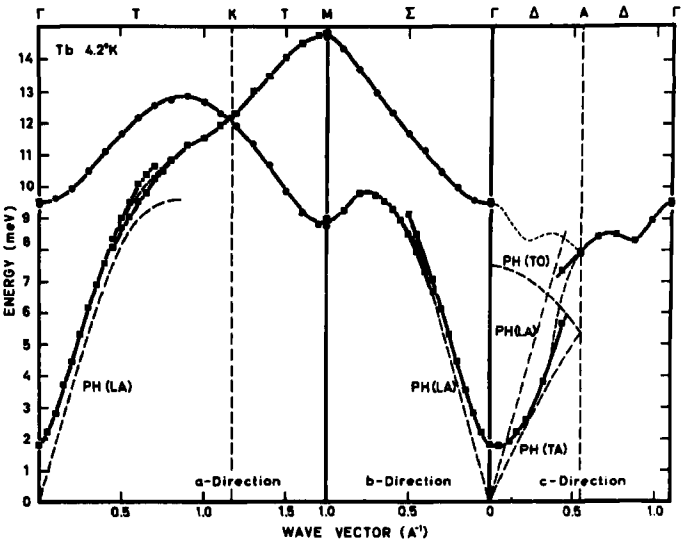

Fig. 2. Magnon dispersion relations for Tb along the symmetry lines in the Brillouin zone at 4.2°K. The effects of magnon - phonon interactions are also shown (after ref. 3).

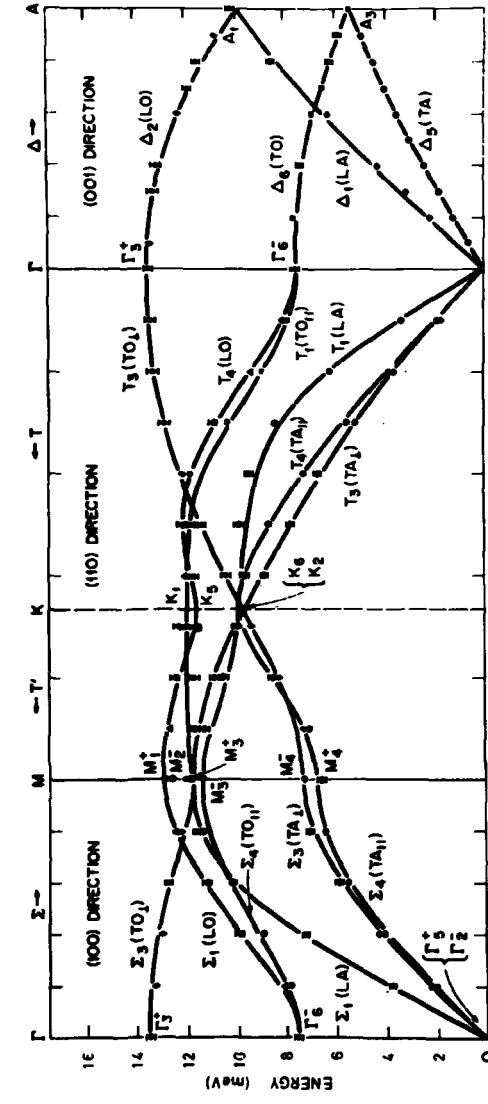

Fig. 3. Phonon dispersion relations for Tb in the symmetry directions at room temperature (after ref. 37).

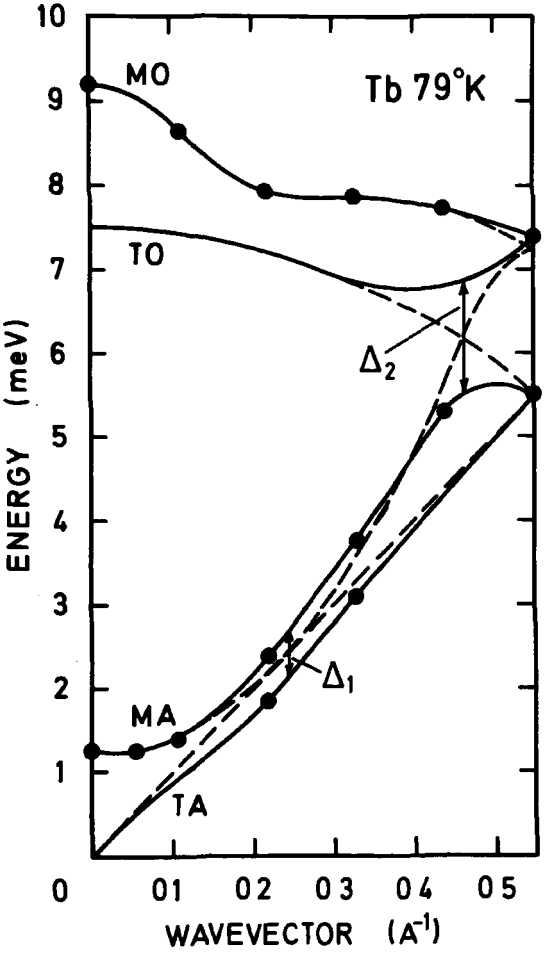

Fig. 4. The magnon and transverse phonon (TA, TO) dispersion relations for Tb in the c-direction at 79°K. The magnon - phonon interaction causes a mixing of the modes and energy gaps Δ_1 and Δ_2 at the crossing points of the unperturbed dispersion relations, indicated by dashed lines.

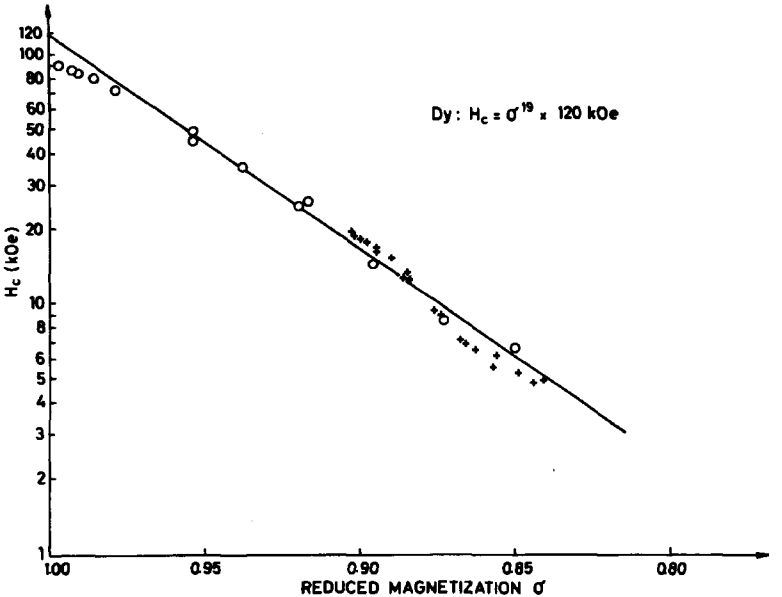

Fig. 5. Comparison between the critical field, H_c, in Dy determined by magnetic anisotropy measurements (o, after ref. 6) and the resonance field obtained in the ferromagnetic resonance experiment at 37 GHz (+, after ref. 43).

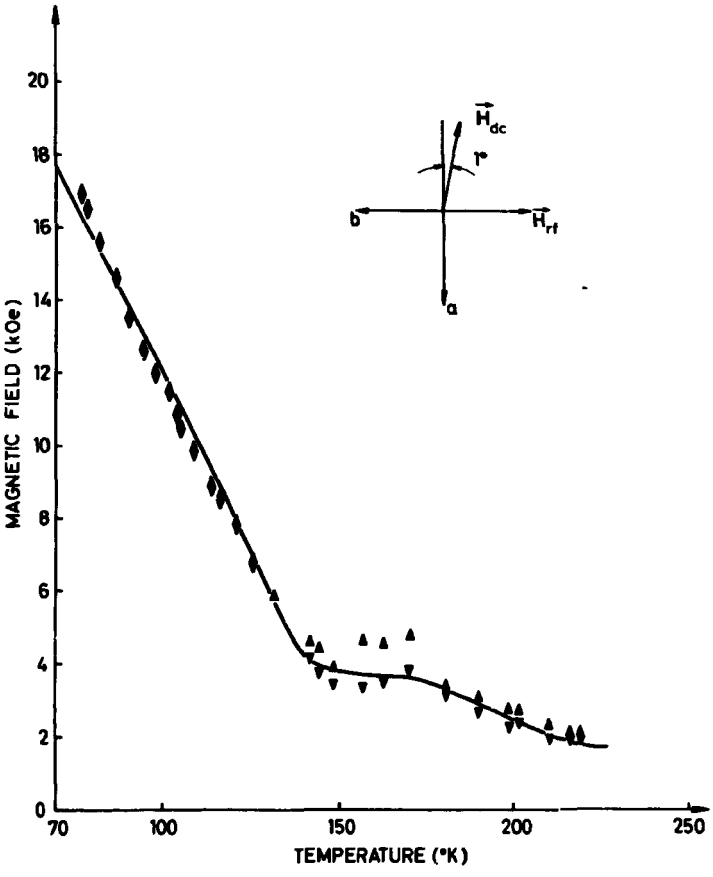

Fig. 6. Plot of the field values of power-absorption maxima as functions of temperature, compared with the calculation by Vigren and Liu of Cooper's free-lattice-model absorption maxima at 24 GHz for H_{dc} along the a-axis (after ref. 46).

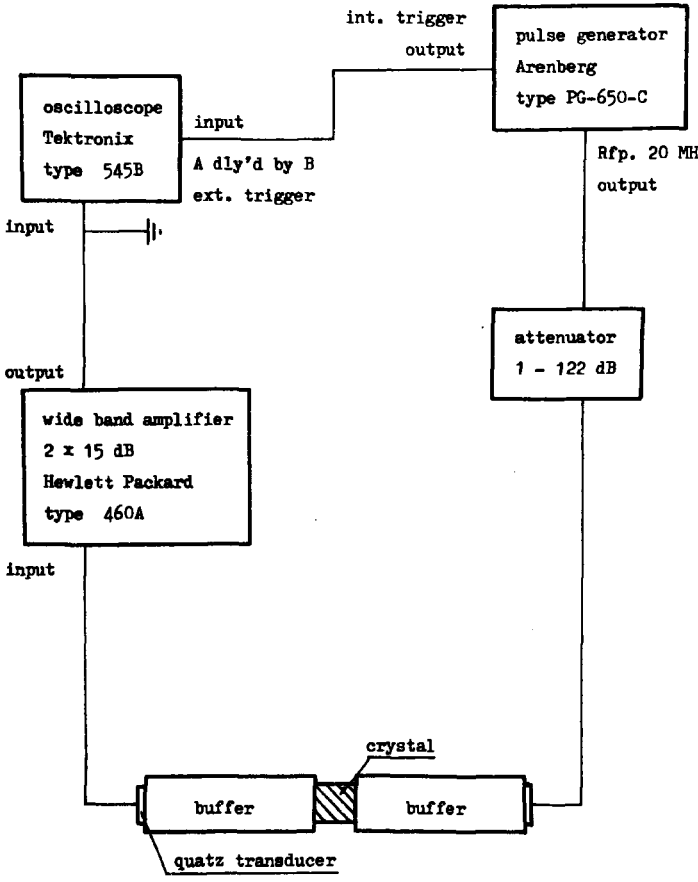

Fig. 7. Simplified diagram showing the experimental set-up for ultrasonic measurements.

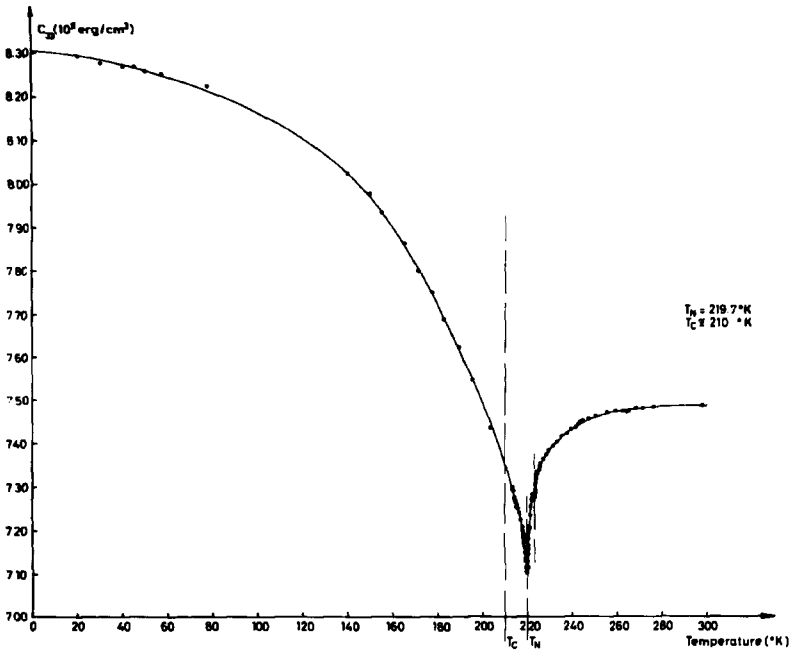

Fig. 8. The variation of c_{33} with temperature (0 - 300°K).

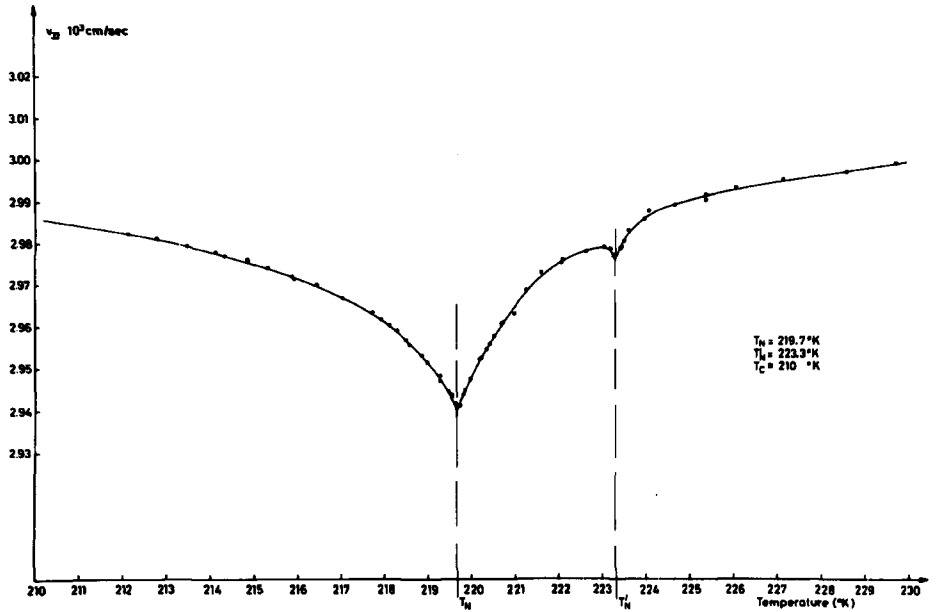

Fig. 9. The variation of the velocity of the longitudinal sound waves propagating in the c-direction (v_{33}) near the transition temperatures. A small critical change at T'_N and a more pronounced critical change at the transition temperature, T_N, of the main domain are shown.

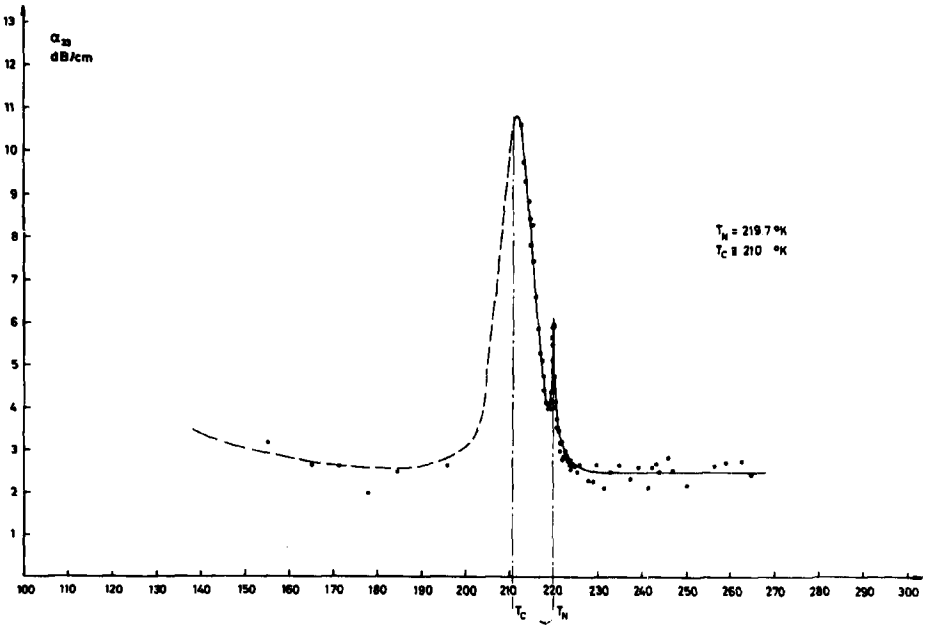

Fig. 10. The variation of the attenuation of v_{33} with temperature; the sound waves are greatly damped at T_N and at the Curie temperature, T_C.

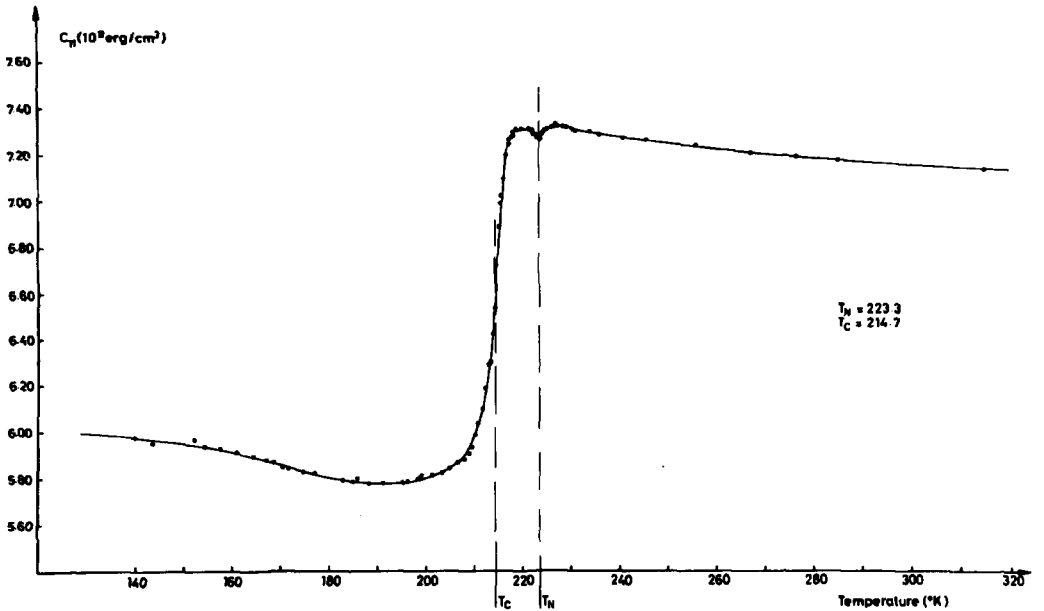

Fig. 11. The variation of c_{11} with temperature (140 - 320°K).

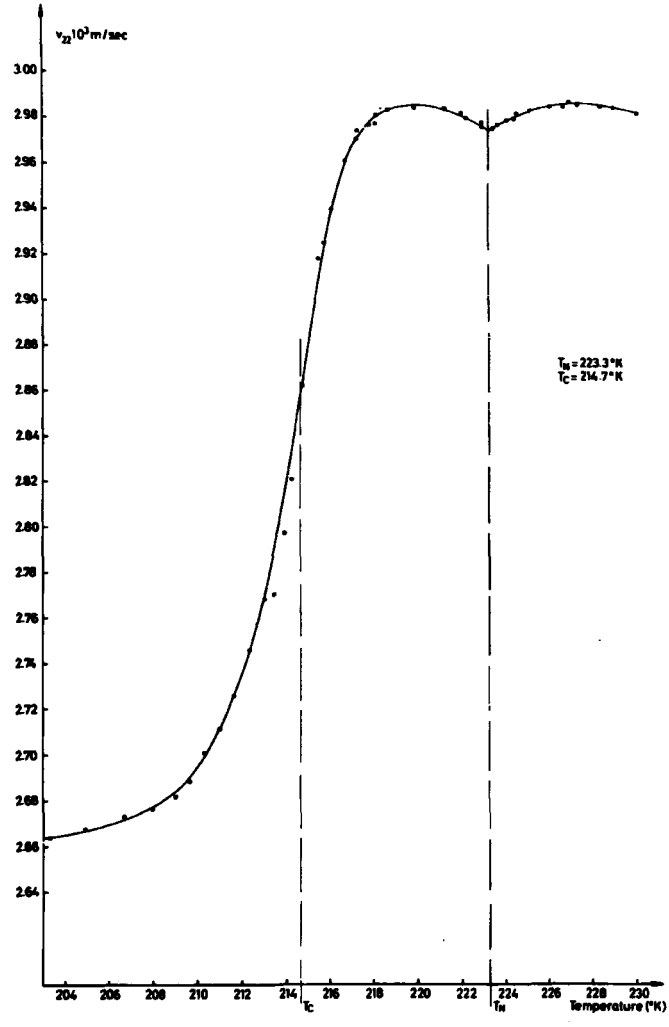

Fig. 12. The variation of the velocity of the longitudinal sound waves propagating in the b-direction (v_{22}) near the transition temperatures.

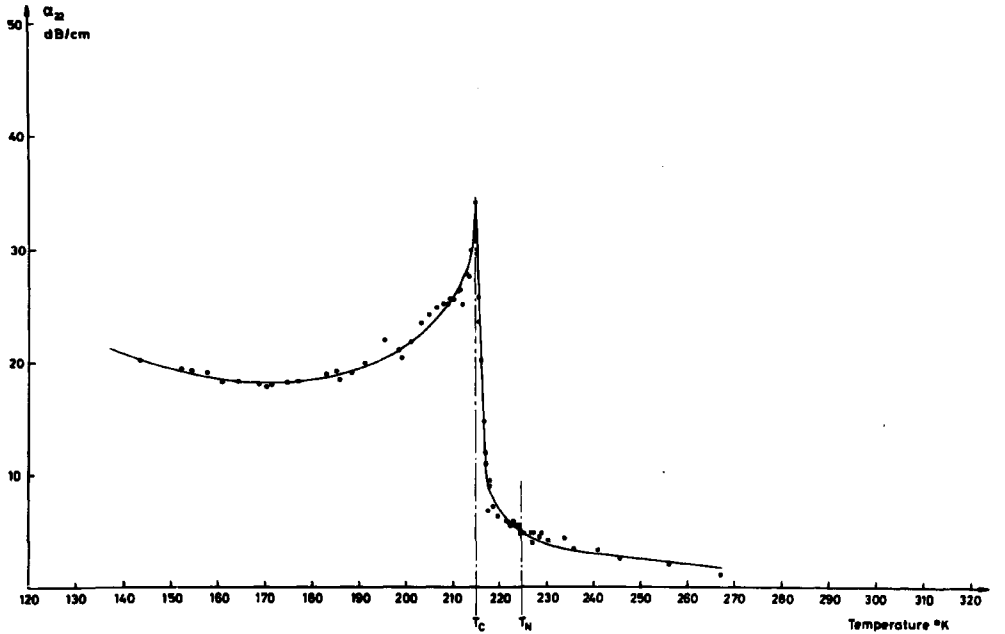

Fig. 13. The variation of the attenuation of v_{22} with temperature, determining T_C.

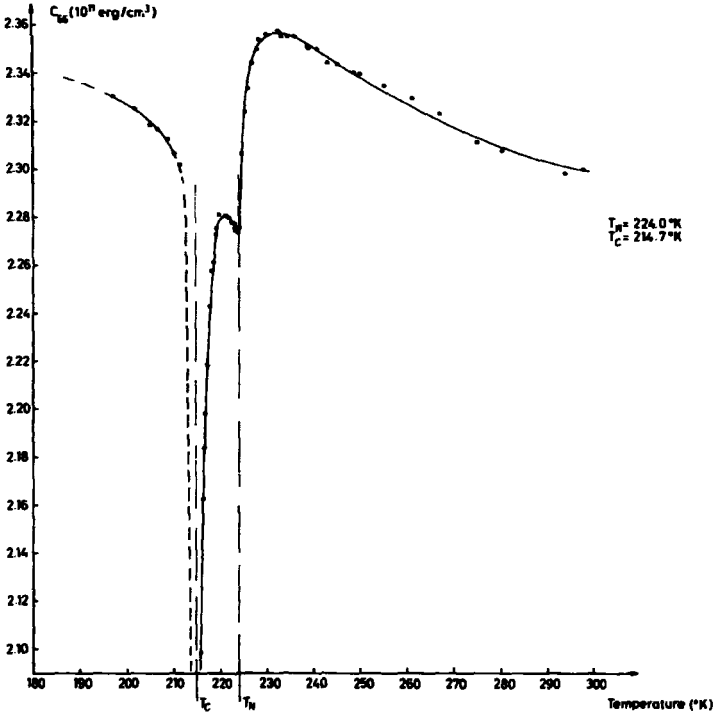

Fig. 14. The variation of c_{66} with temperature (200 - 300^{O}K).

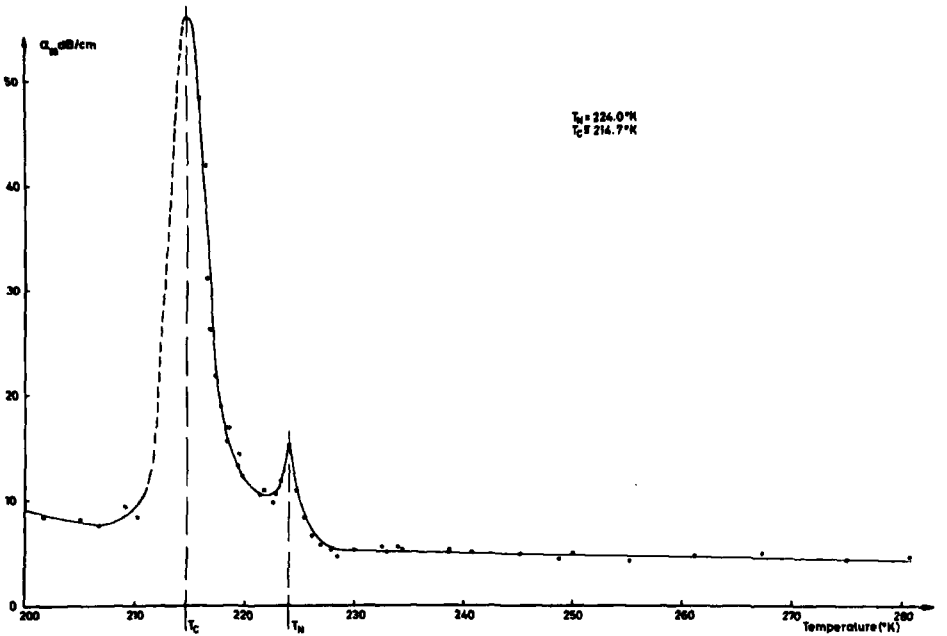

Fig. 15. The variation of the attenuation of the transverse sound waves polarized along an *a-axis* and propagating in a b-direction (α_{66}) with temperature.

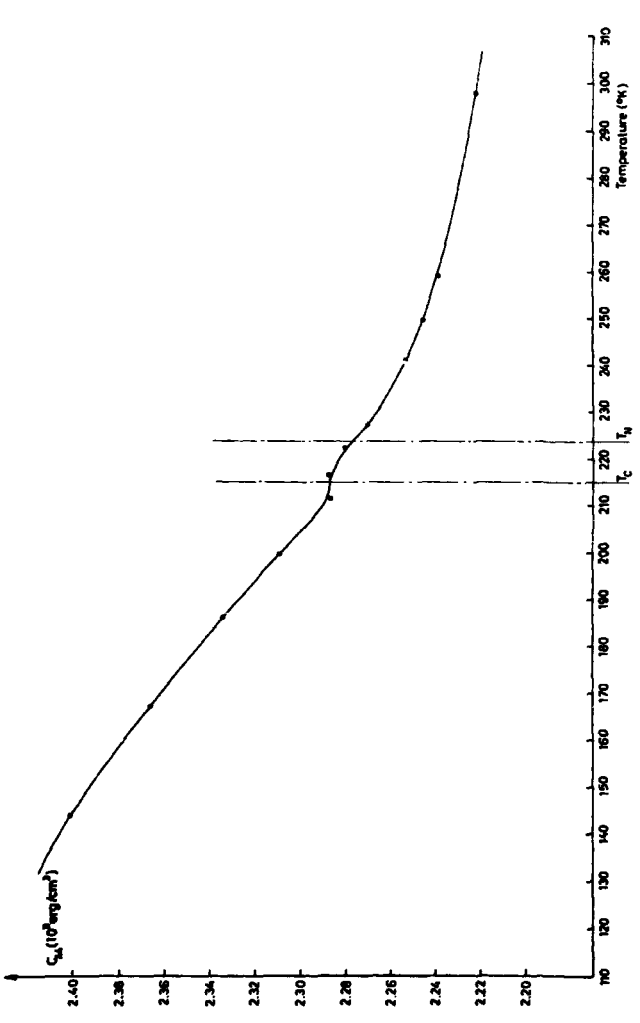

Fig. 16. The variation of c_{44} with temperature (140 - 300°K).

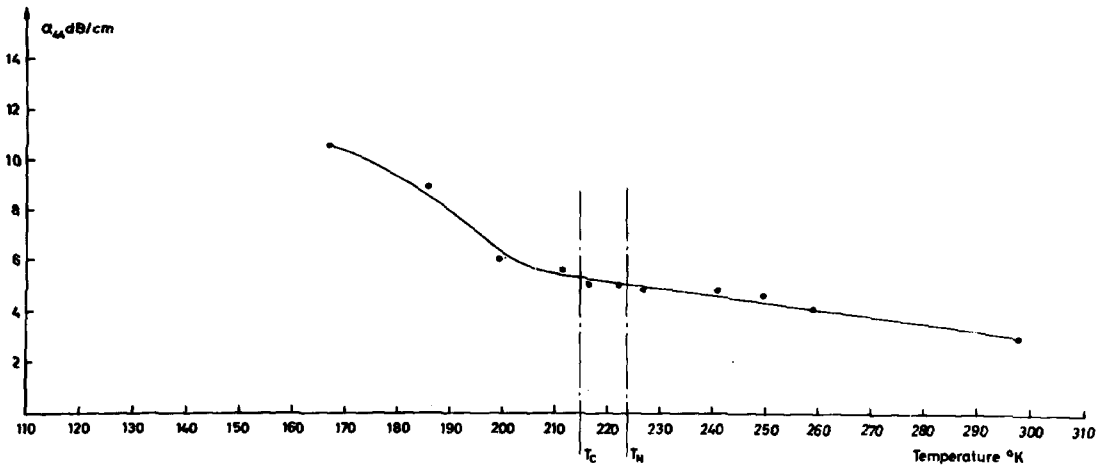

Fig. 17. The variation of the attenuation of the transverse sound waves propagating in the c-direction.

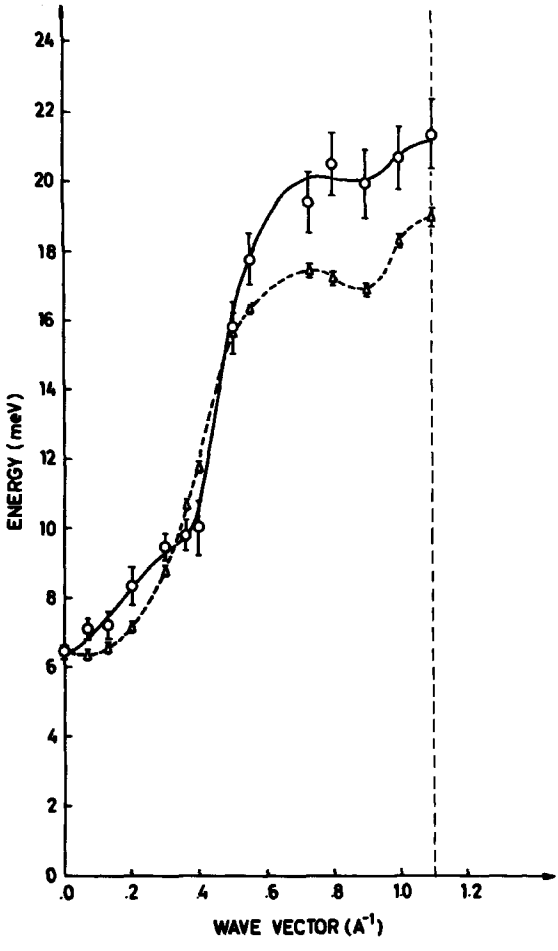

Fig. 18. Comparison between the experimentally measured dispersion relation parameters, the solid line is 2 A(q) and the dashed line $2\,[\epsilon^2(q) + B^2(0)]^{1/2}$, for the spin waves propagating in the c-direction of Tb at 4.2°K. The deviation between the two curves is due to the anisotropy of the two-ion spin interaction.

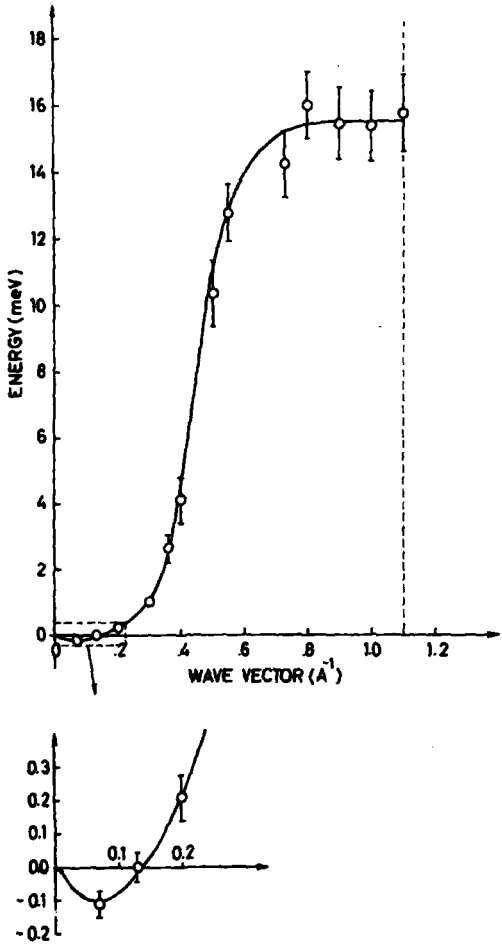

Fig. 19. The exchange function $2J[K^{\xi\xi}(0) - K^{\xi\xi}(q)]$ in the c-direction of Tb at 4.2°K. The insert shows the minimum at $q = 0.08$ Å^{-1}.

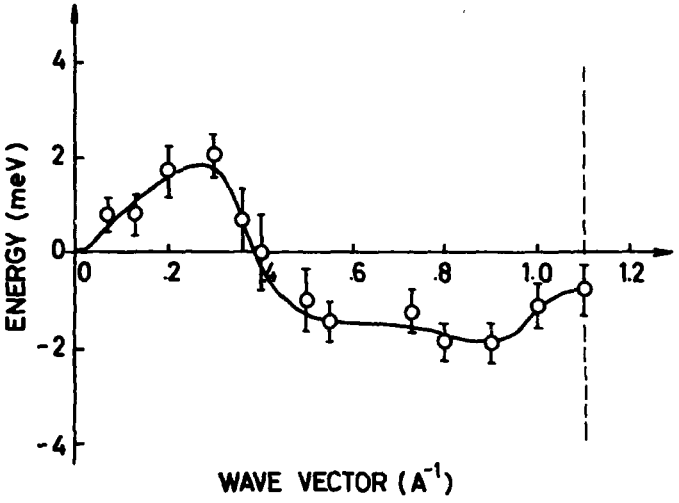

Fig. 20. The exchange function $2J[K^{cc}(0) - K^{cc}(q)]$ in the c-direction of Tb at 4.2°K.